

Abstract

ROE, BARRY GORDON. Durable Non-Fluorine Water-Repellent Fabric Finishing: Surface Treatment Using Silica Nanoparticulates and Mixed Silanes. (Under the direction of Dr. Xiangwu Zhang.)

Due to the cost of processing, materials, and environmental and human hazards, alternatives to fluorine-containing water-repellent finishes have begun to be heavily investigated. One type of chemistry, i.e. surface modification using silica nanoparticles and mixed silanes has recently become of particular interest in the scientific community.

100% cotton fabrics were treated with a combination of silica nanoparticles, silane hydrophobes (such as alkyltrialkoxysilanes), and silane crosslinkers (such as tetraethoxysilane). Fabric samples were prepared using a laboratory-scale dip-dry-cure process. After coating, the performance of the samples was evaluated using a contact angle goniometer. A number of the best performing samples were selected for further investigation, involving durability to laundering and crocking.

Results of the work show that surface modification using silica nanoparticles (both hydrophilic and hydrophobic) and mixed silanes was successful; the contact angle values of finished but unwashed samples ranged between 129° and 144°. Fabric samples made using the silane crosslinker tetramethoxysilane, silane hydrophobe n-decyltriethoxysilane, and silica nanoparticles had the highest water contact angle of all samples tested before laundering and crocking.

Fabric samples had varying levels of performance after being subjected to laundering and crocking. There was a very notable difference in samples after laundering that were allowed to air dry at laboratory conditions to those that was heat dried at the temperature at which the samples were cured. All samples prepared with the crosslinker

bis(triethoxysilyl)ethane showed the best durability to laundering, especially those using solutions that were prepared using an ultrasonic probe. The most durable sample was prepared with an ultrasonicated solution of bis(triethoxysilyl)ethane, n-octyltrimethoxysilane, and Aerosil[®] 90 fumed silica. These samples had an average contact angle of 129.7° before washing (AATCC-type accelerated laundering) and heat-drying and a contact angle of 123.1° after washing and heat-drying. This 94.9% recovery in contact angle shows a lot of promise in the technology that was the focus of this research.

Durable Non-Fluorine Water-Repellent Fabric Finishing: Surface Treatment Using Silica
Nanoparticulates and Mixed Silanes

by
Barry Gordon Roe

A thesis submitted to the Graduate Faculty of
North Carolina State University
In partial fulfillment of the
Requirements for the degree of
Master of Science

Textile and Apparel, Technology and Management

Raleigh, North Carolina

April 1, 2008

APPROVED BY:

Dr. Xiangwu Zhang
Chair of Advisory Committee

Dr. Stephen Michielsen
Co-chair of Advisory Committee

Dr. Richard Kotek
Co-chair of Advisory Committee

Dr. Peter Hauser
Minor Representative

Dr. Henry Boyter, Jr.
ITT Committee Member

Biography

Barry Roe was born and raised in Keene, NH. He graduated Cum Laude from the University of Massachusetts at Dartmouth with a B.S. in Textile Science and a minor in Business Administration. During his undergraduate study, he was on the chancellor's list twice, the dean's list four times, and earned awards from foundations like the AATCC. Barry worked at U-Mass Dartmouth's Advanced Technology and Manufacturing Center as a research intern and operating engineer for their Scanning Electron Microscope. After graduation, Barry will move to Minneapolis, MN to start his job as a purchasing engineer with Industrial Fabrics Corporation.

Acknowledgements

- I would like to thank my Research Committee for the time and effort to support this research and my growth as a student.
 - Xiangwu Zhang, Ph.D. – Committee Chair and P.I.
 - Stephen Michielsen, Ph.D. – TATM Co-Chair
 - Peter Hauser, Ph.D. – Minor Representative
 - Richard Kotek, Ph.D. – Committee Member, Project Co-P.I.
 - Henry Boyter, Jr., Ph.D. – Committee Member
 - Chris Moses – Technical Advisor from the Institute of Textile Technology
- I would especially like to thank my other Research Contributors, without their help this research would not have been possible.
 - Jeff Krauss, Pilot Plant Laboratory Manager – For donation of fabric used in research and invaluable help with fabric sample laundering
 - Birgit Andersen, TECS Research Assistant and Laboratory manager – For training and assistance with the contact angle goniometer
 - Dale Arnold, Vice President of Product Development at International Textile Group – For donation of fabric
 - Judy Elson, TECS Laboratory Manager – For supplies used in research and use of crocking test materials
 - Wendy Krause, Ph.D. – For advising at research meetings
 - Dale Batchelor, Ph.D. and Roberto Garcia, NCSU Analytical Instrumentation Facility – For assistance with SEM analysis

- Bill Roth, senior applications specialist with Hitachi High Technologies, Inc. – For analysis done with FE-SEM
- I would really like to say thank you to Patrice Hill, without whom the ITT Fellows would be lost. Thanks for all your hard work and support.

Table of Contents

List of Figures	viii
List of Tables	xi
Chapter 1: Introduction	1
Chapter 2: Literature Review	3
2.1. Advantages of Using Silica-Nanosol Coatings on Textiles	3
2.2. Important Principles Affecting Water Contact Angle on Textiles	5
2.2.1. Contact Angle and Wettability	6
2.2.2. Thermodynamics of Wetting	8
2.2.3. Other Approaches to Surface Tension and Wetting	10
2.3. Cotton and Polyester/Cotton-Blended Fabrics	11
2.3.1. Cellulose’s Availability for Functionalized Coatings	12
2.4. Fluorinated Coatings	13
2.4.1. Teflon™ and Scotchgard™ Industrial Coatings	14
2.4.2. Water and Oil Repellent Properties of Fluorocarbons	15
2.4.3. Environmental and Processing Concerns with Fluorocarbon Coatings	15
2.5. Silica Nanoparticles	17
2.5.1. Definition and Properties of Silica Nanoparticles	17
2.5.2. Potential Use of Silica Nanoparticles with Textiles	22
2.6. Sol-Gel Coatings	23
2.6.1. Definition of Sol-Gel Technology and Sol-Gel Processes	23
2.6.2. Preparation of Silica Nanoparticle Sol-Gel Coatings	26
2.6.3. Application and Finishing of Silica Nanoparticle Sol-Gel Coatings on Textile Fabric	29
2.7. Silanated Additives to the Sol-Gel Coating Process	32
2.7.1. Definition of a Sol-Gel Additive	32
2.7.2. Variety of Silanated and Fluorosilanated Additives	33
2.7.3. Preparation of Coatings	37
2.7.4. Performance of Coatings	39
2.8. Testing Methods Relevant to Water Repellent Textiles	46
2.8.1. Contact Angle Measurement	47
2.8.2. Water Repellency Under Customary Conditions	49
2.8.3. Testing for Washfastness	49
2.8.4. Analyzing Surface Morphology	50
2.8.5. Additional Test Methods	51
Chapter 3: Methodology and Experimental Procedure	54
3.1. The Approach of this Research and its Advantages	54
3.2. Experimental Procedures	57
3.2.1. Creation of the Design of Experiments	57
3.2.2. Procedure After the Design of Experiments	60
3.2.3. Chemical Structures and Properties	61

3.2.3.1.	Hydrophobic Additive Structures	61
3.2.3.2.	Silane Crosslinker Structures	62
3.2.3.3.	Silica Nanoparticles	64
3.2.4.	Fabric Sample Preparation	65
3.2.5.	Solution Preparation	65
3.2.6.	Fabric Coating, Drying, and Curing	66
3.2.7.	Fabric Sample Laundering (Modified AATCC Test Method)	68
3.2.8.	Fabric Samples Made With Ultrasonicated Solutions	69
3.2.9.	Fabric Sample Crocking (Modified AATCC Test Method)	69
3.3.	Test Methods	70
3.3.1.	Scanning Electron Microscope Analysis	70
3.3.2.	Contact Angle Measurements	71
Chapter 4: Observations and Decisions Regarding Processes, Inputs, and Products		
.....		74
4.1.	General observations on 12 preliminary sets of samples with varying amounts of silica o.w.b. and different crosslinking agents	74
4.1.1.	Samples with 0.02% SiO ₂ on weight of bath	74
4.1.2.	Samples with 0.2% SiO ₂ on weight of bath	75
4.2.	General observations on differences between preliminary samples	77
4.2.1.	On the observable interactions between water droplets and fabric samples	77
4.3.	Decisions made on future proceedings with regards to the design of experiments	78
4.4.	Observations Regarding Samples Made With Noncellulosic Fabrics	80
Chapter 5: Results and Discussion		
.....		82
5.1.	SEM Observations / Analysis of Micrographs	82
5.1.1.	SEM Results of TEOS Samples	82
5.1.2.	SEM Results of the TMOS Sample	84
5.1.3.	Observations Regarding the SEM Micrographs	86
5.2.	Pre-Design of Experiments Results	86
5.2.1.	The Effect of Silica Concentration on Three Crosslinkers	87
5.2.2.	The Effect of Increasing Silica Concentration on TEOS-Crosslinked samples	89
5.2.3.	Results of Two Samples Created with n-Octadecylmethyldimethoxysilane	90
5.3.	Results from the Design of Experiments	91
5.3.1.	Samples Using the Crosslinker Tetraethoxysilane	93
5.5.1.1.	Effect of Silica Type on Hydrophobicity on TEOS Crosslinked Samples	94
5.5.1.2.	Effect of Silane Hydrophobe Chain Length on Hydrophobicity of TEOS Crosslinked Samples	95
5.3.2.	Samples Using the Crosslinker Tetramethoxysilane	96

5.5.2.1. Effect of Silica Type on Hydrophobicity on TMOS Crosslinked Samples	97
5.5.2.2. Effect of Silane Hydrophobe Chain Length on Hydrophobicity on TMOS Crosslinked Samples	98
5.3.3. Samples Using the Crosslinker Bis(triethoxysilyl)ethane	99
5.5.3.1. Effect of Silica Type on Hydrophobicity on Bis(triethoxysilyl)ethane Crosslinked Samples	100
5.5.3.2. Effect of Silane Hydrophobe Chain Length on Hydrophobicity on Bis(triethoxysilyl)ethane Crosslinked Samples	101
5.3.4. Comparison of Hydrophilic Silica to Hydrophobic Silica Regarding Hydrophobicity	102
5.3.5. Analysis of the Design as a Whole	102
5.4. Comparison of Three DOE Samples to Their Counterparts Without Silica	106
5.5. Results of Samples After Washing to Those Before Washing, With and Without Heat Drying	108
5.5.1. Samples Made With Bis(triethoxysilyl)ethane	109
5.5.2. Samples Made With Tetraethoxysilane	112
5.5.3. Samples Made With Tetramethoxysilane	115
5.6. Results of Samples Produced With Ultrasonicated Solutions and Subjected to Laundering	117
5.6.1. Comparison of Sonicated Samples to DOE Samples	118
5.6.2. Comparison of Washfastness Results of Sonicated Samples to Non-Sonicated Samples	120
5.7. Results of Samples After Crocking to Those Before Crocking	123
5.8. Comparison of Results from This Research to Literature	125
5.8.1. Comparison of Results to Literature Review Samples	125
5.8.2. Comparison of Results to Samples Made from Alternate Methods	127
Chapter 6: Conclusions and Recommendations for Future Work	128
6.1. Summary of Results	128
6.2. Recommendations for Future Work	130
Chapter 7: References	133
Appendices	138
Appendix A: Raw Data Used to Make Graphs and Tables	139
Appendix B: Calculations	154

List of Figures

Figure 2.1 Schematic of Contact Angle on a Solid Surface [6].	6
Figure 2.2 Chemical Structure of Poly(ethylene terephthalate) Polymer [46].	12
Figure 2.3 Chemical Structure of Cellulose Polymer [43].	13
Figure 2.4 Chemical Structure of Teflon-AF™ Polymer [4].	14
Figure 2.5 a) Process Reaction and b) Process Diagram of The Continuous Flame Hydrolysis of Silicon Tetrachloride [30].	18
Figure 2.6 Schematic of Chemical After-Treatment of Fumed Silica Nanoparticles [30].	19
Figure 2.8 Preparation of Nanosol Coatings (Sol–Gel Process) [27].	24
Figure 2.9 Partial Hydrolysis of Metal Alkoxides [7].	26
Figure 2.10 Chemical Structure of Tetraethoxysilane (TEOS) [44].	27
Figure 2.11 Polycondensation of Metal Alkoxide Monomers (Sol-Formation) [7].	28
Figure 2.12 Polymerization and Crosslinking of Metal Alkoxide Monomers (Gel-Formation) [7].	29
Figure 2.13 Schematic of Sol Conversion to Xerogel [25].	31
Figure 2.14 Covalent Connection of R to Silica Matrix [27].	33
Figure 2.15 Chemical Structure of Long-Chained Monomeric Alkylsilane [27].	34
Figure 2.16 Chemical Structures of Polysiloxane Derivatives T1, T2, and T3, and Fluorinated Compound TF [24].	35
Figure 2.17 Contact Angle of Water (σ_w) of Sol 1 (left) and 2 (right) with Added Octyltriethoxysilane After Coating on Glass and Textile Fabric [24].	40
Figure 2.18 Apparatus for Measuring Contact Angle [13].	48
Figure 2.19 A) Uncoated Sample, B) HDTMS Coated Sample , and C) Silica Coated Sample [38].	51
Figure 3.1 Simplified Attachment of Chemical Treatment to Cellulose.	55
Figure 3.2 Macroscopic Attachment of Chemical Treatment to Cellulose.	56
Figure 3.3 Chemical Structure of n-Octyltrimethoxysilane [8].	61
Figure 3.4 Chemical Structure of n-Decyltriethoxysilane [8].	62
Figure 3.5 Chemical Structure of n-Octadecylmethyldimethoxysilane [8].	62
Figure 3.6 Chemical Structure of Tetraethoxysilane [8].	62
Figure 3.7 Chemical Structure of Tetramethoxysilane [8].	63
Figure 3.8 Chemical Structure of Bis(triethoxysilyl)ethane [8].	63
Figure 3.9 Chemical Structure of Bis(trimethoxysilyl)ethane [8].	63
Figure 3.10 Chemical Structure of Bis(trimethoxysilyl)hexane [8].	64
Figure 3.11 Chemical Structure of 1,4-Bis(trimethoxysilyl)ethyl)benzene [8].	64
Figure 3.12 Dip-Coating Method and Apparatus Employed in This Research.	66
Figure 3.13 Line Drying Apparatus Employed in This Research.	67
Figure 3.14 Schematic of How Fabric Samples Were Taken for Contact Angle Measurements.	71
Figure 3.15 a) Goniometer Eyepiece and b) Apparatus Used in Measuring Contact Angle.	72

Figure 5.1 Scanning Electron Micrographs of Samples Containing a) TEOS, n-Octyltrimethoxysilane, and 0.2% o.w.b. Aerosil[®] 200 and b) TEOS, n-Octyltrimethoxysilane, and 0.02% o.w.b. Aerosil[®] 200.....	83
Figure 5.2 Scanning Electron Micrographs of Samples Containing a) TEOS, n-Octyltrimethoxysilane, and 0.2% o.w.b. Aerosil[®] 200 (20,000X) and b) TEOS, n-Octyltrimethoxysilane, and 0.02% o.w.b. Aerosil[®] 200 (11,000X).....	84
Figure 5.3 Scanning Electron Micrographs of a Sample Containing TMOS, n-Octyltrimethoxysilane, and 0.2% o.w.b. Aerosil[®] 200 (2,000X).	85
Figure 5.4 Scanning Electron Micrographs of a Sample Containing TMOS, n-Octyltrimethoxysilane, and .02% o.w.b. Aerosil[®] 200 at Higher Magnification {a) 5,000X and b) 15,000X}.	85
Figure 5.5 Graph Comparing Contact Angle on Samples Using Three Different Crosslinkers, n-Octyltrimethoxysilane, and Aerosil[®] 200 at Different Concentrations.	88
Figure 5.6 Graph Comparing Contact Angle on Samples using TEOS, n-Octyltrimethoxysilane, and Aerosil[®] 200 at Five Different Concentrations.	89
Figure 5.7 Graph Comparing Contact Angle on Two Samples Containing TEOS, n-Octadecylmethyldimethoxysilane, (left) 0% and (right) 0.2% Aerosil[®] 90.....	90
Figure 5.8 Graph Comparing Contact Angle on Samples Using TEOS, n-Octyltrimethoxysilane, and Five Types of Aerosil[®] Silica.....	93
Figure 5.9 Graph Comparing Contact Angle on Samples Using TEOS, n-Decyltriethoxysilane, and Five Types of Aerosil[®] Silica.....	94
Figure 5.10 Graph Comparing Contact Angle on Samples Using TMOS, n-Octyltrimethoxysilane, and Five Types of Aerosil[®] Silica.....	96
Figure 5.11 Graph Comparing Contact Angle on Samples Using TMOS, n-Decyltriethoxysilane, and Five Types of Aerosil[®] Silica.....	97
Figure 5.12 Graph Comparing Contact Angle on Samples Using Bis(triethoxysilyl)ethane, n-Octyltrimethoxysilane, and Five Types of Aerosil[®] Silica.	99
Figure 5.13 Graph Comparing Contact Angle on Samples Using Bis(triethoxysilyl)ethane, n-Decyltriethoxysilane, and Five Types of Aerosil[®] Silica.	100
Figure 5.14 Graph Comparing Contact Angle Results for All Samples Prepared for the Design of Experiments.....	103
Figure 5.15 Statistical Data Showing Results from an Effects Test.	104
Figure 5.16 Interaction Profiles for the Design of Experiments.	105
Figure 5.17 Graph Comparing Contact Angle on Samples Chosen from the DOE Made With and Without Silica Nanoparticles.	107
Figure 5.20 Graph Comparing Contact Angle on Bis(triethoxysilyl)ethane Samples Before and After the Accelerated Laundering Test.....	110
Figure 5.21 Graph Comparing Contact Angle on Washed and Unwashed Samples Made With Bis(triethoxysilyl)ethane.	112

Figure 5.18 Graph Comparing Contact Angle of Washed and Heat Dried TEOS Samples to Unwashed Samples.....	114
Figure 5.19 Graph Comparing Contact Angle of Washed and Heat Dried TMOS Samples to Unwashed Samples.....	117
Figure 5.22 Graph Comparing Contact Angle on DOE Samples to Samples Made With Sonicated Solutions and Samples Made Without Silica.	119
Figure 5.23 Graph Comparing Contact Angle on All Unwashed and Washed Samples.	122
Figure 5.24 Graph Comparing Contact Angle on Samples Chosen from the DOE Subjected to Crocking (Before and After).....	124

List of Tables

Table 2.1 Physio-Chemical Data of Aerosil[®] Fumed Silica Particles [30]	21
Table 2.2 Silanated Compounds Used as Hydrophobic Additives [24]	35
Table 2.3 Contact angles of sols coated on different materials.....	41
(additive concentrations of 4 wt.% in the sol) [24]	41
Table 2.4 List of Coating Properties and Effect of Washing [13].....	43
Table 2.5 Physical Properties of Cotton Substrates Before and After Coating [13].	44
Table 2.6 Contact Angle of Water and Methylene Iodide on Cotton Substrates [59]	45
.....	45
Table 2.7 AATCC Repellency of Water and Methylene Iodide on Cotton Substrates	45
[59].....	45
Table 2.8 Surface hydrophobicity and durability evaluation of hydrophobic fumed	46
silica coatings on woven cotton fabrics [38].....	46
Table 3.1 List of Chemicals Used in Experimental Procedures.....	57
Table 3.2 Unrevised Design of Experiments.....	57
Table 3.3 Revised Design of Experiments.....	59
Table 3.4 Abridged Physico-Chemical Data of Aerosil[®] Fumed Silica [30]	65
Table 4.1 Preliminary Observations Made on Water Interaction with Fabric.....	77
Table 5.1 Design of Experiments Results (In Water Contact Angle, WCA)	92
Table 5.2 Comparison of Contact Angle Values on Samples With and Without Silica	107
.....	107
Table 5.3 Comparison of Contact Angle on Washed and Unwashed Samples Made	111
With Bis(triethoxysilyl)ethane	111
Table 5.4 Comparison of Contact Angle on Washed & Heat Dried TEOS Samples to	114
DOE Samples.....	114
Table 5.5 Comparison of Contact Angle on Washed & Heat Dried TMOS Samples	116
to DOE Samples	116
Table 5.6 Comparison of Contact Angle on Sonicated Samples to Unsonicated	118
Samples	118
Table 5.7 Comparison of Contact Angle on All Washed and Unwashed Samples .	121
Table 5.8 Comparison of Contact Angle on Crooked Samples to Uncrooked Samples	123
.....	123

Chapter 1: Introduction

The purpose of this literature review is to describe the usefulness and breadth of functionalized fabric coatings used for water, oil, and soil repellency. This literature review will describe the principles of the science behind water repellency and contact angle. It will also show current practices in use in industry as well as related functionalized coatings currently in research. Some industrial fluorinated compounds used for water repellency are useful for oleophobic as well as soil repellent and soil release coatings. This research, however, will only focus on functionalized hydrophobic coatings. The majority of the literature will be focused on related silanated and silica nanoparticle water repellent coatings. There are some coatings that feature both silane and fluorinated compounds that are important in the scope of this research. The topics that will be covered are: Advantages of Silica Nanosol Coating on Textiles, Important Principles Affecting Water Contact Angle of Textiles, Cotton and Polyester/Cotton Fabrics, Fluorinated Coatings, Silica Nanoparticles, Sol-Gel Coatings, Silanated Additives to the Sol-Gel Coating Process, and Test Methods Relevant to Water Repellent Textiles.

Since high contact angle and water repellency is the desired end result of this research, understanding the science of water repellency and contact angle is extremely important. The fabrics being used for this coating process will be 100% cotton, but polyester/cotton blends will be important for future work. It shows why and how these fabrics are appropriate for functionalized coatings. At present, repellent and release coatings in industry are mainly produced from fluoropolymers. However, sol-gel coatings are

making an impact in research in water-repellent textile-coatings. Within the realm of sol-gel coatings, this research will focus on coatings made with silica nanoparticles. The silanated and siloxane additives to these coatings will ultimately drive the usefulness and performance of the textile coating. The combination of additives and silica nanoparticle sols to different textile fabric will be the focus of this research. Current research shows various methods of applying nanosol coatings; however they do not address the issues concerning durability. These coatings are susceptible to damage from various sources, such as crocking and laundering. There lacks, in current research, the technology or knowledge to increase the durability of these coatings on the face of textile substrates.

Chapter 2: Literature Review

2.1. Advantages of Using Silica-Nanosol Coatings on Textiles

Functional and technical garments are products that should still meet consumer expectations like looks, comfort, hand, care/maintenance, and health issues, but should offer other properties like protection against: physical, thermal, chemical, and biological attacks or stress [27]. This means that it is especially important that these products retain their durability (to stresses like light, laundering, and crocking), feel, and looks [27]. However, these requirements do not solely apply to the garment and clothing markets. These expectations also apply to technical textiles. Functionalization of technical products can offer superior properties in markets such as automobiles, aerospace, construction, and home furnishings [27]. Mahltig et al. [27] list five goals that functionalized textiles should fulfill:

1. Improved stability against: mechanical, chemical, photochemical, or thermal degradation;
2. Improved repellency against: water, oil, and soil;
3. Changed light absorption and emission properties from UV to IR regions;
4. Improved electrical conductivity (and protection from electrostatic or antistatic effects);
5. Immobilization and controlled release of active species (biocidal, therapeutic and well-being effects).

Textile functionalization with silica nanosols (as they are the focus of this research) offers an economic and viable alternative to fluorinated products in the water-repellent

textile market. This is of great interest because functional and high-grade textiles have shown over-proportional market growth; for example, in Germany, sales increased 24.3% in 2002 [27]. There are many reasons to research and implement this particular coating technology in industry. Sols based on modified silica with particle diameter smaller than 50 nm for well-adhering, transparent layers on textiles [27]. These coatings will not alter the appearance of the substrate on which they are coating, which is especially important when implementing coatings on consumer apparel. These oxide layers are stable against light, heat, chemical, and microbial attacks [27]. With even more research, they can also be made to be durable against normal textile stresses, such as laundering and crocking. In some instances, nanosol coatings can help to improve the mechanical properties of the textile, meaning that the end product may have high mechanical strength and high wear and abrasion resistance [27]. In most instances, it is important for chemical processing of textiles not to severely damage or adversely affect the mechanical strength of the fabric (i.e. bleaching). These coated fabrics are extremely well suited for applications where mechanical properties are a consideration. Perhaps the most advantageous aspect of these coatings is the fact that they can be prepared at room temperature and atmospheric pressure [27]. Not only that, but they can also be processed in conventional coating devices commonly used for textile finishing, such as pad application or exhaust finishing [27]. Not only can they be traditionally processed, but silica nanosol coatings are annealed at 120°C, a considerably lower temperature than fluorochemicals that provide similar water-repellent performance. This means that should they be implemented, this technology will not require a substantial amount of additional capital in either processing

or finishing. This research will work to develop a process and coating formula that is economically advantageous by using lower-cost high-performance materials to show that it is indeed economical to implement this technology.

2.2. Important Principles Affecting Water Contact Angle on Textiles

Contact angle, not to be confused with the term water repellency, is a measure of fluid-surface and fluid-vapor interaction. Understanding the science behind contact angle will help us to better understand how to achieve desired end properties for functionalized coatings. In order to do so, there are certain important topics that must be understood that cover how a material interacts with liquids, the most important of which for water repellent textile materials is water.

As a clarification, it must be understood that water repellency and contact angle are not interchangeable terms. Water repellent materials are those that have the ability to resist the absorption, penetration, or wetting of water on the surface of the textile material. Measuring the contact angle of a liquid on a solid surface is a way of quantitatively classifying the interaction of the liquid with the surface of said material and also the interaction of the liquid with the vapor surrounding the liquid-solid interface. Moreover, the measurement of the contact angle is a way to quantify the surface energy of the material. It is extremely important to note that though a material may have extremely low surface energy due to a coating imparted to it, it may not be water repellent as measured by conventional tests as specified by the American Association of Textile

Chemists and Colorists (AATCC). This effect can be a product of fabric construction, coating type, or fabric basis weight, among other things.

2.2.1. Contact Angle and Wettability

The contact angle of a liquid on the surface of a material is a measurable value, a measure of wettability, and is defined by the surface tensions of all the components of the multiphase system (liquid, gas, and solid) and their interactions. The most common way of measuring contact angle on a solid surface is to place a drop of liquid of predetermined volume on to a the horizontal surface of the solid that is being observed. The measurements are taken by optical methods [57]. This concept may be better understood by referencing **Figure 2.1**, a schematic of the contact angle of a liquid on a solid surface.

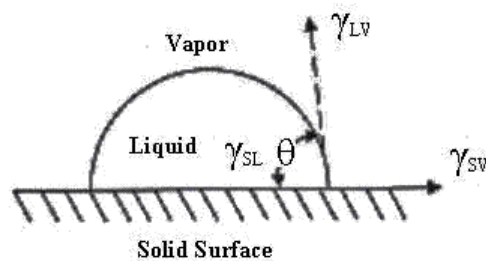


Figure 2.1 Schematic of Contact Angle on a Solid Surface [6].

When $\theta \leq 90^\circ$, the drop is said to wet the surface of the solid material. Perfect wetting occurs when the corresponding contact angle is equal to 0° . If a material has a contact angle of 0° , it is known that the attraction between solid and liquid is at least as great as the liquid-liquid attraction. Conversely, at values of $\theta = 180^\circ$ we can understand that there is no interphase attraction [57]. It is known that at values of $\theta > 90^\circ$ that wetting does not occur, as the droplet is showing less affinity for the surface of the fabric than the

vapor boundary. In these cases, the fluid and the surface are generally not capable of secondary bonding. For example, this occurs in a system where water is the fluid and the non-wetting surface is not generally capable of hydrogen bonding. Fluids and surfaces typically need similar solubility parameters for good wetting to occur [56].

In many cases, increasing the surface roughness of a solid is known to increase the contact angle [56]. Likewise, it is through the lotus leaf that nature tells us that it is not absolutely necessary to have $-\text{CH}_3$ or F-containing groups to have superhydrophobic effects [22]. By these two mechanisms we can specifically modify surfaces to mimic the lotus effect. Lotus leaves can obtain a water contact angle of greater than 160° using paraffinic wax crystals containing predominantly $-\text{CH}_2-$ groups [22]. These crystals manifest themselves as papillae or “bumps” on the leaf surface. Their sizes are on the order of single-digit micrometers, as shown by Burton and Bhushan [11] (these values, as seen later in **Section 5.1** are similar to the nanoparticle clusters deposited on the test substrates used). For more information on the lotus effect, refer to the work of its discoverers, Barthlott and Neinhuis [9]. Ma and Hill [22] state that extremely low surface energy is not necessary to achieve superhydrophobic effects and that controlling surface morphology at the nanometer scale is the key.

Knowing the relationship between contact angle and wettability allows us to understand the definition of wetting, which can be defined as “the process in which a fluid phase is totally or partially separated from contact with the surface of a solid by another fluid phase” [32]. The most common example of wetting describes the case where a liquid displaces air from a surface [32]. Wettability is driven by interfacial tensions between

the solid, liquid, and vapor phases. It can be defined by many equations depending on the situation, the most common of which is Young's Equation [32]. Surface roughness also plays a very important role in determining the wetting behavior of solids. It is a positively correlated relationship, as increasing the surface roughness of a hydrophobic material can enhance the surface water repellency greatly [59]. The sol-gel process is one of many techniques that can be used to achieve an increased surface roughness from the manipulation of nanoparticles [59].

2.2.2. Thermodynamics of Wetting

Always, when referring to **Figure 2.1**, will the work of Thomas Young be mentioned.

His work has been the basis for much of the modern work done with surface energy, wetting, and contact angle [47]. The Young-Dupree Equation, more commonly known as Young's Equation and shown as **Equation (2.1)**, gives an explanation of contact angle, θ , of a liquid on a solid surface [48][32].

$$(\gamma_{LV}) \cos\theta = \gamma_{SV} - \gamma_{SL} \quad (2.1)$$

where: γ_{LV} = Interfacial Tension of the Liquid-Vapor Interface

γ_{SV} = Interfacial Tension of the Solid-Vapor Interface, and

γ_{SL} = Interfacial Tension of the Solid-Liquid Interface

As wetting and wettability are characterized by the measurement of contact angle and in turn defined by the surface energies of the components of the system, it is important to examine the thermodynamics of the systems in which these phenomena occur. There are two types of wetting that are of particular interest in the finishing of textiles: spreading wetting and adhesional wetting [47].

In spreading wetting, a liquid in contact with a solid surface spreads over the surface and displaces the vapor phase from that surface. During the process of spreading, the interfacial area between the solid and the initial phase (defined by P1, normally air) is decreased by the amount A. This occurs while the area between the solid and the wetting liquid phase (P2) increases by an equal amount. Also, the interfacial area between (P1) and (P2) increases during the process. The change in interfacial area in each case will be the same, so that the total change (decrease) in the energy of the system will be:

$$-\Delta G = A (\gamma_{SP1} - \gamma_{SP2} - \gamma_{P1P2}) \quad (2.2)$$

where: γ_{SP1} = Interfacial Tension of the Solid-Vapor Interface
 γ_{SP2} = Interfacial Tension of the Liquid-Vapor Interface, and
 γ_{P1P2} = Interfacial Tension of the Solid-Liquid Interface

The term in Equation 2.2 in the parenthesis is called the spreading coefficient, S, and can be re-written as:

$$S = \gamma_{SV} - \gamma_{SL} - \gamma_{LV} \quad (2.3)$$

If S is positive, then a liquid will spread over the surface of the material to the greatest extent possible. For example, if γ_{SV} is large, S will be greater and the liquid will spread more. Now, if Young's equation (2.1) is rewritten as:

$$\cos\theta = \frac{\gamma_{SV} - \gamma_{SL}}{\gamma_{LV}} \quad (2.4)$$

and combined with the equation for the spreading coefficient (2.3), it gives the following:

$$S = \gamma_{LV} (\cos\theta - 1) \quad (2.5)$$

and if values of $\theta > 0$, S cannot be positive or zero and spontaneous spreading will not occur.

In adhesional wetting, if a drop of liquid is placed on the surface of a substrate and forms a contact angle, a change in free energy occurs. This change is shown by:

$$\Delta G_w = A (\gamma_{SV} + \gamma_{LV} + \gamma_{SL}) \quad (2.6)$$

where A is the surface area of the substrate in contact with the liquid. The work of adhesion can be defined as such:

$$W_a = \gamma_{SV} + \gamma_{LV} - \gamma_{SL} \quad (2.7)$$

This equation was first proposed by Dupré in his work *Théorie Mécanique de la Chaleur* and with modification by **Equation (2.1)** will read [47]:

$$W_a = (\gamma_{LV}) \cos\theta + \gamma_{LV} = \gamma_{LV} (\cos\theta + 1) \quad (2.8)$$

2.2.3. Other Approaches to Surface Tension and Wetting

Because not all systems are ideal, many researchers have tried to expand upon the original work done by Young. For systems with a rough solid surface, another relationship can be defined. Wenzel's Equation, shown by **Equation 2.9**, describes the effects of the surface's microstructure, for a contact angle θ' on a rough solid surface [48].

$$(\gamma_{LV}) \cos\theta' = r (\gamma_{SV} - \gamma_{SL}) \quad (2.9)$$

where: r = Wenzel's Roughness Factor.

Wenzel's roughness factor is defined as the ratio of actual area of rough surface to the geometric projected area. The relationship of θ to θ' is given by: $\cos\theta' = r \cos\theta$ [48]. Pilotek and Schmidt [37] cited work done by Cassie and Baxter, where hydrophobic textiles were investigated. They concluded that a drop of water cannot rest solely on the solid (textile) but also has contact to air at the substrate-side of the drop.

$$\cos \theta_{\text{obs}} = Q_1 \cos \theta_0 - Q_2 \quad (2.10)$$

where: θ_{obs} = Observable Contact Angle
 θ_0 = Intrinsic contact angle of ideal surface material

Their equation (shown by **Equation 2.10**) expresses this idea by reflecting the area where a liquid is in contact with the material (Q_1 , with contact angle θ_0) and where the liquid is in contact with air (Q_2 , with contact angle $\theta_{\text{air}} = 180^\circ$) normalized to the nominal area, respectively [37].

For polar liquids and surfaces (for example, cotton and water), both dispersion and hydrogen forces are important at the surface [53,54]. The Owens-Wendt-Kaelble Equation, shown by **Equation 2.11**, describes this situation [53,54].

$$(1 + \cos\theta) \gamma_L = 2\sqrt{(\gamma_S^d)(\gamma_L^d)} + 2\sqrt{(\gamma_S^h)(\gamma_L^h)} \quad (2.11)$$

where: γ^h = Component of Surface Tension Caused by Hydrogen and Dipole-Dipole Interactions

2.3. Cotton and Polyester/Cotton-Blended Fabrics

The approach of attaching a functionalized coating to a material surface involves analyzing the chemical structure of the material itself. Poly(ethylene terephthalate), commonly known as polyester, in fibrous form is a non-polar material and therefore has

no natural affinity for water. The chemical structure of polyester is shown in **Figure 2.2**. Though polyester polymer is an inherently hydrophobic material because it is non-polar, one researcher reported 100% polyester fabric as having a water contact angle of 76° [52]. This value, being below 90°, is considered to be hydrophilic. However in comparison, any prepared (desized, scoured and bleached) 100% cotton fabric has a contact angle of 0° (full wetting). Though polyester has no little affinity for water, a fabric made of a blend of polyester and cotton does. Therefore, it is still desirable to assess functionalized coatings on blended fabrics.

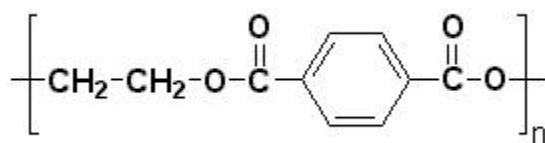


Figure 2.2 Chemical Structure of Poly(ethylene terephthalate) Polymer [46].

Cotton, as a polar polymer, has great affinity for polar fluids. This is true to the extent that there is no measurable contact angle of water on cotton. Therefore, it is a naturally hydrophilic, or “water-loving”, material. In applications where this quality is not desirable, water-repellent coatings can be attached to the polymer itself by exploiting knowledge of the chemistry of both the substrate and the coating materials.

2.3.1. Cellulose’s Availability for Functionalized Coatings

Cotton, as a naturally occurring polymer, is about 90% cellulose [54]. Its structure, as such, has six functional hydroxyl groups per repeat unit. **Figure 2.3** shows the structure of cellulose polymer with two repeat units.

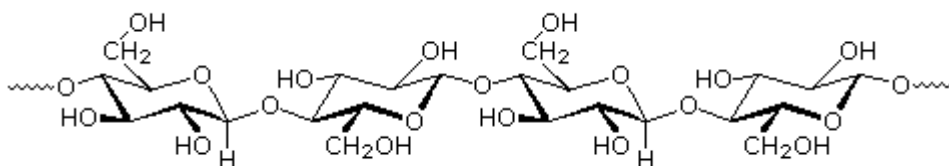


Figure 2.3 Chemical Structure of Cellulose Polymer [43].

The cellulose polymers that make up a cotton fiber have a degree of polymerization (DP) in the order of 1500. That gives the average polymer of DP 1500 and a 40% amorphous structure 3600 hydroxyl groups available for bonding, be it primary or secondary. These hydroxyl groups play an important part in this research, as they are the primary functional group for attachment of silanes. During an attachment reaction, silane oligomers form hydrogen bonds with the hydroxyl groups of the substrate and are then converted to covalent bonds during the drying and curing steps [7].

2.4. Fluorinated Coatings

Fluorinated compounds and polymers are known for their inert chemical behavior, owing to the fact that fluorine is such an electronegative element. Because they are so inert, fluorocarbon polymers have been widely used in industry for repellent and release coatings. They are useful as surfactants, fire-extinguishing agents, coolants, electrical insulators, inhalation anesthetics and transport systems for dissolved oxygen in medical applications [31]. Particularly in the textile industry, fluorocarbons are used for water repellency, oil repellency, and soil release coatings.

2.4.1. Teflon™ and Scotchgard™ Industrial Coatings

There are a number of companies that produce fluorocarbon treatments for textile substrates, two of which are the DuPont and 3M Corporations. One of the world's most well known repellent coatings among many substrates is DuPont's Teflon™ fluoropolymer. It is not entirely possible to detail everything about either Teflon™ or 3M's trademarked fluoropolymer, Scotchgard™ because both chemicals are protected by proprietary formulas. 3M has two particular chemicals that it claims are their most effective and popular among customers. Their PM-490 coating is a non-ionic fluorochemical resin solution, for use as a soil release treatment and also for limited water and oil repellency [40]. 3M's PM-930 is a high-performance fluorochemical emulsion, providing oil and water repellency to all types of natural and synthetic fibers. It has excellent durability to laundering and dry cleaning [42]. Both of these chemicals are made from a proprietary fluorochemical urethane, ranging from 28-32% in water, with the PM-930 containing an additional 0.5-1.5% of ammonium dodecyltrimethyl chloride [40][42]. Similar to the 3M products, DuPont's Teflon™ AP-II contains a fluorinated substituted urethane, as well as a fluorinated acrylic copolymer [50]. An example of a Teflon polymer (Teflon-AF™) can be seen in **Figure 2.4**.

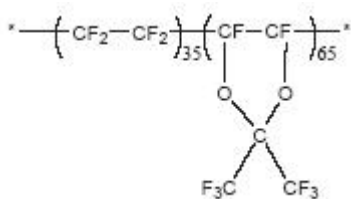


Figure 2.4 Chemical Structure of Teflon-AF™ Polymer [4].

2.4.2. Water and Oil Repellent Properties of Fluorocarbons

It is never easy to classify a general rule for the performance of a group of coatings or materials. A lot of how a material behaves depends on how it was processed. For example, knit and woven goods do not necessarily interact the same with water any more than do two different yarns of the same material. It can depend on how tightly a fabric is knit or woven, the finish on the yarn, yarn twist, or the amount of texture imparted into the yarn surface. Qualitatively, fluorocarbon coatings like Teflon™ can be considered hydrophobic and oleophobic, meaning they are repellent of both water and oil [4]. How repellent, however, depends on the type of polymer used and how it was processed. To give a practical example of the hydrophobicity of Teflon™, it is useful to look at Anamelechi et al.'s [4] work. They were able to quantify the contact angle of a water droplet on Teflon-AF™ to be $108 \pm 2.6^\circ$ [4]. This value was high in comparison to literature available from DuPont, stating the coating should give a water contact angle of 104° [4].

2.4.3. Environmental and Processing Concerns with Fluorocarbon Coatings

Numerous researchers have reported in their literature the importance of replacing fluorinated compounds in industry. Mahltig et al. [27] state that it is of great interest to avoid fluorinated compounds because of their high cost, potential risk with skin contact, and the environmental risks involved with the emission of fluorine compounds during or after textile impregnation. Many fluorinated organics, especially perfluorinated compounds (PFC), are environmentally persistent, bioaccumulative, and potentially harmful [20]. In addition, little is known about the occurrence, transport, biodegradation,

and toxicity of these compounds in the environment [20]. Another concern is that certain volatile fluorinated compounds can be oxidized in the troposphere, yielding nonvolatile compounds such as trifluoroacetic acid [20]. Material safety data sheets for the compounds detailed in **Section 2.5.1** list a number of hazardous thermal-decomposition products for the coatings. Both the PM-490 and PM-430 made by 3M may evolve hazardous byproducts of hydrogen fluoride and perfluoroisobutylene; the PM-930 is of particular interest because may decompose to a known carcinogen, methyl ethyl ketoxime [39][41]. Teflon™ products list only hydrogen fluoride (HF) as a byproduct of thermal decomposition, in addition to carbon dioxide and carbon monoxide [49][50]. At the processing level, some workers handling fluorinated organic compounds (FOC) have had organic fluorine levels in their blood serum from 1 to 71 ppm (where a normal organic fluorine level in blood serum is from 0 to 0.13 ppm) [20]. Apart from health and environmental concerns, the processing of fluorocarbon polymers is difficult and expensive. Therefore, it is very desirable to find an industrial replacement for these polymers. In particular, fluorocarbon compounds such as PTFE are difficult to handle because of their viscosity, melt strength (the mechanical strength of polymer in the melting state), and insolubility [31]. Some researchers have also brought up issues with fluorosilanated additives when used in sol-gel and modified sol-gel processes. Daoud et al. [13] states that some studies have been done on fluoroalkyltrimethoxysilanes that have discovered: economic (high cost) disadvantages; environmental and ecological disadvantages, such as risk for human health with skin contact and environmental concerns in the case of fluorine emission during and after the coating process; and that a

high temperature is usually required for their production. Mondea et al. [31] reinforce this statement by saying that making branched chains of perfluoroalkyl silane is an important technology because linear chains with $\text{CF}_2\text{-CH}_2$ bonds tend to evolve undesirable and dangerous hydrogen fluoride (HF) gas upon heating.

2.5. Silica Nanoparticles

Research in nanotechnology is now becoming of great interest all over the world.

Currently, research and development spending in the United States is at about \$2 billion [5]. Silica nanoparticles, when properly prepared, can be used to create functionalized coatings for textile fabrics. These coatings can be used with additives to impart hydrophobic properties or hydrophilic properties, or carry dyes, polymers, biomolecules, or bioactive agents [27][25][26].

2.5.1. Definition and Properties of Silica Nanoparticles

Silica nanoparticles are a solid state of matter made of silicon dioxide, SiO_2 . These particles are extremely small; their order of magnitude lies in the nanometer (nm) range [30]. The particles are nearly spherical and their diameter can range from 7 to 40 nanometers [30]. The primary silica particles are built up of about 10,000 SiO_2 units, with a Si-Si distance of about 0.31nm [30].

This research will use specially produced, hydrophilic and hydrophobic fumed silica nanoparticles made by Degussa Corporation, under the trade name Aerosil[®]. These particles start hydrophilic and are produced by continuous flame hydrolysis using silicon tetrachloride, SiCl_4 , known as the “Aerosil[®] Process” [30][60]. In this process, SiCl_4 is converted to the gas phase and then reacts spontaneously and quantitatively in an

oxyhydrogen flame with the intermediately formed water to produce silicon dioxide [30].

The process reaction and diagram are shown in **Figure 2.5**.

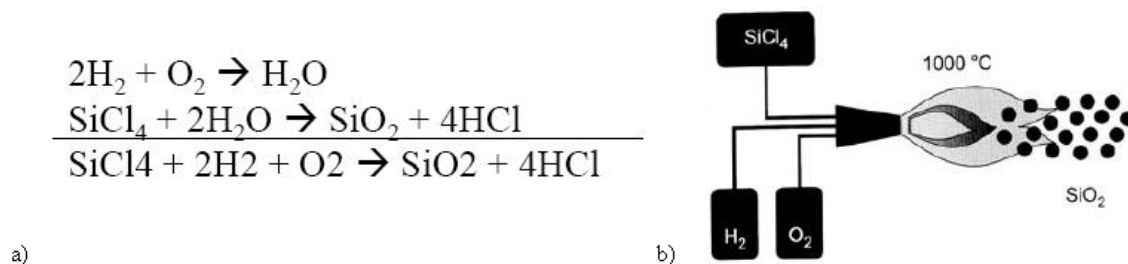


Figure 2.5 a) Process Reaction and b) Process Diagram of The Continuous Flame Hydrolysis of Silicon Tetrachloride [30].

By varying the concentration of the co-reactants, flame temperature, and dwell time of silica in the combustion chamber, makes is possible to influence particles size, particles size distribution, and surface properties of the silica within wide boundaries [30].

It is also possible, and extremely advantageous in certain applications, to attach a chemical after-treatment process to the continuous flame hydrolysis of silicon tetrachloride [30]. Here, hydrophilic silica can be made hydrophobic. It is especially reactive while still in the production system; the after-treatment is done with an after-treatment silane [30]. **Figure 2.6** shows the direct after treatment process of fumed silica nanoparticles.

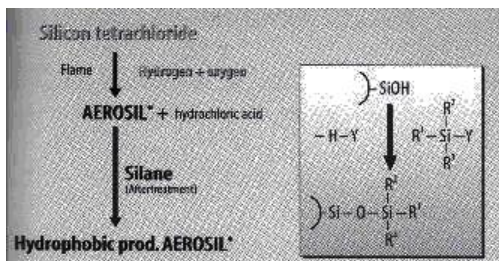


Figure 2.6 Schematic of Chemical After-Treatment of Fumed Silica Nanoparticles [30].

The chemical treatment can be done with halogen silanes, alkoxy silanes, silazanes, or siloxanes [30]. The reaction is done in the presence of dimethyldichlorosilane (DDMS) in a fluid bed reactor [30]. When reacted, the particles have additional siloxane groups that are largely chemically inert. The inert siloxane groups lead the particles to be strongly hydrophobic. These particles offer a lower silanol group density than the hydrophilic particles, and therefore have lower water vapor adsorption [30]. The hydrophobic particles are easier to disperse in air than are the hydrophilic and exhibit a less pronounced network structure [30]. Regardless of affinity for water, the primary silica particles form a loose network structure, where the smaller the particle diameter, the more pronounced the aggregation or agglomeration [30]. **Figure 2.7** shows a transmission electron micrograph (TEM) showing agglomeration differences between hydrophilic and hydrophobic fumed silica particles.

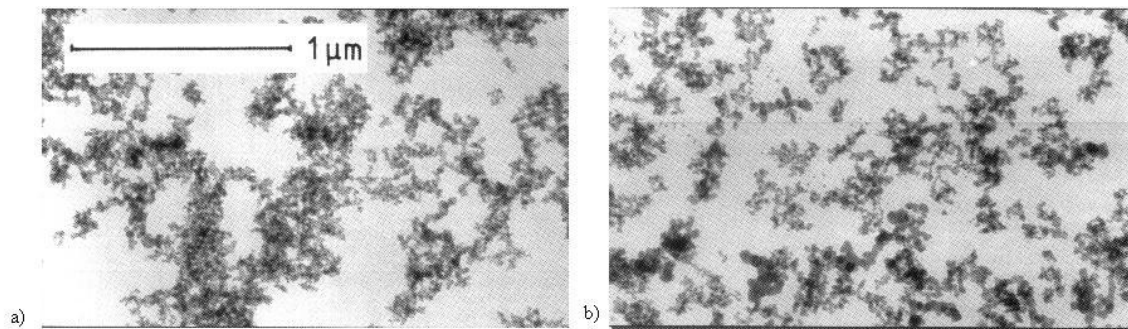


Figure 2.7 TEM Micrographs of a) Hydrophobic and b) Hydrophilic Fumed Silica Particles [30].

Hydrophilic particles, as can be seen, show a higher agglomeration tendency in air, but have much more affinity for water than their hydrophobic counterparts. Also, dispersion difficulty of particles increases with decreasing particle size, especially in the hydrophilic particles, due to the high concentrations of OH^- groups and extremely high surface area [30]. To complement the microscope images, **Table 2.1** outlines some special physical and chemical attributes of Aerosil[®] fumed silica particles.

Table 2.1 Physio-Chemical Data of Aerosil[®] Fumed Silica Particles [30]	
Property:	Value:
Refractive Index	1.46
Solubility in water (pH 7, 25C)	150 mg/L
Specific Weight	2.2 g/cm ³
Thermal Capacity Cp of Aerosil [®] 200	10°C: 0.79 J/(g K)
	50°C: 0.85 J/(g K)
Wetting Heat of Water on Aerosil [®] 200	-150x10 ⁻⁷ J/m ²
Molar Adsorption Coefficient for Free Silanol Groups (3750 cm-1)	(4.4±0.4) x 10 ⁵ cm ² /mol
Temperature Stability of Aerosil [®] Hydrophobic Types	850°C
Ignition Temperature of Aerosil [®] Hydrophobic Types According to DIN 51794	Aerosil [®] R 974: 530°C
	Aerosil [®] R 805: 480°C
	Aerosil [®] R 812: 460°C
	Aerosil [®] R 202: 440°C
Stability:	
With Respect to Acids	Excellent
With Respect to Ammonia, 5%	Slight
With Respect to Sodium Hydroxide Solution, 5%	Very Slight
With Respect to Oxidizing Agents	Excellent
With Respect to Reducing Agents	Excellent

One of the most important characteristics of the hydrophilic silica particles is their abundance of silanol (SiOH) groups. In other words, the particles are “water attractive” and are responsible for the fact that these hydrophilic silica types are easily wetted by water. These groups also have very good capacity for chemical reactions, which makes this research possible and the manufacture of hydrophobic particles (like Aerosil[®] R805) possible [30].

2.5.2. Potential Use of Silica Nanoparticles with Textiles

There are two important reasons for the functionalization of textiles. The first is the maintenance and improvement of current properties; the second is the creation of new material properties [27]. Chemically and physically modified sol coatings of silica can allow for the creation of advantageous properties and functions (i.e. water repellency) [27]. Silica nanoparticles can be prepared in the sol-gel process, in combination with other additives, such as silanes, to give desired end-properties to fabric. Sols based on modified silica, and other metal oxides, with particle diameters smaller than 50 nm (nanosols) form well-adhering, transparent oxide layers on textiles [27]. This sol-gel process is an alternative to methods of applying metal or silicon oxides by deposition from the gaseous phase, which requires vacuum devices and a high technical standard [25]. Compared to some commercially organic coatings, these inorganic silica coatings show increased stability at higher temperatures, approximately 180°C [24]. This means that the silica sol-coatings could be used in products with a higher application temperature [24]. These coatings have come under scrutiny because issues with washfastness. It has become necessary to balance properties, because with these particular coatings, the additives to the process determine adhesion. Specifically, the washfastness of the coating decreases because the adhesion of the sol-gel layer decreases with increased hydrophobicity [25]. This research will attempt to specifically address both of these issues by creating coatings that are super-hydrophobic as well as extremely durable to a textile substrate.

2.6. Sol-Gel Coatings

Silicas, silanes, metal oxides, and other materials can be prepared, or combined and prepared, in the sol-gel process to prepare thin, transparent coatings on a variety of substrates [27][60]. These coatings are used to modify or enhance the surface properties of the substrate on which they are applied. Hydrophilic materials can be made to be hydrophobic (and vice versa) or the coatings can be used to carry dyes, polymers, biomolecules, or bioactive agents [27][25][26]. These coatings can be applied to a number of substrates: (not limited to) cotton, glass (solid or fabric), wood, plastics, stainless steel, and silicon [33][58][29][14][13].

2.6.1. Definition of Sol-Gel Technology and Sol-Gel Processes

Classifying sol-gel technology can be ambiguous, as it is difficult to determine what does or does not fall under the umbrella of its definition. Sol-gel technology can be said to be “the fabrication of nanoparticles by hydrolysis and condensation processes or controlled precipitation processes” [45]. It is a method of preparing special metal oxide glasses and ceramics by hydrolyzing a chemical precursor (or mixture of chemical precursors) that pass sequentially through a solution state and a gel state before being dehydrated to a glass or ceramic [7]. Much literature is available on hybrid organic-inorganic nanocomposite coatings made using sol-gel reactions via hydrolysis and polycondensation of hexadecyltrimethoxysilane (HDTMS), tetraethoxyorthosilicate (also known as tetraethoxysilane and TEOS), and 3-glycidyloxypropyltrimethoxysilane (GPTMS) mixtures [38]. Through a sol-gel process prepared with the preceding chemicals, contact

angles of up to 141° have been achieved. The state of superhydrophobicity in these cases, defined by the contact angle greater than 140° , have been attributed to the following:

1. A change in the surface geometry from smooth to rough
2. The hydrophobic properties of the roughness surface [38].

However, Pipatchanchai and Srikulkit [38] state that because previous sol preparations were done in an alcohol-based media that commercial applications for the technology are limited or restricted. In order to fully understand the meaning behind the definition, it is best to look at examples of how the technology is used in the preparation and application of these coatings. The final coating will pass through four main stages of preparation and application, shown in **Figure 2.8**.

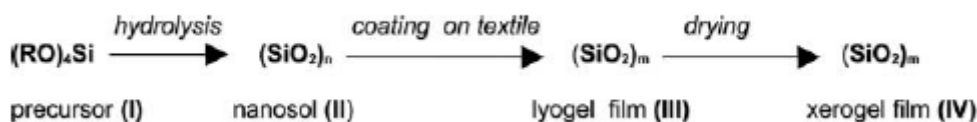


Figure 2.8 Preparation of Nanosol Coatings (Sol–Gel Process) [27].

To create a silica nanosol coating, it is possible to use tetraalkoxysilanes (TAOS); they undergo hydrolysis and condensation steps to form sols and then gels. When the sol-gel process is complete, an inorganic silicate group free of organic groups is formed [29].

Mai and Militz [28] state that in forming a sol-gel, the process proceeds in two general steps. In the first step (when creating silica sols-gels), silicon alkoxide groups (silicic acid esters) are hydrolyzed by water molecules to form siloxanes; the process can be catalyzed by acids or bases [28]. The second step is characterized by siloxanes

condensing to polysiloxanes. The condensation of two siloxane molecules releases a molecule of water, which is able to further contribute to the hydrolysis [28]. The alkoxy groups of silanes can be hydrolyzed to form silanols, and later are able to condense to three dimensional units [14]. Condensation starts while hydrolysis is still in progress, leading first to the formation of colloid oligometric particles called sols [14]. Further reaction leads to crosslinking of the particles so that highly condensed gels are formed [14]. In the first phase of these processes, sols are formed that are soluble, for example, in the corresponding alcohol of the alkoxy silanes. However, the sols formed are “living” systems that perform further hydrolysis and condensation until a certain molecular weight and degree of crosslinking is reached and an insoluble gel is formed [28]. As polymerization and crosslinking progress, the viscosity of the sol increases until the sol-gel transition point is reached [7]. At this point, the viscosity abruptly increases and gelation occurs [7]. To further promote crosslinking, the coated substrate is dried and other dehydration techniques are employed [7]. For best results, the substrate will pass through a process called densification (where maximum density is reached) in which the isolated gel is heated about its glass transition temperature (T_g) [7]. Arkles and Larson [7] state that the densification rate and temperature of sintering are primarily influenced by the morphology and composition of the gel. It is important to note, that in the coating of textiles, hydrolysis and drying conditions govern the density, porosity, mechanical properties, and the critical thickness for cracking [27]. This is especially true in the crosslinking in the coating. In Mai and Militz’s [28] research, the degree of crosslinking in polysiloxanes was steered by the concentration of TEOS in ethanol and by other

parameters such as reaction time. Mahltig et al. [23] dedicated research to the analysis of similar topics. They concluded that the presence of organic solvent has the advantage of shorter drying times and lower curing temperatures, resulting in less energy consumption and reduction of processing time [23]. However, in contrast, for practical application aqueous media are preferred because they are non-flammable and environmentally more accepted [23]. Acid-hydrolyzed coatings are weakly crosslinked condensation products with a denser layer structure [27]. Base-hydrolyzed coatings form particle aggregates with larger pores [27]. To get a final coating on a substrate, the sol-gel needs to be prepared from its precursor, applied to the material, dried, and thermally after-treated.

2.6.2. Preparation of Silica Nanoparticle Sol-Gel Coatings

The preparation stage of sol-gel coatings can also be considered to be the hydrolysis stage; it is the first of three basic steps. The partial hydrolysis of metal alkoxides to form reactive monomers is shown in **Figure 2.9**.

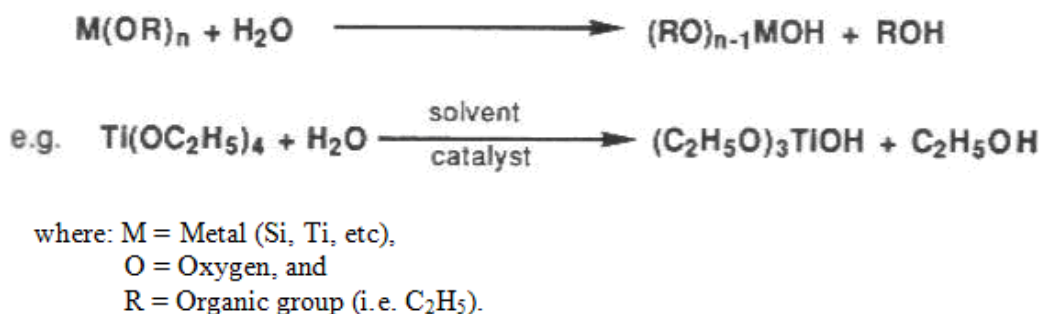


Figure 2.9 Partial Hydrolysis of Metal Alkoxides [7].

In the sol-gel process, it is intuitive to think that first a sol would need to be made, then converted to a gel. Ebbing and Gammon [15] state that a sol “consists of solid particles dispersed in a liquid”. A silica sol can be prepared a number of ways. It can be prepared from either acid- or alkali-catalyzed hydrolysis, for example: a silicon alkoxide hydrolyzed in water and an organic solvent miscible in water (usually ethanol) [27]. In their work, Mahltig et al. [27][24][26][25] claimed the coatings are transparent, stable, nanosized dispersions with between 4-20% solids (by weight) and particle diameters of less than 50 nm. Many researchers find it to be advantageous to use tetraethoxysilane (TEOS, **Figure 2.10**), sometimes in combination with other materials, as their hydrolysable precursor, using acid as a catalyst [24][29][13][31][25].

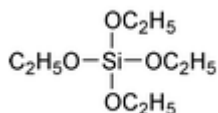


Figure 2.10 Chemical Structure of Tetraethoxysilane (TEOS) [44].

There is, of course, different ways to produce these coatings. In one of their papers, Mahltig and Böttcher [24] prepared a pure silica sol by combining 20 mL of TEOS, 4 mL of 0.01 N hydrochloric acid (HCl), and 84 mL of 96% ethanol. This mixture was stirred at room temperature for 24 hours [24]. They were also able to produce a modified silica sol by combining 43 mL of TEOS, 12 mL of 0.01 N hydrochloric acid (HCl), 50 mL of 96% ethanol, and 4 mL of 3-glycidoxypropyl triethoxysilane (GLYEO or GPTMS), again stirring for 24 hours at room temperature [24]. Sol-formation occurs with the

polycondensation of the hydrolyzed monomers to form colloid-like oligomers [7]. The chemistry behind the transformation is shown in **Figure 2.11**.

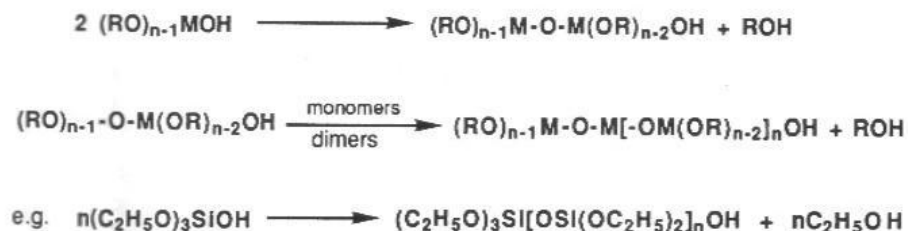


Figure 2.11 Polycondensation of Metal Alkoxide Monomers (Sol-Formation) [7].

In Daoud et al.'s [13] research, sols were also prepared with TEOS (98%), 3-glycidoxypropyltrimethoxysilane (GPTMS) (97%) and HCl in 99.8% ethanol. They were best made with a molar ratio of 1:0.118:0.008 of TEOS:GPTMS:HCl [13]. The sol was prepared with an additive and stirred for a total of 24 hours [13]. Textor et al. [52] created their coating by pre-hydrolyzing GPTMS with 1.5 mol of water (0.01 mol HCl), stirring for at least 2 hours to build the base sol, to which they incorporated a variety of additives. Yu et al. [59] prepared coatings using a mixture of 11.5 mL of TEOS, 25.0 mL of ethanol, 3.6 mL of water, and 0.5 mL of ammonia. Again, the mixture was stirred for 2 hours at room temperature. Yu et al. [59] claimed an SiO₂ particle size of 198.4 nm. Two different research teams, one lead by Mai and Miltz [29] and the other by Donath et al. [14], were able to create sol-gel coatings on and in wood substrates by using the moisture and free water in the wood to initiate hydrolysis of alkoxysilanes to conduct the sol-gel process in the wood and cell wall. As noted, additives can and have been added to these sols before substrate (i.e. fabric) treatment to further enhance the properties of

the coating, and will be covered in **Section 2.8**. Nanosols also usually contain alcohol from the hydrolyzed precursor when prepared in Mahltig et al.'s [27] fashion. The alcohol promotes good storage stability, good adhesion to any textile fiber type, and fast drying at low temperatures [27]. After the sol is prepared, it is applied to the substrate and further treated to make the final coating.

2.6.3. Application and Finishing of Silica Nanoparticle Sol-Gel Coatings on Textile Fabric

There are three steps through which the coating, now in sol form, must now go. The sol needs to physically be applied to the substrate, made to a lyogel, and finally converted to a xerogel [25]. To complete the conversion, additional hydrolysis of the polycondensed sol occurs [7]. It does so to promote polymerization and crosslinking, which leads to a three dimensional matrix, known as gel-formation (as shown chemically by **Figure 2.12**) [7].

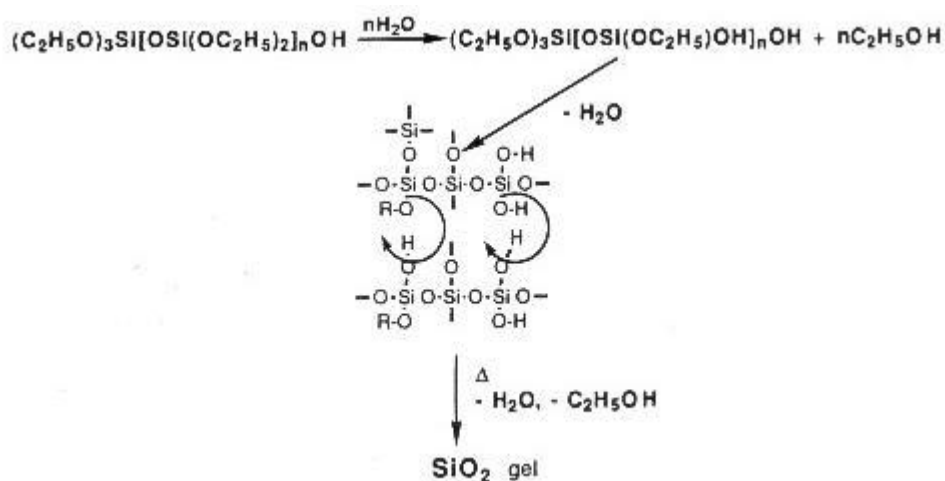


Figure 2.12 Polymerization and Crosslinking of Metal Alkoxide Monomers (Gel-Formation) [7].

One of the most appealing aspects of this particular type of coating is that it can be applied to textile fabrics in a number of conventional methods. The easiest method in which the coating can be applied is by dip coating; Mahltig and Böttcher [24] dip-coated their samples at a speed of 30 cm/min. In one paper, Mahltig et al. [23] cited using three separate substrates: a PET fabric of basis weight 85 g/m², a nylon fabric of basis weight 113 g/m², and a PET/Cotton blend of basis weight 201 g/m². Daoud et al. [13] also chose to dip-coat their samples, instead keeping the samples submerged for 1 minute. However, their procedure went another step, and padded at a nip pressure of 2.75 kg/cm² [13]. Yu et al [59] treated plain woven, cotton samples of basis weight 140 g/m² in the gel and padded them to 70% wet pick-up. Though not necessarily done as much in research because of cost limitations, it is also possible to apply these coatings by spray-coating and knife-coating [52]. After the sol is applied to the surface of the substrate, the nanoparticles tend to aggregate and condensate into three dimensional networks due to their high surface to volume ratio [27]. This forms a solvent-containing lyogel layer on the surface of the textile [27]. To form the final layer, the lyogel is heated and dried to remove solvent from the coating. This forms the final xerogel layer which is free of solvent molecules and has a porous structure [27]. **Figure 2.13** shows the step-wise difference between the sol, lyogel, and xerogel forms.

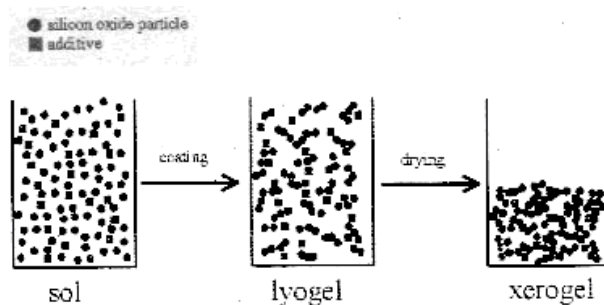


Figure 2.13 Schematic of Sol Conversion to Xerogel [25].

To finish the fabric treatment, both Mahltig and Böttcher [24] and Daoud et al. [13] allowed their samples to dry at room temperature for at least 2 hours, then annealed them at 120°C for 1 hour. Textor et al. [52] chose to treat their samples at 130°C for 1 hour, not disclosing if they allowed the samples to dry at room temperature first. Yu et al.'s [59] finishing treatment was fairly different from the other disclosed methods. After padding, the samples were dried at 80°C for 3 minutes before being padded in a methanol solution containing perfluorooctylated quaternary ammonium silane coupling agents [59]. The fabric was padded twice to a wet pick-up of 70%, dried at 80°C for 3 minutes, and finally cured at 160°C for a further 3 minutes [59]. A thermal post-coating treatment is necessary to obtain good adhesion and coating stability [27]. Mechanical properties and stability during washing will be improved by increasing the duration and temperature of annealing [27]. It is important that for these coatings that thermal treatment does not go exceed 180°C because of risk of thermal destruction of the textile [27]. After treatment, these xerogel coatings can be modified easily by physical or chemical means; this alters the coating properties and a wide range of options are available [27].

2.7. Silanated Additives to the Sol-Gel Coating Process

In order for nanosols to be used as effective hydrophobic coatings, they are usually made from inorganic silica sols [27]. In these cases, the silica is either physically or chemically modified with hydrophobic additives [27]. There are a number of additives available for this process, usually monomeric alkylsilane compounds, polysiloxanes with hydrophobic groups, or fluorinated compounds (i.e. perfluorooctyltriethoxysilane) [27]. These additives can severely alter the fluid interaction properties of the coating by greatly increasing its hydrophobicity. They may also work as crosslinking and coupling agents in the final gel coating.

2.7.1. Definition of a Sol-Gel Additive

An additive to the sol-gel process is just that, an additive. These modifiers do not have a set purpose or function, other than they are used to alter the properties of the coating in some way. In the scope of this research, additives will serve two main purposes: crosslinking the network of silica particles and increasing the hydrophobic nature of the coating. These functions can be achieved with two distinct types of chemical additives. Increasing the hydrophobicity of the coating can be done with a variety of hydrophobic alkyltrialkoxysilanes. The hydrophobic properties of the coating can be altered using different long-chained monomeric alkylsilane compounds [27]. Crosslinking in these coatings is done with crosslinkable silane compounds. These compounds act as crosslink centers that improve the durability of water-repellent finishing. To some extent, silane coupling agents could be used to increase interaction with the silica nanoparticles or the additives with the substrate surface. Arkles and Larson [8][6] state that silane coupling

agents are recommended for applications in which a surface has hydroxyl groups and the hydroxyl groups can be converted to stable oxane bonds by reaction with the silane.

There are a number of additives and chemicals being researched for these purposes, as can be seen in **Section 2.6.2**.

2.7.2. Variety of Silanated and Fluorosilanated Additives

Since there are a number of functions that an additive can perform, there are a number of forms in which they can be configured. Crosslinking and chemical modification can be done with trialkoxysilanes, TAOS, having a chemical structure $R-(SiOR)_3$ and containing an organic substituent, R [27]. The trialkoxysilanes work as crosslinking agents because they are covalently connected to the silica matrix via the hydrolysis and co-condensation steps [27]. **Figure 2.14** shows how the organic substituent R is chemically bonded to the silica matrix.

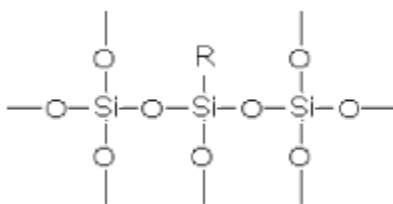


Figure 2.14 Covalent Connection of R to Silica Matrix [27].

By incorporating different chemical structures of R, the nanosol can be modified to great number of uses. This means that hydro- or oleophobic properties can be obtained by using alkyl- or perfluoroalkyl-containing trialkoxysilanes [27]. It is important to note that only oil and soil repellency can be achieved by using silane compounds that are fluorinated or that have fluorinated side chains [27]. However, in the interest of this

research, alkylsilane compounds without fluorine substituents can lead to excellent water repellency [27].

To achieve the best non-fluorinated hydrophobic coatings, a viable option is to use long-chained monomeric alkylsilane compounds [27]. It is known that increasing the chain length of the monomers increases the hydrophobicity of the textile coating [27]. It is certainly possible to use other compounds for hydrophobic additives as well. Mahltig et al. [27] state that it is possible to achieve contact angles of greater than 110° using methyltriethoxysilanes. With alkylsilane long-chain monomers, the best water repellency comes from structures where 'n' is greater than twelve for the structure in **Figure 2.15** [27].

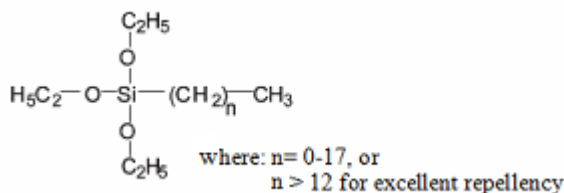


Figure 2.15 Chemical Structure of Long-Chained Monomeric Alkylsilane [27].

The idea behind using alkylsilanes where 'n' is greater than twelve works well because very good repellent coatings can be produced by using small concentrations of the alkylsilane [27]. In experimental research, a great number of silanated additives for the purpose of increasing the hydrophobicity of the coating. Mahltig and Böttcher [24] based some of their research on using two varieties of silanated and, for comparison purposes, one fluorinated compound as additives to a pure silica sol. The two silanated varieties

used were alkyltrialkoxysilanes, with different alkyl chain-lengths, and hydrophobic polysiloxanes derivatives, as shown in **Table 2.2** [24]. The chemical structures of the polysiloxane derivatives as well as the fluorinated compound (denoted TF) can be seen in **Figure 2.16**.

Table 2.2 Silanated Compounds Used as Hydrophobic Additives [24]		
Alkyltrialkoxysilanes	Hydrophobic Polysiloxane Derivatives	Fluorinated Compound
C1 - Methyltriethoxysilane	Polysiloxane T1	TF - Triethoxytridecafluorooctylsilane
C4 - Iso-Butyltriethoxysilane	Polysiloxane T2	
C8 - Octyltriethoxysilane	Polysiloxane T3	
C16 - Hexadecyltriethoxysilane		
C6 - Phenyltriethoxysilane		

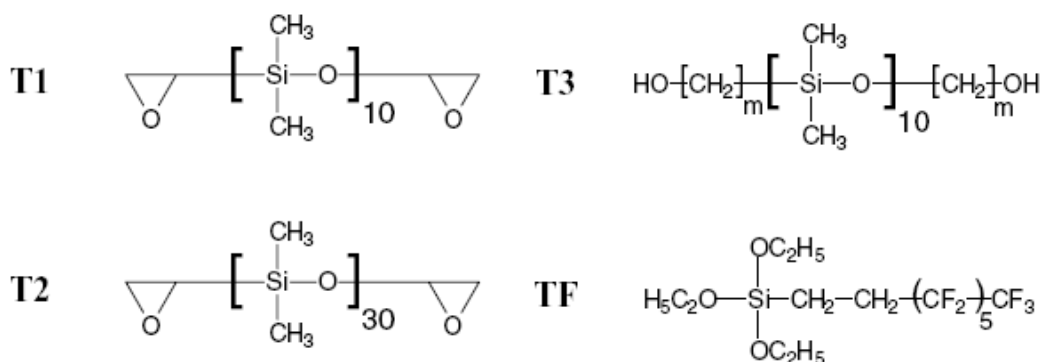


Figure 2.16 Chemical Structures of Polysiloxane Derivatives T1, T2, and T3, and Fluorinated Compound TF [24].

Depending on the goal of the research and the substrate being treated, a large amount of additives can be used for hydrophobic treatments. The majority of researchers have worked to create hydrophobic treatments on glass, wood, or textile substrates. For

hydrophobic modification of textiles, Textor et al. [52] used tridecafluoro-1,1,2,2-tetrahydrooctyltriethoxysilane. Their work was on the surface modification of technical polyester fabric and glass fiber fabric, both with hydrophobic additives and epoxy crosslinking agents [52]. Daoud et al. [13] chose to prepare their hydrophobic coating with hexadecyltrimethoxysilane (HDTMS) as an additive, as well as a crosslinking agent on cotton fabric. On other substrates, researchers chose to use more fluorinated additives for hydrophobicity. To create water-repellent coatings on glass, Yoneda and Morimoto [58] chose to use perfluoroalkyl isocyanine silane for its good mechanical durability. Similarly, Mondea et al. [31] worked with glass, but chose to use a polyfluoroalkylsilane (triethoxy[4, 4-bis(trifluoromethyl)-5,5,6,6,7,7,7-heptafluoroheptyl]silane) for water-repellent coatings. Mai and Militz [29] used a variety of additives to impregnate and create hydrophobic coatings on wood substrates. They worked with 3,3,3-trifluoropropyltrimethoxysilane (TFPTMOS), 2-heptadecafluorooctylethyltrimethoxysilane (HFOETMOS), and decyltrimethoxysilane (DTMOS) [29]. Also working with wood, Donath et al. [14] used two proprietary oligomeric silane systems under the trade names Dynasytan® HS 2909 and Dynasytan® F 8815 to impart hydrophobic properties.

Some researchers chose to further modify their coatings with silanated crosslinking agents. Though it is not a compulsory component to achieve maximum hydrophobicity, they can increase the durability of the coating. Among the options, there are epoxy-functional crosslinkers that some researchers have chosen to use. Mahltig and Böttcher [24] added a co-condensed crosslinkable 3-glycidoxypropyl triethoxysilane (GLYEO) to

crosslink their silica sol. They conjectured that the GLYEO functions to form covalent bonds with the textile surface and the inorganic coating, which helps to enhance washfastness [24]. Similar to this research, Nakagawa [33] used 1,4-bis(trimethoxysilylethyl)benzene (BTB) to assist in the creation of alkaline-resistant and water-repellent thin films on stainless steel and silicon wafers. They estimated that the ethyl groups near the siloxane bonds and three-dimensional BTB polymer network helped to protect and/or prevent OH⁻ groups from breaking siloxane bonds [33]. Daoud et al. [13] used 3-glycidoxypropyltrimethoxysilane (GPTMS) as a crosslinker in their research. Textor et al. [52] did not specifically add a separate crosslinker when preparing sols. To their silica sols created from GPTMS, they added 1-methylimidazol as an agent to catalyze the crosslinking of the epoxy groups on the GPTMS [52]. In the creation of their hydrophobic coatings, a secondary sol was prepared from n-propyl trimethoxysilane by partly hydrolyzing 1 mol of the silane with 1.5 mol 0.01 M HCl for at least 5 hours.

2.7.3. Preparation of Coatings

The work done to prepare these coatings is essentially identical to the work done to create the normal sol-gel coatings (**Section 2.6.2**), though slightly modified. Similar to their silica sol, Mahltig and Böttcher [24] were also able to produce a modified silica sol, containing a crosslinker, by combining 43 mL of TEOS, 12 mL of 0.01 N hydrochloric acid (HCl), 50 mL of 96% ethanol, and 4 mL of 3-glycidoxypropyl triethoxysilane (GLYEO or GPTMS), again stirring for 24 hours at room temperature. Again, in Daoud et al.'s [13] research, sols were also prepared with TEOS (98%), GPTMS (97%) and HCl in 99.8% ethanol at a molar ratio of 1:0.118:0.008 of TEOS:GPTMS:HCl. However, the

process was modified with the additive HDTMS [13]. The HDTMS was added at 10% by weight of the TEOS [13]. Half of the amount (5%) was added to the sol and the mixture was stirred for 6 hours before the other half was added and stirred for an additional 18 hours at room temperature [13]. Textor et al. [52] created their coating by pre-hydrolyzing GPTMS with 1.5 mol of water (0.01 mol HCl), stirring for at least 2 hours to build the base sol. The addition of the crosslinker was done immediately, in an undisclosed amount, before the coating of the textile material [52]. Though the preparation of these coatings is done in a slightly modified manner, the coating and finishing techniques use are the same as in **Section 2.6.3**.

Pipatchanchai and Srikulkit [38] took a unique approach to creating their water-repellent coating, though they used materials not uncommon to textile and sol-gel processing. Their starting materials consisted of Aerosil[®] 200 silica nanoparticles (a material used in this research), glacial acetic acid, HDTMS, and Triton X-100 non-ionic surfactant [38]. Two padding solutions were prepared, the first being made up of a set weight percentage of silica nanoparticles and water, sonicated in an ultrasonic bath for 30 minutes. After the bath was created, fabric was padded through at a set pressure and oven-dried at 60°C. A second bath was prepared of HDTMS, varied from 1.3-5%, in a bath of 0.02% X-100 in water with a pH between 3 and 4, adjusted with acetic acid.. The solution was sonicated in an ultrasonic bath for 5 minutes. The dry samples padded with solution 1 were again padded in solution 2 to a wet pick-up of 70%. The samples were placed into a plastic bag and batched at room temperature for 24 hours. This allows the condensation

reaction to occur on the silica particle surface. The fabrics were finalized by washing to remove residual surfactant and allowed to air dry [38].

El Ola et al. [16] carried out a sol-gel style polymerization by combining their AEM5700 chemical (a 3-(trimethoxysilyl)propyldimethyloctyldecyl ammonium chloride) and de-ionized water. The mixture was brought to pH 4 with glacial acetic acid at ambient temperature. Polyester fabric was padded through the solution to a wet pick-up of 100%. Excess water was evaporated in an oven and polymerization was carried out at 70°-140° for 30 minutes [16].

2.7.4. Performance of Coatings

Since literature details work done with fluorinated and non-fluorinated additives, the coatings can be considered hydrophobic, oleophobic, or both. In most cases, because of the nature of the additives, fluorinated coatings will be more hydrophobic than their non-fluorinated counterparts. In addition to being strongly hydrophobic, the fluorinated coatings also have the advantage of being oleophobic as well. Mahltig and Böttcher [24] worked with a number of hydrophobic additives and concluded that the non-fluorinated additives (hydrocarbon repellency only) were only effective at a chain length of no less than 8. They showed that contact angles between 112° and 135° could be achieved with the additive octyltriethoxysilane in the sol containing the crosslinker and the sol without the crosslinker [24]. These results are represented graphically in **Figure 2.17**. In this graph, **sol 1** is prepared without a crosslinking agent and **sol 2** is prepared with a crosslinking agent. The coatings were prepared on a polyamide fabric and a

polyester/cotton blended fabric; the results were compared to the same coating on a piece of glass.

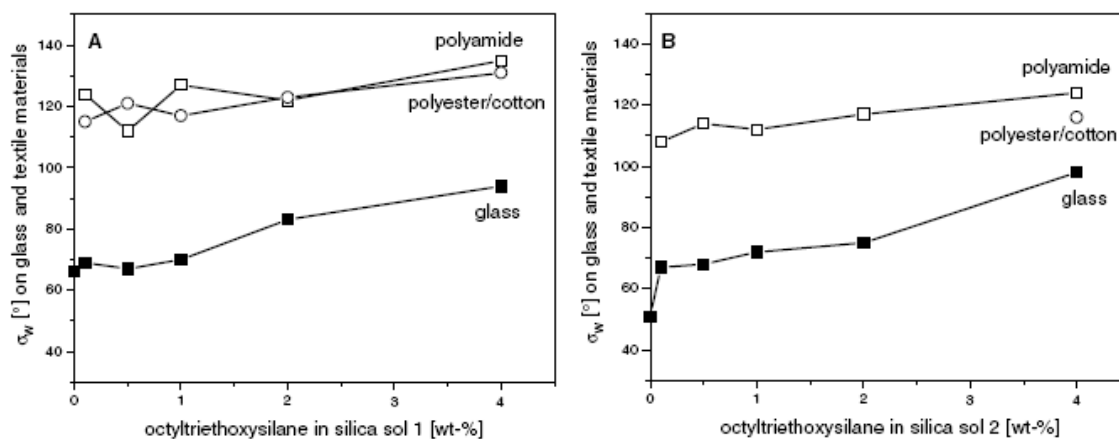


Figure 2.17 Contact Angle of Water (σ_w) of Sol 1 (left) and 2 (right) with Added Octyltriethoxysilane After Coating on Glass and Textile Fabric [24].

As can be seen with **sol 2**, the hydrophobic behavior of the textile decreases with the addition of the crosslinking agent. The coating prepared with **sol 2** on the polyamide fabric had measurable contact angles between 108° and 124° , compared to angles between 124° and 135° with coatings prepared with **sol 1** [24]. This effect was attributed to the presence of the compound 3-glycidyloxypropyltriethoxysilane (GLYEO) in **sol 2**, which they claim to make the coatings more hydrophilic. An interesting point to note is that only at 4 wt.% addition of octyltriethoxysilane was there a measurable contact angle of 116° on the polyester/cotton fabric [24]. Mahltig and Böttcher's [24] work reinforces the fact that the hydrophobicity of coatings does increase with the addition of hydrophobic additives with longer chain lengths of the alkyl groups. They also attributes the fact that coatings prepared with **sol 2** contain the GLYEO crosslinking chemical,

which should lead to a slightly more hydrophilic coating, resulting in a lower contact angle [24]. Since their results lead him to believe that coatings on polyester/cotton fabrics were only effective with 4 wt.% of the additive added, Mahltig and Böttcher [24] prepared a comparative table of contact angles by additive type, shown as **Table 2.3**.

Table 2.3 Contact angles of sols coated on different materials					
(additive concentrations of 4 wt.% in the sol) [24]					
<i>Sol</i>	<i>Additive</i>	σ_w on Glass	σ_{mi} on Glass	σ_w on PA	σ_w on P/C
1	-	66°	46°	N/M	N/M
1	-	51°	41°	N/M	N/M
1	C1	70°	46°	112°	121°
1	C4	74°	48°	117°	123°
1	C8	94°	43°	131°	135°
1	C16	100°	53°	135°	142°
1	C6	71°	43°	121°	120°
2	C1	54°	38°	115°	N/M
2	C4	66°	42°	109°	108°
2	C8	98°	49°	124°	116°
2	C16	101°	44°	130°	131°
2	C6	72°	46°	96°	108°
1	T1	102°	29°	122°	118°
1	T2	91°	44°	122°	128°
1	T3	99°	52°	126°	120°
1	TF	104°	62°	128°	138°

where: PA represents polyamide fabric, P/C represents polyester/cotton fabric, N/M represents a non-measurable value, and σ_{mi} represents the contact angle of methylene iodide (CH_2I_2).

In this table there are no columns representing the contact angle of methylene iodide on either of the fabric types because they do not have sufficient oleophobic properties and therefore a measurable contact angle could not be obtained [24]. The coatings C1-C16 had no effect on the oleophobic properties of the coating [24]. The polysiloxane coatings T1-TF had some effect, but not enough to be considered oleophobic. Tests with

methylene iodide gave a contact angle of 29° on T1 and as 62°, the highest measured value, for TF [24].

Mahlting and Böttcher [24] also evaluated the water uptake and washfastness of their coatings. As a control, they determined that the submersive water-uptake of the polyester/cotton fabric led to an increase in weight of 157% [24]. Further work was done with unmodified **sol 1** and **2** to determine that water uptake was reduced to 109% and 92%, respectively [24]. Finally, they concluded that with the addition of 4 wt.% of the C16 additive that the water uptake could be further reduced to values of 17% (in **sol 1**) and 12% (in **sol 2**) [24]. To better simulate customary conditions, like rain, Mahlting and Böttcher [24] also performed a spray-test evaluation. They concluded that the weight increase due to the uptake of water could be reduced from 99% with the untreated polyester/cotton fabric to about 5% with the addition of 4 wt.% of the C16, T2 and TF additives, making these fabrics suitable for applications such as rain protection [24].

Mahlting and Böttcher [24] also evaluated washing fastness properties of the coatings on polyester/cotton fabrics and determined that only the C16, T2, and TF additives resisted washing enough to maintain their hydrophobicity. However, to simulate ironing, they annealed all washed samples for 1 hour at 120°C to discover that this process brought back the hydrophobic nature of all coatings [24]. Due to these findings, Mahlting and Böttcher [24] were led to believe that the addition of the GLYEO crosslinking agent did nothing to increase the washfastness of the coatings.

Daoud et al. [13] also looked to measure the contact angle of water on their substrates, as well as the durability to washing, surface roughness, water uptake, and change in physical

properties due to the coating. Their knit cotton substrate achieved a final contact angle of 141°, compared to 0° for the uncoated substrate [13]. A comprehensive list of water repellency and water uptake properties from Daoud et al.'s [13] research is shown in

Table 2.4.

Table 2.4 List of Coating Properties and Effect of Washing [13]		
<i>Knit Substrate:</i>	<i>Before Coating</i>	<i>After Coating</i>
Contact Angle	0°	141°
Contact Angle After 30 Washings	-	105°
Water Uptake	170%	3%
Water Uptake After 30 Washings	-	17%
<i>Woven Substrate:</i>	<i>Before Coating</i>	<i>After Coating</i>
Contact Angle	0°	135°
Contact Angle After 30 Washings	-	104°
Water Uptake	120%	5%
Water Uptake After 30 Washings	-	20%

The effectiveness of the chosen crosslinker, GPTMS, is the reason Daoud et al. [13] believes the coatings were so durable to the washing cycles. As can be seen from the table, the coatings maintained the majority of their integrity after washing. Though the values for contact angle did decrease, they are still over 90° and are therefore still hydrophobic.

In observing the samples, Daoud et al. [13] noted that compared to the relatively smooth, uncoated appearance of cotton under an electron microscope, the coated fabric appeared rough and grainy, with a surface roughness of about 30-70 nm; under further magnification, the grains appeared to be spheres with a diameter of about 75 nm [13]. Finally, the physical properties of the fabrics were examined to see what overall effect the coating had. The results from the physical testing can be seen in **Table 2.5**.

<i>Property</i>	<i>Parameter</i>	<i>Before Coating</i>			<i>After Coating</i>		
		<i>Weft</i>		<i>Weft</i>	<i>Weft</i>		<i>Warp</i>
Tensile	Length at Maximum Load (mm)	15.9		8.6		15.5	8.4
	Maximum Load (kg*m/s ²)	666.4		401.3		574.6	346.2
	Strain (%)	21.1		11.4		20.7	11.1
Bursting	Pressure (kg/cm ²)		7.2			7.5	
Tearing	Mean Force (kg*m/s ²)	166.4		142.9		161.7	138.2
Permeability	Air Resistance (kPa*s/m)		0.36			0.33	

We can gather from the table that though there was a decrease in almost every physical property, the changes were very slight. Daoud et al. [13] points out that the slight increase in the bursting strength came at a cost of a <5% decrease in the tensile strength. All other properties were comparable to the point where the change would most likely go unnoticed.

Textor et al. [52] reported a number of findings about the effect of the GPTMS modified sols on the properties of polyester fabric. Though they created both hydrophilic and hydrophobic coatings, this literature review will only focus on the hydrophobic coatings. The sol made with tridecafluoro-1,1,2,2-tetrahydrooctyl triethoxysilane was able to achieve a contact angle of up to 95° with as little as 1-2% added to the sol [52]. They also tested the oil resistance of the fabric, achieving a repellency grade of “satisfactory” (grade 4), which was much improved over the “unsatisfactory” (grade 0) rating of the unfinished fabric [52]. Textor et al. [52] also noted that the sol gave the fabrics a clear,

but distinctively yellow shade, a slightly increased tensile strength, slightly increased stiffness, and a decreasing wrinkle recovery angle.

Yu et al. [59] reported results of their fluorochemical treated fabric as being successfully hydrophobic and oleophobic. This was done with both objective contact angle measurements and subjective AATCC repellency ratings. **Tables 2.6** and **2.7** show the results of Yu et al.'s [59] work.

Table 2.6 Contact Angle of Water and Methylene Iodide on Cotton Substrates [59]						
	<i>Sample:</i>	1	2	3	4	5
H ₂ O		134°	137°	134°	145°	137°
CH ₂ I ₂		125°	125°	119°	131°	125°

Table 2.7 AATCC Repellency of Water and Methylene Iodide on Cotton Substrates [59]						
	<i>Sample:</i>	1	2	3	4	5
H ₂ O		3	3	3	4	3
CH ₂ I ₂		4	4	4	5	4

Yu et al. [59] noted that the only distinction between the samples (1 through 5) was the size of the silica nanoparticles. Though there was not a significant difference between the contact angles achieved on the samples, the differences could certainly be attributed to the nanoparticle sizes ranging from 115.4 nm to 198.4 nm [59].

Pipatchanchai and Srikulkit [38] found that because of the nature of Aerosil[®] particles is to agglomerate in and out aqueous dispersions that it was necessary to sonicate the baths in order to break up the agglomerates and better disperse the particles. In doing so, and when applied to fabric, the particles sizes and microagglomerates stayed small enough to

be invisible to the naked eye [38]. **Table 2.8** shows Pipatchanchai and Srikulkit's [38] results regarding contact angles of treatments and the resulting washfastness ratings.

Table 2.8 Surface hydrophobicity and durability evaluation of hydrophobic fumed silica coatings on woven cotton fabrics [38]				
HDTMS wt. %	Fumed Silica wt. %	<i>Water Contact Angle</i>		
		Before Wash	5 Wash Cycles	10 Wash Cycles
1	0	114.0	112.6	110.4
3	0	115.2	112.6	110.8
5	0	115.6	113.4	110.0
1	1	118.8	118.4	117.6
3	1	120.2	118.6	117.4
5	1	121.0	119.6	118.8
1	3	120.0	118.8	118.2
3	3	121.2	118.6	117.4
5	3	121.6	120.2	118.6
1	5	120.6	120.0	116.4
3	5	120.6	120.2	117.4
5	5	121.6	121.2	117.2

As can be seen by **Table 2.8**, the addition of HDTMS to the system does not significantly increase the contact angle that can be achieved. However, it is plain that the addition of fumed silica does add to the hydrophobicity of the system. It is also evident that only a small addition of fumed silica is needed to create a contact angle increase. A 1 wt. % addition of fumed silica is enough to increase the contact angle of 1 wt.% HDTMS upon fabric almost 5°. Upon investigation with FTIR, the analysis showed strong Si-O absorption bands after washings, indicating that the treatment is durable to washing [38].

2.8. Testing Methods Relevant to Water Repellent Textiles

As in all disciplines of physical science and materials processing, it is essential to have a clear set of testing methods to ensure the outcome of what was done was as desired or to

gain insight into the unknown. There are a number of tests most common to water repellent textiles and wet-processed textile in general that will be useful to evaluate the performance of the finished goods and the process in which they were produced. Some researchers find it valuable to test the mechanical properties of the fabrics before and after processing to ensure there have been no detrimental losses in strength or other properties due to the chemical treatment.

2.8.1. Contact Angle Measurement

Perhaps the most common method of measuring water repellency on a small scale is done by measuring the contact angle of a liquid on the textile surface. The significance of the measurements was delineated in **Section 2.3.1**. In measuring contact angle in their various papers, Mahltig et al. [24][23] used a device by Surf tens (OEG GmbH, Germany). their tests were done with water (σ_w) and methylene iodide (σ_{MI}). Measurements were performed 20 seconds after the drop was placed on the textile substrate. Any non-repellent substances took less than 20 seconds to absorb the liquid and did not have measurable values [24][23]. Daoud et al. [13] measured contact angle using a Tante c contact-angle meter 60 seconds after the drop was placed on the textile substrates. Mondea et al. [31] used the device in **Figure 2.18** to measure contact angles and the contact angle, θ , was derived from the θ_a (advancing contact angle), θ_r (reducing contact angle), and **Equation (2.12)**.

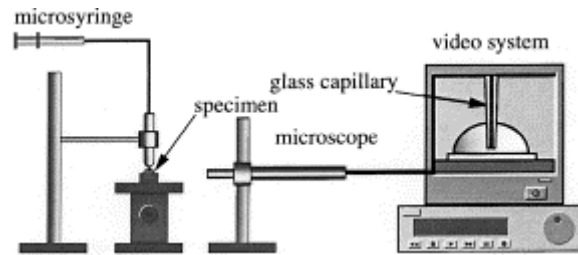


Figure 2.18 Apparatus for Measuring Contact Angle [13].

$$\cos \theta = \frac{\cos \theta_s + \cos \theta_r}{2} \quad (2.12)$$

Textor et al. [52] chose to measure the contact angle of water on their substrate with a Krüss G40 measuring system. They also followed the TEGEWA test to investigate the drop penetration behavior of distilled water on the textiles [52]. Yu et al. [59] did contact angle tests with water and oil using an automatic video contact-angle testing apparatus (Dataphysics). The test was completed by applying 3 μL of the test liquid to the fabric, waiting 20 seconds, and finally measuring the contact angle with the video camera system [59]. Pipatchanchai and Srikulkit [38] did water contact angle measurements using a contact angle meter (protractor), performed 20 seconds after the drop was placed on the fabric surface. In their work, Pilotek and Schmidt [37] determined contact angles by variation of the drop volume on a Krüss GII. They also performed a unique tilt-angle test. This tilt-angle was determined by using an apparatus that tilts a substrate with a drop of liquid until the drop moves. The apparatus stops and the respective angle can be read. Liquids of different surface tensions can be made using appropriate mixtures of

acetone and water. The surface tension of each mixture can be determined by a tensiometer (Krüss).

2.8.2. Water Repellency Under Customary Conditions

There are a small number of tests that are used to test how effectively textile substrates repel water under customary conditions. That is to say, these tests attempt to recreate circumstances that the textiles will face during normal, everyday use. Mahltig et al. [24][23] used two tests, the first of which was done to determine water uptake of textiles under full contact with water. A 10 cm x 10 cm sample was taken and placed them in 300 mL of water for 60 seconds. The sample's mass was taken with a balance and compared with the dry, original sample. The second method was a rain (spray) test, in AATCC styling; this test was also adopted by Daoud et al. [13]. A 20 cm x 20 cm sample was set at a 45° angle at a 16 cm distance. Then, 250 mL of water was sprayed on to the sample over a 30 second period. Again, the mass was taken and compared to the original [24][13][23].

2.8.3. Testing for Washfastness

In making functional textile coatings, it is extremely important to ensure that the coatings will not be compromised when laundered. There are scientific and controlled methods that can be employed to simulate repeated launderings in a laboratory environment. Mahltig et al. [24][23] investigated leaching behavior at 40°C using a thermostatic dissolution tester PTWS3 (Pharma Test, Germany) with a paddle stirrer. The washing solution used was a 1% aqueous solution of sodium lauryl sulfate of pH 7. Leaching was done for 2 hours and then samples were rinsed thoroughly with water and air-dried at

room temperature. Contact angles were measured after the samples had dried completely. After the taking the contact angles (done with water) were measured, the samples were annealed at 120°C for 1 hour to simulate ironing and subjected again to contact angle measurements [24][23]. Daoud et al. [13] used a similar test in a different apparatus. Their test was done in an Atlas Launder-Ometer at 49°C in 1.2 L stainless-steel lever-lock canisters. The substrates were leached in a 200 mL of 0.15% of sodium lauryl sulfate with 50 steel balls for 45 minutes. This is the equivalent of 5 washing cycles, in the style of AATCC Test Method 61-1996. After laundering, the samples were rinsed thoroughly, dried at room temperature and then tested for contact angle (water) [13]. Pipatchanchai and Srikulkit [38] also followed AATCC Test Method 61-2001, using a Gyrowash laundering machine at 40°C in a 500 mL canister. The fabric was leached in 200 mL of 0.37% AATCC standard reference detergent.

2.8.4. Analyzing Surface Morphology

Substrate surface analyzation, though a qualitative observation, can be a very useful method of process control. Different forms of microscopy and other analytical techniques can give a visual approximation of particle dispersion on the surface of a textile substrate or insight as to how the surface was modified. Daoud et al. [13] and Pipatchanchai and Srikulkit [38] analyzed the surface morphology of their substrates using field-emission scanning electron microscopy (Jeol, Tokyo, Japan), Daoud et al.'s [13] work done at a 3 kV acceleration voltage. **Figure 2.19** shows the surface morphology of Pipatchanchai and Srikulkit's [38] samples. Sample (a) is an uncoated

fiber surface at 20,000x, (b) is a fiber surface coated only with HDTMS at 20,000x, and (c) shows a fiber surface coated with silica at 60,000x [38].

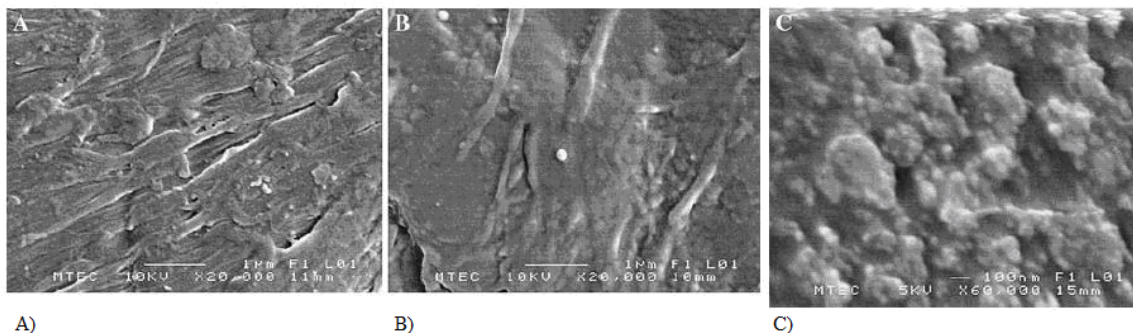


Figure 2.19 A) Uncoated Sample, B) HDTMS Coated Sample , and C) Silica Coated Sample [38].

Yu et al. [59] and Mahltig et al. [23] also used a scanning electron microscope to analyze surface morphology. Pilotek and Schmidt [37] analyzed and measured surface roughness with both a Collotec Nanosurf 500 profilometer and an atomic force microscope.

2.8.5. Additional Test Methods

Many researchers have tests that they feel are important and enable them to better analyze their process and product when performing experiments. Creating a functional coating on a textile substrate usually demands wet processing. These processes use chemicals and interact heavily with the fibers in the substrate. As such, of the most important needs is for the textile to retain (or stay very close to) its original mechanical properties. Daoud et al. [13] felt it important to test three of a textile substrate's most common tensile properties. They subjected their finished and original fabrics to three ASTM test methods: Standard Test Method for Breaking Force and Elongation of Textile Fabrics

(Strip Method), ASTM Designation D5035-95; Standard Test Method for Hydraulic Bursting Strength of Textile Fabrics-Diaphragm Bursting Strength Tester Method, ASTM Designation D3786-01; and Standard Test Method for Tearing Strength of Fabrics by Falling-Pendulum Type (Elmendorf) Apparatus, ASTM Designation D1424-96 [13].

Daoud et al. [13] also saw fit to compare the air permeability of the finished goods to the unfinished using an air permeability tester (Kato Tech Co., Kyoto, Japan). Constant air flow was generated and passed through specimens and resistance was measured by loss of air pressure [13].

Since silica nanoparticles have been used in similar research experiments to improve the wear-resistance of glass-fiber and other fabrics, Textor et al. [52] used a Martindale Abrasive test to determine the effects of the treatment on wear-resistance. Their climatized fabrics were scrubbed radially over a defined testing fabric. After 5,000 cycles, the samples were visually inspected [52].

Yu et al. [59] took a different route to inspect the repellent properties of their fabrics. They measured them according to test methods 3M-II-1988 and AATCC TM 118-2002. The ratings given to fabrics were the highest numbered test liquid that will not wet the fabric within a period of 10 seconds (for water) and 30 seconds (for oil) [59]. Yu et al. [59] were also able to measure nanoparticle sizes in the sol with a Zetasizer Nano ZS particle sizer and a Zeta potential analyzer.

Mahltig et al. [23] implemented a test that allowed them to determine the amount of silicon deposited on the fabrics. The samples were leached in NaOH_{aq} and the amount of silicon in the leaching solution was measured by Inductively Coupled Plasma

Spectroscopy (ICP) (Zeiss, Jena) [23]. Pipatchanchai and Srikulkit [38] also sought to determine silica concentrations on their fabric. However, their approach was to use Fourier Transform Infrared Spectroscopy (FTIR) (Perkin Elmer FR-2000) as opposed to chemical methods.

Chapter 3: Methodology and Experimental Procedure

3.1. The Approach of this Research and its Advantages

The approach of this research is to use silica nanoparticles and mixed silanes

(hydrophobic alkyltrialkoxysilanes and crosslinkable silanes) to treat cotton and other fabrics to obtain durable non-fluorine water-repellent surfaces. The main objective is to obtain a fabric finishing technology that has the advantages of:

1. High water contact angle,
2. Excellent durability, and
3. Easy processability.

After initial treatment, the coatings were also tested for durability, by attempting to disturb the coating and retesting the coating's ability to repel water.

To complete this research, silica nanoparticles and mixed silanes were first used to surface-treat 100% cotton fabrics to obtain durable water-repellent surfaces. In this work, fumed silica was used as a nanoparticle material to improve the roughness and durability of water-repellent surface. This effect is achieved using said particles because of their small diameter (<20 nm) and ability to form a large amount of covalent bonds, about 800 bonds per particle at a diameter of 10 nm. Increased surface roughness is known to increase contact angle on material surfaces through the lotus effect (refer to **Section 2.2.2**). The ability to form a large amount of covalent bonds not only helps the silica particles to be strongly attached to the fabric surface, but it also provides the opportunity to grow more hydrophobic surface chains. Long chain alkyltrialkoxysilanes (such as n-decyltriethoxysilane) will be used to provide water repellency through a non-polar

repulsion of polar liquids. Crosslinkable silanes (i.e., TMOS and TEOS) were used in our work as crosslink centers to improve the durability of water-repellent finishing.

Figure 3.1 shows a simplified attachment mechanism of the chemicals to the 100% cotton surface.

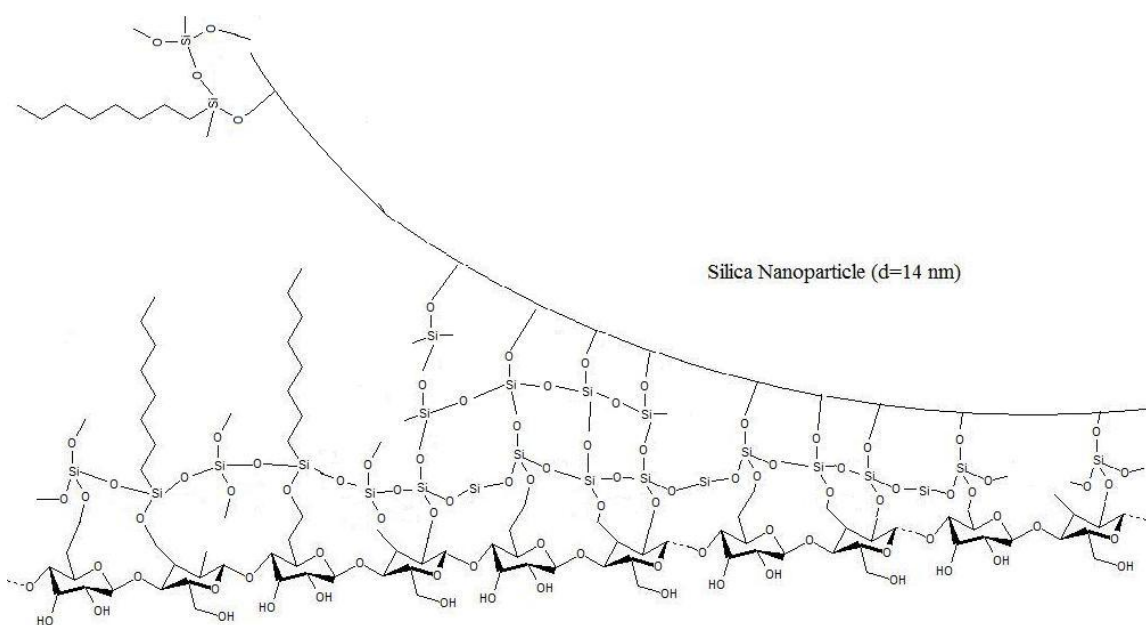


Figure 3.1 Simplified Attachment of Chemical Treatment to Cellulose.

This picture is, of course, not a perfect representation nor is it perfectly to scale. It does, however, give a working representation of the treatment at the molecular level. The overall scale of the picture is in order, where the diameter of the silica nanoparticle (in this case, 12nm, the same as Aerosil[®] 200) is on the order of eight times the length of the hydrophobic additive (shown here to be n-octyltrimethoxysilane). To get a better overall macroscale picture of the treatment, refer to **Figure 3.2** below.

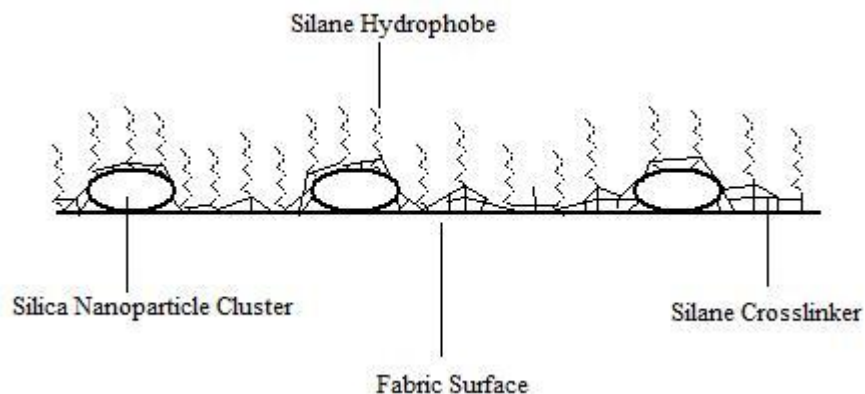


Figure 3.2 Macroscopic Attachment of Chemical Treatment to Cellulose.

Again, this picture is idealized and not to scale. It does give a better idea of the actual attachment of the treatment to a cellulosic fabric. Silica nanoparticles do not attach to the fabric as single particles; rather they attach in clusters at random intervals. It is possible that the hydrophobic additives or the silane crosslinkers will attach directly to the fabric surface, as shown above. The crosslinkers work to form a three-dimensional network between particle clusters and hydrophobic additives. The attachment of the hydrophobic additives to surface of the fabric through direct bonding and through the crosslinkers (essentially as an extender) and on top of the silica nanoparticles help to give an uneven and rough surface which gives better repellency. A three-dimensional “forest” of crystallized, long hydrocarbon chains is created and as a result acts as the hydrophobic intermediary between water and the surface of the fabric. In addition to cotton fabric, the feasibility of using silica nanoparticles and mixed silanes on other fabrics (such as nylon, polyester, and wool) was also investigated.

3.2. Experimental Procedures

3.2.1. Creation of the Design of Experiments

A number of chemicals were purchased at the beginning of this research project as possible candidates for the design of experiments (DOE). The chemicals fell into three categories: hydrophobic additives, silane crosslinkers, and silica nanoparticles. **Table 3.1** shows the original chemicals purchased for research. A description of the chemicals in **Table 3.1** can be found in **Section 3.2.3.1**.

Table 3.1 List of Chemicals Used in Experimental Procedures		
Hydrophobic Additives	Silane Crosslinkers	Silica Nanoparticles
n-Octyltrimethoxysilane	Tetraethoxysilane	Aerosil [®] 90
n-Decyltriethoxysilane	Tetramethoxysilane	Aerosil [®] 150
n-Octadecylmethyldimethoxysilane	Bis(triethoxysilyl)ethane	Aerosil [®] 200
	Bis(trimethoxysilyl)ethane	Aerosil [®] 380
	Bis(trimethoxysilyl)hexane	Aerosil [®] R805
	1,4-Bis(trimethoxysilyl)ethylbenzene	

Due to reasons outlined in **Section 4.3**, bis(triethoxysilyl)ethane, bis(trimethoxysilyl)hexane, and 1,4-bis(trimethoxysilyl)ethylbenzene were deemed unfit to continue in the research. This change led to the creation of a DOE containing the three hydrophobic additives, the three remaining silane crosslinkers, and the five types of silica nanoparticles. **Table 3.2** shows the original design.

Tetraethoxysilane	n-Octyltrimethoxysilane	Aerosil® 90
		Aerosil® 150
		Aerosil® 200
		Aerosil® 380
		Aerosil® R805
	n-Decyltriethoxysilane	Aerosil® 90
		Aerosil® 150
		Aerosil® 200
		Aerosil® 380
		Aerosil® R805
	n-Octadecylmethyldimethoxysilane	Aerosil® 90
		Aerosil® 150
		Aerosil® 200
		Aerosil® 380
		Aerosil® R805
Tetramethoxysilane	n-Octyltrimethoxysilane	Aerosil® 90
		Aerosil® 150
		Aerosil® 200
		Aerosil® 380
		Aerosil® R805
	n-Decyltriethoxysilane	Aerosil® 90
		Aerosil® 150
		Aerosil® 200
		Aerosil® 380
		Aerosil® R805
	n-Octadecylmethyldimethoxysilane	Aerosil® 90
		Aerosil® 150
		Aerosil® 200
		Aerosil® 380
		Aerosil® R805
Bis(Triethoxysilane)Ethane	n-Octyltrimethoxysilane	Aerosil® 90
		Aerosil® 150
		Aerosil® 200
		Aerosil® 380
		Aerosil® R805
	n-Decyltriethoxysilane	Aerosil® 90
		Aerosil® 150
		Aerosil® 200
		Aerosil® 380
		Aerosil® R805
	n-Octadecylmethyldimethoxysilane	Aerosil® 90
		Aerosil® 150
		Aerosil® 200
		Aerosil® 380
		Aerosil® R805

However, due to further reasons outlined in **Section 4.3**, n-octadecylmethyldimethoxysilane created problems that also made it unfit to continue with. A revised DOE, shown in **Table 3.3**, is the final version used for this research.

Table 3.3 Revised Design of Experiments		
Tetraethoxysilane	n-Octyltrimethoxysilane	Aerosil [®] 90
		Aerosil [®] 150
		Aerosil [®] 200
		Aerosil [®] 380
		Aerosil [®] R805
	n-Decyltriethoxysilane	Aerosil [®] 90
		Aerosil [®] 150
		Aerosil [®] 200
		Aerosil [®] 380
		Aerosil [®] R805
Tetramethoxysilane	n-Octyltrimethoxysilane	Aerosil [®] 90
		Aerosil [®] 150
		Aerosil [®] 200
		Aerosil [®] 380
		Aerosil [®] R805
	n-Decyltriethoxysilane	Aerosil [®] 90
		Aerosil [®] 150
		Aerosil [®] 200
		Aerosil [®] 380
		Aerosil [®] R805
Bis(Triethoxysilyl)Ethane	n-Octyltrimethoxysilane	Aerosil [®] 90
		Aerosil [®] 150
		Aerosil [®] 200
		Aerosil [®] 380
		Aerosil [®] R805
	n-Decyltriethoxysilane	Aerosil [®] 90
		Aerosil [®] 150
		Aerosil [®] 200
		Aerosil [®] 380
		Aerosil [®] R805

A full design was run using three fabric samples for each combination of samples. The results of this design were used to determine which combination of chemicals gave the highest contact angle and therefore which combination(s) of chemicals would be suitable for further investigation.

3.2.2. Procedure After the Design of Experiments

Once all the water contact angle values were obtained from the design of experiments, three samples were chosen to continue investigating. It was decided that the best sample (the one with the highest contact angle) would be chosen from each of the three crosslinkers. The following three chemical combinations were chosen:

- Tetraethoxysilane, n-Decyltriethoxysilane, Aerosil[®] R805;
- Tetramethoxysilane, n-Decyltriethoxysilane, Aerosil[®] 380; and
- Bis(triethoxysilyl)ethane, n-Octyltrimethoxysilane, Aerosil[®] 90.

It was felt that these combinations made a suitable lot for investigation (Refer to **Section 5.3**). Each of the three crosslinkers were represented, both of the hydrophobes were represented, one silica was hydrophobic, and the two hydrophilic silicas chosen represent the opposite ends of the diameter spectrum.

After the chemical combinations were chosen, further work was done to investigate the durability of the fabric to which they were applied. The durability of the finishes was tested using modified AATCC methods to simulate laundering and abrasion (these test methods are outlined in **Section 3.2.7** and **Section 3.2.8**, respectively). After the

respective laundering and abrasion, the samples were measured for water contact angle again for comparative values.

In order to fully demonstrate the advantages of the chemicals chosen for this research, an additional three sets of the three chosen samples were prepared without silica. These were done to mirror those samples made for the durability testing. The samples prepared were:

- Tetraethoxysilane, n-Decyltriethoxysilane, No Silica;
- Tetramethoxysilane, n-Decyltriethoxysilane, No Silica; and
- Bis(triethoxysilyl)ethane, n-Octyltrimethoxysilane, No Silica.

One set of samples was kept unchanged, to compare to the sample's water contact angle values from the design of experiments, one set was subjected to abrasion, and one set was subjected to laundering. All of the sets were measured for water contact angle to compare to their silica-containing counterparts and the samples that were not subjected to either laundering or abrasion.

3.2.3. Chemical Structures and Properties

3.2.3.1. Hydrophobic Additive Structures

- n-Octyltrimethoxysilane, shown in **Figure 3.3**

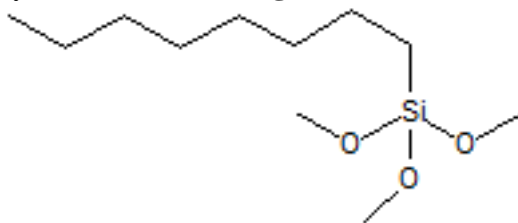


Figure 3.3 Chemical Structure of n-Octyltrimethoxysilane [8].

- n-Decyltriethoxysilane, shown in **Figure 3.4**

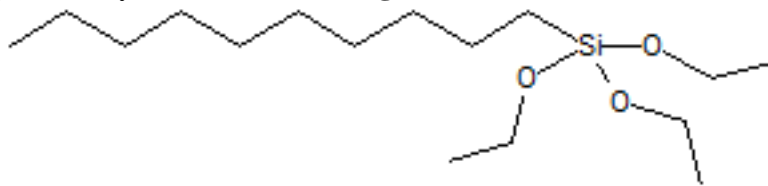


Figure 3.4 Chemical Structure of n-Decyltriethoxysilane [8].

- n-Octadecylmethyldimethoxysilane, shown in **Figure 3.5**

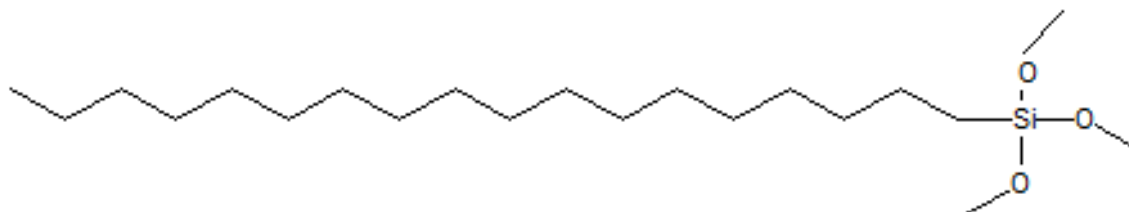


Figure 3.5 Chemical Structure of n-Octadecylmethyldimethoxysilane [8].

3.2.3.2. Silane Crosslinker Structures

- Tetraethoxysilane, shown in **Figure 3.6**

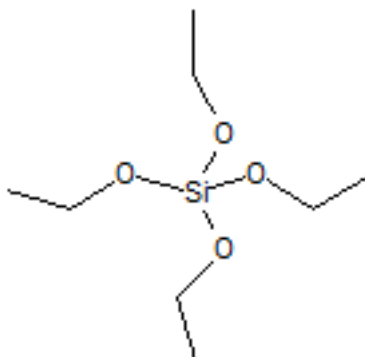


Figure 3.6 Chemical Structure of Tetraethoxysilane [8].

- Tetramethoxysilane, shown in **Figure 3.7**

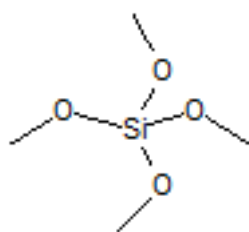


Figure 3.7 Chemical Structure of Tetramethoxysilane [8].

- Bis(triethoxysilyl)ethane, shown in **Figure 3.8**

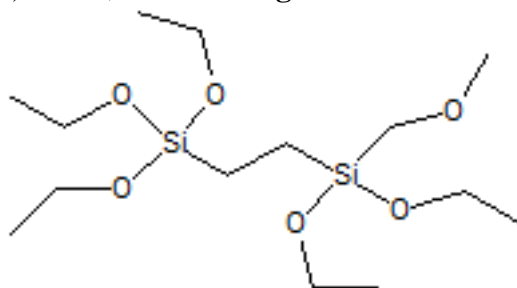


Figure 3.8 Chemical Structure of Bis(triethoxysilyl)ethane [8].

- Bis(trimethoxysilyl)ethane, shown in **Figure 3.9**

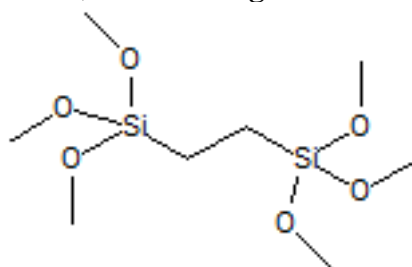


Figure 3.9 Chemical Structure of Bis(trimethoxysilyl)ethane [8].

- Bis(trimethoxysilyl)hexane, shown in **Figure 3.10**

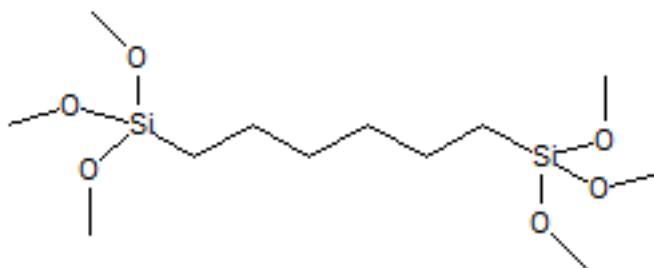


Figure 3.10 Chemical Structure of Bis(trimethoxysilyl)hexane [8].

- 1,4-Bis(trimethoxysilylethyl)benzene, shown in **Figure 3.11**

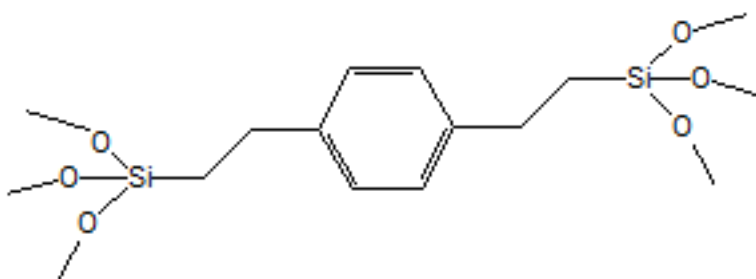


Figure 3.11 Chemical Structure of 1,4-Bis(trimethoxysilylethyl)benzene [8].

3.2.3.3. Silica Nanoparticles

Aerosil[®] silica nanoparticles can be either hydrophilic or hydrophobic and come in a variety of diameters. In the case of this research, four hydrophilic varieties were chosen: Aerosil[®] 90, Aerosil[®] 150, Aerosil[®] 200, and Aerosil[®] 380. The one hydrophobic silica chosen was Aerosil[®] R805. The number denoting the variety of hydrophilic silica denotes its surface area (and therefore its diameter). **Table 3.4** shows the particle diameter and surface area of the particles used in this research.

Silica Type	Particle Diameter (nm)	Surface Area (m²/g)
Aerosil [®] 90	20	90±15
Aerosil [®] 150	14	150±15
Aerosil [®] 200	12	200±25
Aerosil [®] 380	7	380±30
Aerosil [®] R805	12	150±25

3.2.4. Fabric Sample Preparation

A roll of scoured and bleached, 4 oz/yd², plain-woven cotton fabric was obtained from the College of Textiles Pilot Plant. The roll was conditioned in the College of Textiles Physical Testing Laboratory at standard laboratory conditions (i.e. 21.1°C and 65% RH). When needed, 22.86 cm x 22.86 cm samples were cut from the roll for the coating process.

3.2.5. Solution Preparation

Coating solutions were prepared using a modified version of Mahltig and Böttcher's [24] method. The following recipe was used to create the solutions for the design of experiments:

- 86 mL 96% Reagent Grade Ethanol - Sigma-Aldrich Co.
- 24 mL 0.01 N Hydrochloric Acid (HCl) - Sigma-Aldrich Co.
- 20 mL Silane Crosslinker - Gelest, Inc.
- 4 mL Silane Hydrophobe - Gelest, Inc.
- 0.2% on weight of bath (o.w.b.) Aerosil[®] Silica Nanoparticles - Evonik Industries AG (Formerly Degussa GmbH)

The ethanol, hydrochloric acid, silane crosslinker, and silica nanoparticles were all added at the same time and allowed to stir for 24 hours. Two hours before the coating of the fabric, the silane hydrophobe was added and stirring was continued.

3.2.6. Fabric Coating, Drying, and Curing

Fabric coating was done in a 12 in. Linzer Products Corp. paint tray purchased from The Home Depot. The stirred solution was emptied into the tray's reservoir and the 22.86 cm x 22.86 cm samples were manually dipped into the solution. **Figure 3.12** shows how the fabric was passed through the solutions.

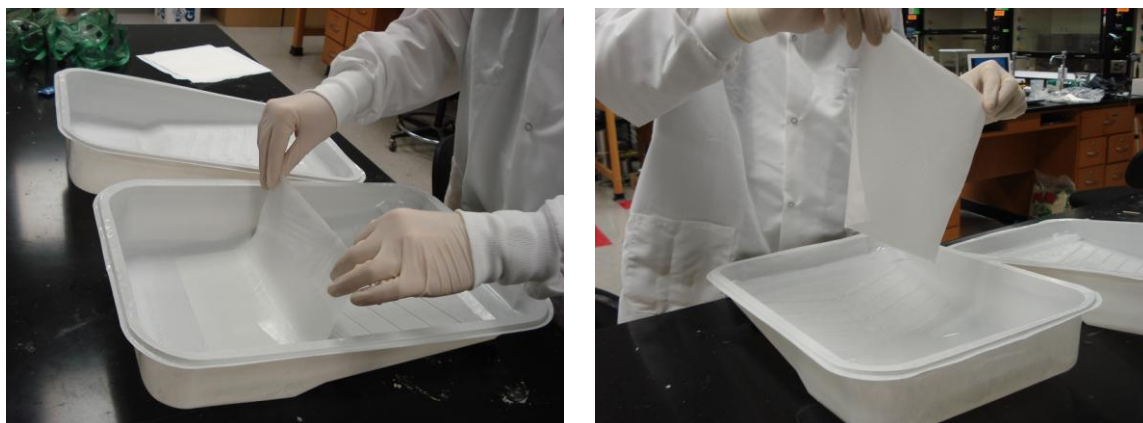


Figure 3.12 Dip-Coating Method and Apparatus Employed in This Research.

To ensure as complete a coating as possible, the fabric was passed through the solution several times. Once dipped, the excess solution was allowed to drain off of the fabric and samples were hung to dry on a self-made drying line, shown in **Figure 3.13**:



Figure 3.13 Line Drying Apparatus Employed in This Research.

After the samples were sufficiently dry, they were cured. Fabric samples were placed into an oven at 100°C for 1 hour. Once cured, fabric samples were set aside until they were tested for water contact angle. After the samples outlined in Section 3.2.2 were chosen, the samples were tested for % solids add-on. Samples were taken from the 22.86 cm x 22.86 cm originals and allowed to condition for 24 hours in at standard laboratory conditions. It was determined by using the following formula:

$$\left(\frac{\text{Dry Wt. of Treated Fabric} - \text{Dry Wt. of Untreated Fabric}}{\text{Dry Wt. of Untreated Fabric}} \right) \times 100 \quad (3.1)$$

that the % solids add-on for the three different sample types was:

- Tetraethoxysilane, n-Decyltriethoxysilane, Aerosil[®] R805: 11.7%
- Tetramethoxysilane, n-Decyltriethoxysilane, Aerosil[®] 380: 7.6%
- Bis(triethoxysilyl)ethane, n-Octyltrimethoxysilane, Aerosil[®] 90: 6.8%

3.2.7. Fabric Sample Laundering (Modified AATCC Test Method)

A modified methodology taken from the AATCC test method 61-2006 [2] was used in the laundering (washing) of finished fabric samples. This test method is an accelerated laundering method that is used to help evaluate the washfastness of fabrics that are expected to withstand frequent laundering. This method simulates the surface changes of a fabric from the detergent solution and abrasive action of five hand or home launderings. A stock solution of 0.15% AATCC standard reference detergent was made from 3.0 L of water and 4.5 g of AATCC standard reference detergent. Portions of the stock solution in 150 mL increments and fifty 6 mm stainless steel balls were dispensed into eighteen Stainless Steel Lever Lock Canisters Type 2 1200 mL. The lids to the canisters and PTFE gaskets were secured onto the canisters. All canisters (without fabric) were loaded into an Atlas LEF Launder-Ometer, which was preheated to 45°C, and run for two minutes to preheat. Samples were cut from the original 22.86 cm x 22.86 cm sample to a test specimen size of 5 cm x 15 cm. The fabric samples were loaded into the preheated canisters and run for forty five minutes. At the end of the laundering cycle, the canisters were emptied and the fabric samples rinsed thoroughly with DI water [2]. The rinsed samples were partially dried by putting them into a Bock CP-8/183 Centrifugal Extractor. The fabric samples were allowed to air dry for 24 hours in laboratory conditions to avoid complications that could arise with drying. Drying them with any amount of heat may or may not have influenced the test results. After laundering, the fabric was kept aside to be tested for water contact angle, as in **Section 3.3.2**.

In order to evaluate the effect of heat drying, selected samples were subjected to an additional heat drying step. This was done at 100°C for thirty minutes to simulate the act of ironing, where the process may help to make the samples more hydrophobic again.

3.2.8. Fabric Samples Made With Ultrasonicated Solutions

To improve the durability of the finish to laundering, additional steps needed to be taken to increase fixation of the finish to the fabric surface. Three sample sets were produced with solutions that were done with an additional ultrasonication step. This was done to further disrupt the silica nanoparticle agglomerates so they could fix more to the fabric surface than to themselves.

This was done by creating the solutions as stated in **Section 3.2.5**. At least two hours after the silane hydrophobes were added to the solutions, the samples were sonicated. This was done by placing the solution jar in an ice bath and placing a ultrasonic wand powered by an Ultrasonic Power Corporation sonicator into the middle of the solution. The sonication was carried out for 30 minutes and the fabric samples were immediately dipped, dried, and cured after the sonication was complete.

3.2.9. Fabric Sample Crocking (Modified AATCC Test Method)

A modified methodology taken from the AATCC test method 8-2005 [1] was used in the crocking (abrasion) of finished fabric samples. Crocking is defined as the transfer of a colorant from the surface of a colored yarn or fabric to another surface or to adjacent area of the same fabric principally by rubbing. This method was adopted to simulate a similar rubbing (abrasion) action that may potentially wear off the applied finish. This method is

perhaps more applicable to this research than something like Martindale or Wyzenbeek abrasion tests, which mainly record cycles to failure and may destroy the fabric rather than test wear of the finish.

Samples were cut from the original 22.86 cm x 22.86 cm sample to an approximate test specimen size of 5 cm x 13 cm. The test specimen was placed on the base of the crockmeter (apparatus used: AATCC Model CM-1 Crockmeter) resting flat on the abrasive cloth with its long dimension in the direction of the rubbing. The specimen holder was placed over the specimen as an added means to prevent slippage. A white test cloth square was mounted over the end of the finger which projects downward from the weighted sliding arm. The cloth square was held in place with the special ring clip with the loops pointing upwards. The covered finger was lowered onto the test specimen and the meter arm was cranked ten times. This was done at a rate of one turn per minute to slide the finger back and forth twenty times. Once the crocking motion was finished, the white test cloth was discarded [1]. After crocking, the fabric was kept aside to be tested for water contact angle, as in **Section 3.3.2**.

3.3. Test Methods

3.3.1. Scanning Electron Microscope Analysis

Field-emission scanning electron microscopy (FESEM) was performed with the help of Roberto Garcia in the Analytical Instrumentation Facility at North Carolina State University (NCSSU). The FESEM was a Jeol model 6400F with EDS attachment. High-resolution field-emission scanning electron microscopy was performed with the help of Bill Roth, senior applications specialist with Hitachi High Technologies, Inc., in

the Analytical Instrumentation Facility at NCSU. The high-resolution FESEM was a Hitachi model S-5500 In-Lens FESEM.

3.3.2. Contact Angle Measurements

Preliminary contact angles on coated cotton fabric were done with an A-100 CA

Goniometer made by Ramé-Hart, Inc. Fabric samples measuring approximately 2.54 cm x 2.54 cm were cut from the coated sample-fabric in three approximate spots, as shown below in **Figure 3.14** (not to scale):

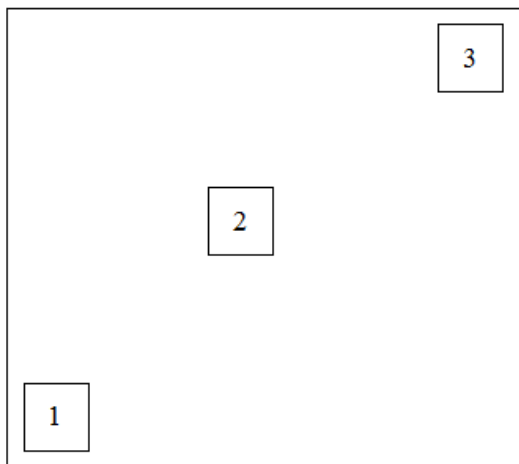


Figure 3.14 Schematic of How Fabric Samples Were Taken for Contact Angle Measurements.

The 2.54 cm x 2.54 cm samples were placed on the sample platform of the goniometer and held in place using scotch tape. It is important that the samples are kept as flat as possible so that readings taken will be accurate. A 2 mL syringe, made by Gilmont Industries, was filled with HPLC (high performance liquid chromatography) water and placed in its holder above the fabric platform. Once the syringe was suspended over the fabric sample, 0.014 mL of HPLC water was dropped onto the fabric (corresponding to

seven notches on the cylinder of the syringe). A Reichert Scientific Instruments No. 610 Illuminator light source was placed directly behind the goniometer to allow for readings to be taken through the scope. The goniometer was physically adjusted so that the fabric was level with the base line. **Figure 3.15** shows both the scope of the goniometer and the goniometer apparatus as a whole.

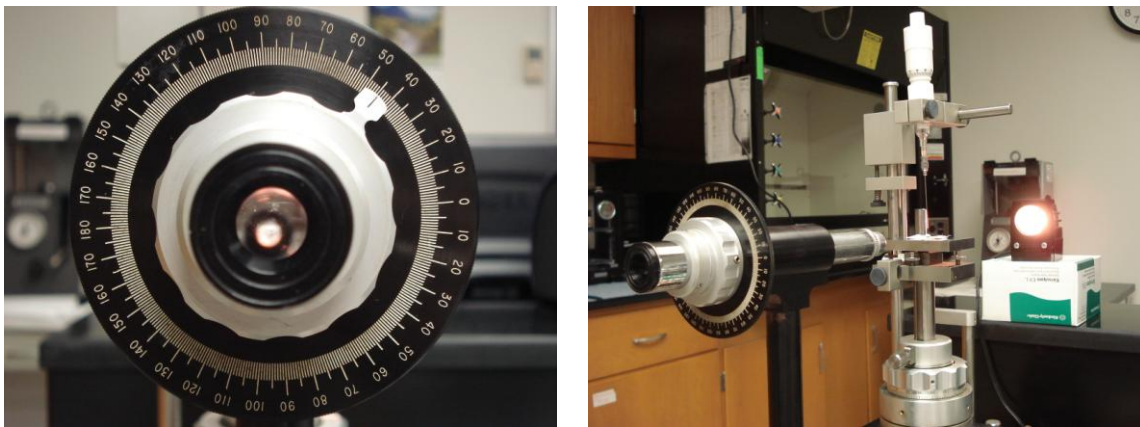


Figure 3.15 a) Goniometer Eyepiece and b) Apparatus Used in Measuring Contact Angle.

Once the drop was placed on the fabric sample, the scope was moved so that the drop was completely viewable through the eyepiece. After the drop was in view, the focus knob was manipulated so that the drop image sharpened and was in focus. The contact angle measurement was taken through the measurement apparatus on the goniometer scope. Two measurements were taken with the apparatus, one on either side of the drop. This was done by aligning and adjusting the knob on the scope's protractor. The second, adjustable line controlled by the knob was placed so that it formed the corresponding

contact angle between the drop and the fabric line. The measurements were recorded and averaged for each fabric type tested.

Chapter 4: Observations and Decisions Regarding Processes, Inputs, and Products

4.1. General observations on 12 preliminary sets of samples with varying amounts of silica o.w.b. and different crosslinking agents

4.1.1. Samples with 0.02% SiO₂ on weight of bath

- Sample: Bis(trimethoxysilyl)hexane, Aerosil[®] 200, n-Octyltrimethoxysilane
 - Sols created with bis(trimethoxysilyl)hexane formed solids rapidly upon contact with water. This made clean-up almost impossible because the solid product adhered to glass and plastic (solution jar and dipping tray) and would not come off.
 - Fabric samples, after coating, became very stiff/inflexible. The fabric felt like and behaves like oak tag paper.
- Sample: Bis(triethoxysilyl)ethane, Aerosil[®] 200, n-Octyltrimethoxysilane
 - Fabric samples, after coating, felt softer in comparison to other treated samples, but were still somewhat stiffer than those without the hydrophobic treatment.
- Sample: Bis(trimethoxysilyl)ethane, Aerosil[®] 200, n-Octyltrimethoxysilane
 - Fabric sample had a similar hand to the bis(triethoxysilyl)ethane sample, but it was perhaps a little less stiff
- Sample: 1,4-Bis(trimethoxysilylethyl)benzene, Aerosil[®] 200, n-Octyltrimethoxysilane
 - Sols created with 1,4-bis(trimethoxysilylethyl)benzene formed solids rapidly upon contact with water. This made clean-up almost impossible

because the solid product adhered to glass and plastic (solution jar and dipping tray) and would not come off.

- Coated fabric sample probably had the stiffest hand of all the fabrics created. The hand was similar to samples made with bis(trimethoxysilyl)hexane, but felt slightly worse.
- Sample: Tetraethoxysilane, Aerosil[®] 200, n-Octyltrimethoxysilane
 - The fabric sample had the softest hand of all fabric samples created and was the least stiff.
- Sample: Tetramethoxysilane, Aerosil[®] 200, n-Octyltrimethoxysilane
 - Sample had softer fabric hand than all other samples but the one created with TEOS. The feel of the fabric was good, but was still slightly stiffer than an uncoated fabric.

4.1.2. Samples with 0.2% SiO₂ on weight of bath

- Sample: Bis(trimethoxysilyl)hexane, Aerosil[®] 200, n-Octyltrimethoxysilane
 - Fabric was very stiff, even more so than the sample containing 0.02% SiO₂. The tenfold increase in silica nanoparticles appeared to make the samples stiffer, perhaps due to the higher degree of surface crosslinking.
 - Solid byproducts created by the sol were created in earnest at this concentration of silica. The creation was so extreme that immovable solids were left on the fabric surface. The appearance of the fabric was that of one with melted plastic in spots on the face and back. The

problems with cleaning the solution were the same as the samples containing 0.02% SiO₂.

- Sample: Bis(triethoxysilyl)ethane, Aerosil[®] 200, n-Octyltrimethoxysilane
 - Fabric was again stiff. It appeared to be stiffer than the sample containing 0.02% SiO₂.
- Sample: Bis(trimethoxysilyl)ethane, Aerosil[®] 200, n-Octyltrimethoxysilane
 - On one of the three samples, a water drop was absorbed into the fabric after about 10-15 minutes.
 - Consistent with other samples, fabric samples were much stiffer with the increased silica percentage.
- Sample: 1,4-Bis(trimethoxysilylethyl)benzene, Aerosil[®] 200, n-Octyltrimethoxysilane
 - This solution gave the worst fabric samples. Solids created by the sol covered the entire fabric surface and left the samples very stiff.
- Sample: Tetraethoxysilane, Aerosil[®] 200, n-Octyltrimethoxysilane
 - These samples were stiffer again than the 0.02% o.w.b. SiO₂, however they appeared to have the softest hand of the samples containing 0.02% o.w.b. SiO₂.
- Sample: Tetramethoxysilane, Aerosil[®] 200, n-Octyltrimethoxysilane
 - The hand of these samples was considerably stiffer than their counterparts containing ten-times less silica in the bath.

4.2. General observations on differences between preliminary samples

4.2.1. On the observable interactions between water droplets and fabric samples

One water droplet appeared to have less affinity for the surface of the fabric containing 0.2% silica than in samples with 0.02% silica o.w.b. The droplet glided easily over the surface if moved or tilted. A water droplet of the same size showed more affinity for samples of 0.02% silica. The droplet “stuck”, even if the fabric was held at 90° or even upside-down. However, the droplet fell off or moved with slight agitation. This means the fabric must be moved carefully for the droplet to stick, but it will stick.

Similarly, the droplet of water also glided on the samples using bis(triethoxysilyl)ethane as a crosslinker. However, on samples using bis(trimethoxysilyl)ethane and bis(trimethoxysilyl)hexane the droplet stuck at both concentrations of silica. The sample containing 0.02% o.w.b. silica and 1,4-bis(trimethoxysilylethyl)benzene allowed for the water droplet to glide. By contrast, the sample with 1.0 % silica caused the droplet to stick.

Table 4.1 below clarifies water interactions with the sample set:

Table 4.1 Preliminary Observations Made on Water Interaction with Fabric		
Sample/Crosslinker	0.02% o.w.b. Silica	0.2% o.w.b. Silica
Tetraethoxysilane	Droplet Stuck	Droplet Glided
Tetramethoxysilane	Droplet Stuck	Droplet Glided
Bis(triethoxysilyl)ethane	Droplet Glided	Droplet Glided
Bis(trimethoxysilyl)ethane	Droplet Stuck	Droplet Stuck
Bis(trimethoxysilyl)hexane	Droplet Stuck	Droplet Stuck
1,4-Bis(trimethoxysilylethyl)benzene	Droplet Glided	Droplet Stuck

4.3. Decisions made on future proceedings with regards to the design of experiments

- Research continued without the use of the following crosslinkers:
 - Bis(trimethoxysilyl)ethane: Use of SiO₂ nanoparticles did not appear to improve the water-repellent nature of the fabric when using this product as a crosslinker. Product costs between \$2.24-\$2.76 per gram (research grade).
 - 1,4-Bis(trimethoxysilyl)benzene: Use stopped because of difficulty in handling and cleaning after hydrolysis, poor fabric hand & appearance, and initial performance. The performance did not appear to improve with higher concentrations of SiO₂ nanoparticles. Product costs between \$3.30-\$2.64 per gram (research grade).
 - Bis(trimethoxysilyl)hexane: This product was extremely difficult to handle, especially with increasing concentrations of SiO₂ nanoparticles. The “gliding” effect with water was not achieved with either concentration of silica. Product costs between \$3.60-\$2.88 per gram (research grade).
- Comparative product cost of the three crosslinkers:
 - Bis(triethoxysilyl)ethane: Product costs between \$0.21-\$0.60 per gram (research grade).
 - Tetramethoxysilane (99+% Purity): Product costs between \$0.16-\$0.80 per gram (research grade).
 - Tetraethoxysilane (99+% Purity): Product costs between \$0.075-\$0.09 per gram (research grade).

- Tetraethoxysilane (Low Purity): Product costs between \$0.013-\$0.10 per gram (research grade).
- Tetramethoxysilane (Low Purity): Product costs between \$0.132-\$0.60 per gram (research grade).
- On the behavior of the hydrophobe n-octadecylmethyldimethoxysilane:
 - When creating the standard recipe (shown in **Section 3.1.3**) using n-octadecylmethyldimethoxysilane as a hydrophobe, irregular behavior was observed. Within five minutes of the n-octadecylmethyldimethoxysilane hydrophobe being added to the solution, a gel-like substance was formed. Viscosity of the solution greatly increased (visibly) and was turned to a milky/white semi-solid. After this phenomenon happened, the solutions were taken off the stirring plate. Following the removal from the stirrer, the viscosity of the solution decreased and the silica dropped out of the suspension.
 - As a control and to determine the effect of the silica on the formation of gels with n-octadecylmethyldimethoxysilane, two solutions were prepared. One solution was made using Aerosil[®] 90 silica, tetraethoxysilane, and n-octadecylmethyldimethoxysilane with the standard recipe. The other solution was made only using tetraethoxysilane and n-octadecylmethyldimethoxysilane *without* using any silica. The same phenomena were observed in both sample solutions.

- Fabric samples were created using the solutions containing n-octadecylmethyldimethoxysilane to evaluate if they exhibited the same hydrophobic behavior as previous samples created with n-octyltrimethoxysilane and n-decyltriethoxysilane as hydrophobes. When contact angle measurements were performed, fabric samples left a white powdery residue on the sample tray. Of the two samples compared, one with silica and one without, it was found that the use of silica did not appear to have the same effect on contact angle as it did with the other two hydrophobes of interest in this research. This is discussed in greater detail in **Section 5.2.3**.
- Because of difficulty with processing and behavior both in solution and on the fabric, n-octadecylmethyldimethoxysilane was no longer of interest in this research and its use was discontinued.

4.4. Observations Regarding Samples Made With Noncellulosic Fabrics

- Wool, polyester and nylon fabrics were used as received from the International Textile Group.
- The samples were treated with the same recipe as all the cotton fabrics. Adjustments were made for the differing basis weights of all the fabrics treated and the amount of silica used (0.2% o.w.b.)
- Due to the fact that the samples were unlabeled and there was not sufficient time to investigate any surface treatments or to do preparation on the fabric, the trials were unsuccessful.

- The red fabric used (assumed to be polyester) was not wet well by the coating solution. When the fabric was dipped, dye from the fabric started to leach into the solution. Coating of this fabric was unsuccessful and it was discovered that the samples were water repellent.
- The blue fabric used (assumed to be nylon) was stiff after air-drying and curing. Some dye from the fabric was leached into the coating solution. These fabric samples were not repellent after curing.
- The green fabric used (assumed to be wool) also leached dye into the coating solution. This fabric was not repellent after curing.

Chapter 5: Results and Discussion

5.1. SEM Observations / Analysis of Micrographs

SEM analysis was performed on three different sample sets:

- TEOS, 0.02% Aerosil[®] 200, and n-octyltrimethoxysilane;
- TEOS, 0.2% Aerosil[®] 200, and n-octyltrimethoxysilane; and
- TMOS, 0.2% Aerosil[®] 200, and n-octyltrimethoxysilane.

The analysis was only performed on three sets of samples to see if the silica nanoparticles appeared on the fabric and fiber surfaces, rather than to draw specific conclusions about the attachment of nanoparticles to the fabric surface or to serve as a representation of all the produced samples.

5.1.1. SEM Results of TEOS Samples

The analysis showed in both samples that there was a dispersion of silica nanoparticle clusters on the fabric/fiber surface which indicates the formation of a rough surface and is beneficial in increasing the hydrophobicity of a surface. **Figures 5.1** and **5.2** show two separate comparative SEM micrographs at different magnifications of the TEOS samples containing 0.2% (left image) and 0.02% (right image) Aerosil[®] 200 silica o.w.b.

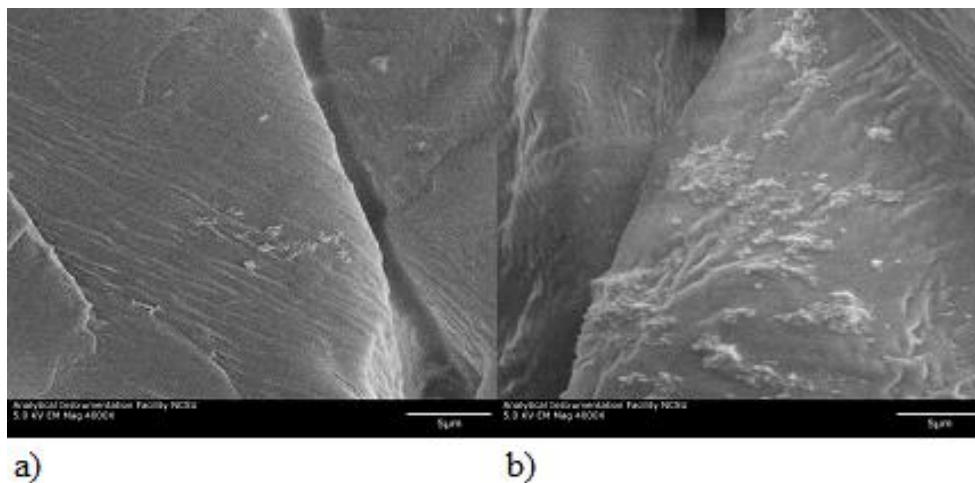


Figure 5.1 Scanning Electron Micrographs of Samples Containing a) TEOS, n-Octyltrimethoxysilane, and 0.2% o.w.b. Aerosil[®] 200 and b) TEOS, n-Octyltrimethoxysilane, and 0.02% o.w.b. Aerosil[®] 200.

Contrary to intuitive thought, the sample containing 0.02% silica o.w.b. appears to have a better coating dispersion than that of the sample containing 0.2% silica o.w.b. However, at this magnification, these two images do not fully represent the entire sample or the set of samples. It is entirely possible that during sample transfer, handling, and preparation that some particles were scraped off of the surface, leaving the resulting image. As these were only two samples in a sample set of three, it should not be taken that these samples represent the entire sample set.

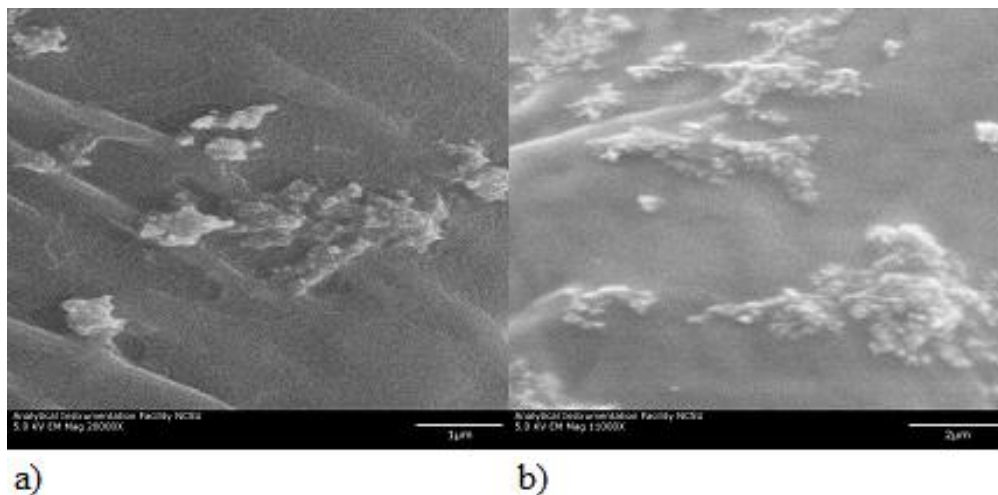


Figure 5.2 Scanning Electron Micrographs of Samples Containing a) TEOS, n-Octyltrimethoxysilane, and 0.2% o.w.b. Aerosil® 200 (20,000X) and b) TEOS, n-Octyltrimethoxysilane, and 0.02% o.w.b. Aerosil® 200 (11,000X).

The right-hand image of **Figure 5.2** shows a close up of the silica clusters at 11,000X magnification and the left-hand image of **Figure 5.2** is at 20,000X magnification. These clusters differ in size and shape on the fabric surface, as well as proximity to one another on these specific samples.

5.1.2. SEM Results of the TMOS Sample

A high-resolution FESEM analysis was performed on a sample prepared with TMOS, 0.2% Aerosil® 200, and n-octyltrimethoxysilane. This analysis gave extremely high resolution images as well as measurements as to the size of some of the silica clusters on the fiber surface. **Figure 5.3** shows an image of the FESEM analysis of a view of a number of fibers in the coated fabric. **Figure 5.4** shows two close-up views of the central silica cluster in **Figure 5.3** as well as provides a measurement of said cluster.

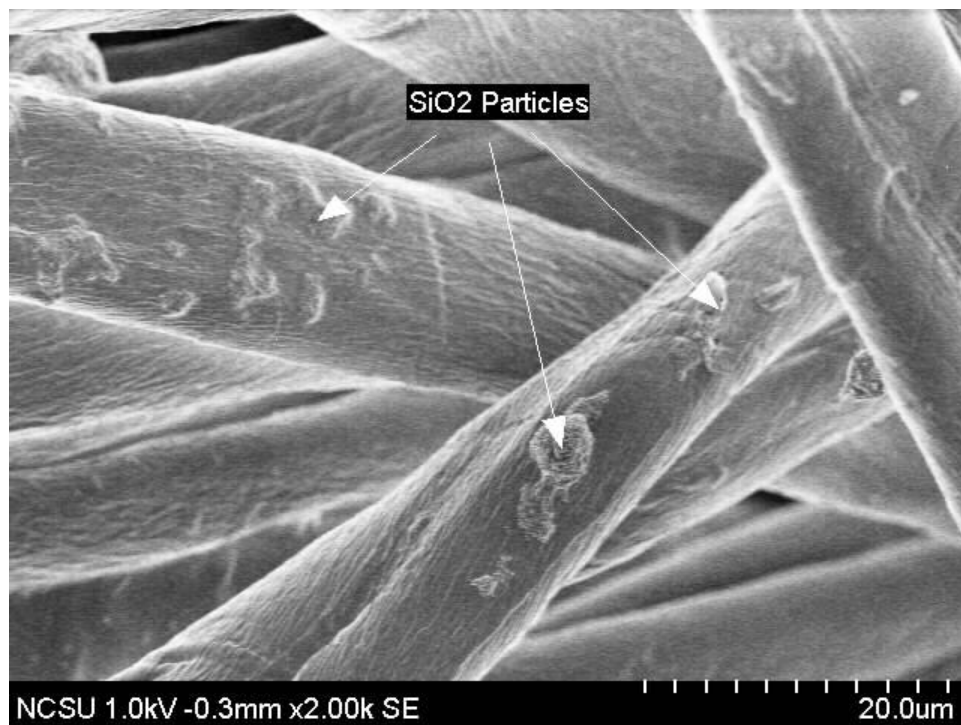


Figure 5.3 Scanning Electron Micrographs of a Sample Containing TMOS, n-Octyltrimethoxysilane, and 0.2% o.w.b. Aerosil[®] 200 (2,000X).

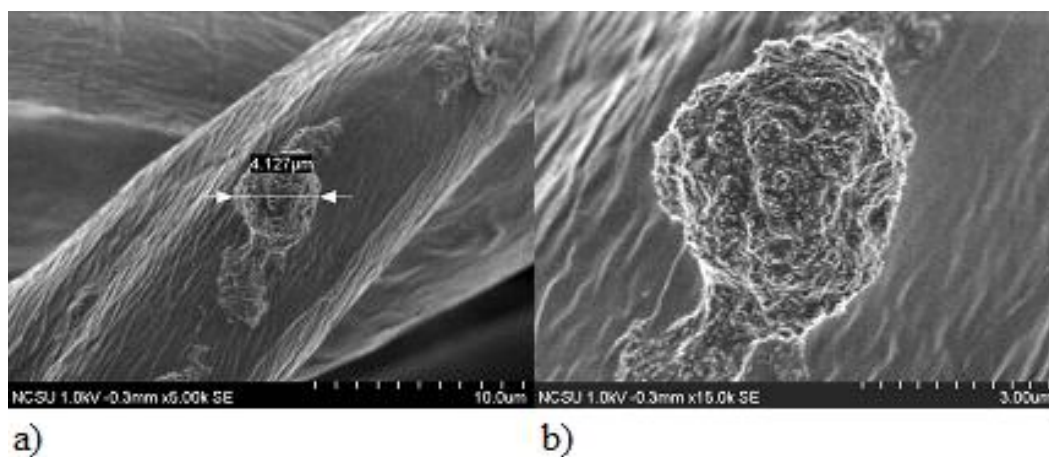


Figure 5.4 Scanning Electron Micrographs of a Sample Containing TMOS, n-Octyltrimethoxysilane, and .02% o.w.b. Aerosil[®] 200 at Higher Magnification {a) 5,000X and b) 15,000X}.

5.1.3. Observations Regarding the SEM Micrographs

All three analyzed samples give insight as to the coating behavior of the solutions under investigation in this research. The coatings on these three sample sets don't give an even, thin coating; instead, the silica nanoparticles tend to cluster and attach to the fiber surfaces at random. In some cases in these three sample sets, the clustering is thin, rather than spherical in **Figure 5.4**, and gives better surface coverage. Using the left-hand picture in **Figure 5.4** as a gauge, it can be seen that a number of clusters of nanoparticles on this sample can be of approximate spherical diameter of 5 μm or less. The right-hand image in **Figure 5.4** gives a good comparative idea of the size of the silica nanoparticles (about 14 nm) to the size of the clusters on the fiber surface of this sample. A simple ultrasound procedure should work to further reduce the size of the silica nanoparticle clusters and was performed on certain solutions before fabric treatment. The ultrasonication procedure can be found in **Section 3.2.8** and the results of the fabrics prepared with said solutions can be found in **Section 5.6**.

5.2. Pre-Design of Experiments Results

Prior to the creation of the DOE, hydrophobic fabric samples were made using only n-octyltrimethoxysilane and Aerosil[®] 200 at various concentrations with the different crosslinkers. This was done to get a preliminary idea of the behavior of the chemicals and the effect that the addition of silica nanoparticles has on the fabric. Aerosil[®] 200 was chosen as a constant for these experiments because of the five types of silica nanoparticles used in this research, Aerosil[®] 200 has the median diameter (Refer to **Table 3.4**). Each chemical combination was applied to three fabrics and from each fabric, three

samples were taken. This gave eighteen data points for each sample type, from which the average value (shown) was taken.

5.2.1. The Effect of Silica Concentration on Three Crosslinkers

This study was carried out to compare the performance of samples containing 0.02%

o.w.b. silica nanoparticles to those containing 0.2% o.w.b. silica nanoparticles. The

samples tested used Aerosil[®] 200 silica nanoparticles, n-octyltrimethoxysilane

hydrophobe, and three crosslinkers: TEOS, TMOS, and bis(triethoxysilyl)ethane. As

Figure 5.5 shows, the contact angle of water (WCA) increases with increasing silica content on every sample.

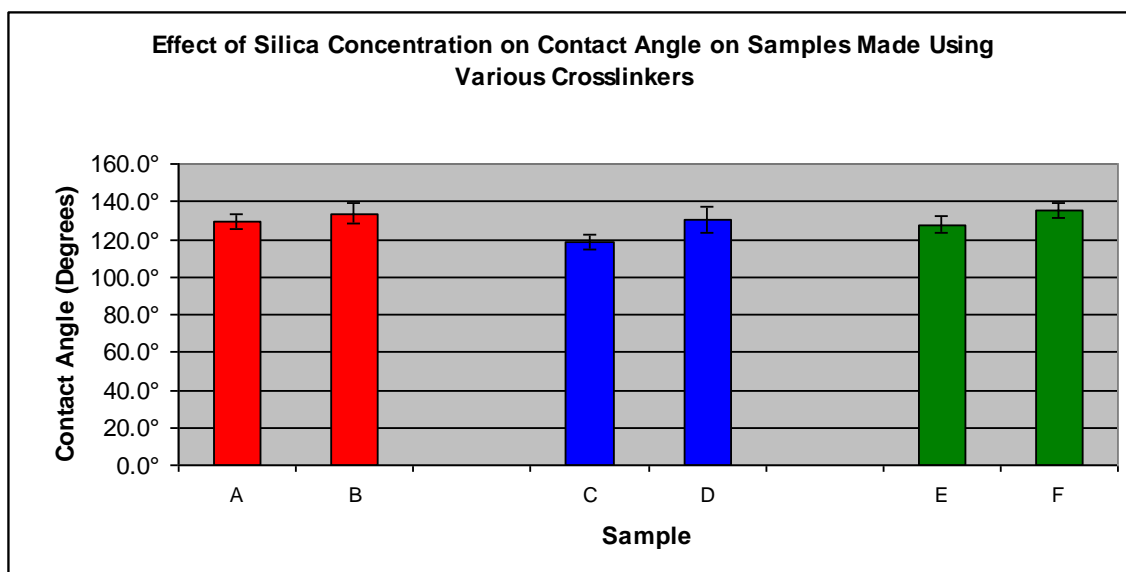


Figure 5.5 Graph Comparing Contact Angle on Samples Using Three Different Crosslinkers, n-Octyltrimethoxysilane, and Aerosil® 200 at Different Concentrations.

where:

- A is TEOS, n-Octyltrimethoxysilane, and 0.02% o.w.b. Aerosil® 200
- B is TEOS, n-Octyltrimethoxysilane, and 0.2% o.w.b. Aerosil® 200
- C is TMOS, n-Octyltrimethoxysilane, and 0.02% o.w.b. Aerosil® 200
- D is TMOS, n-Octyltrimethoxysilane, and 0.2% o.w.b. Aerosil® 200
- E is Bis(triethoxysilyl)ethane, n-Octyltrimethoxysilane, and 0.02% o.w.b. Aerosil® 200
- F is Bis(triethoxysilyl)ethane, n-Octyltrimethoxysilane, and 0.2% o.w.b. Aerosil® 200

The samples all exhibited an increase in contact angle, though none higher than the samples using TMOS as a crosslinker. A tenfold increase in silica from 0.02% o.w.b. to 0.2% o.w.b. resulted in an increase of 11.5° (from 118.9° to 130.4°). All samples gave a water contact angle greater than 130°, with the sample containing bis(triethoxysilyl)ethane, Aerosil® 200, and n-octyltrimethoxysilane giving the highest resulting WCA at 135.1°.

5.2.2. The Effect of Increasing Silica Concentration on TEOS-Crosslinked samples

Further investigations were made as to gain greater knowledge of the effect silica concentration has on the resultant fabric. Five sets of samples were made with silica concentration (Aerosil[®] 200) increasing from 0% o.w.b. to 0.2% o.w.b. using TEOS as a crosslinker and n-octyltrimethoxysilane as a hydrophobe. The results, shown in **Figure 5.6**, give an idea of the behavior of the samples.

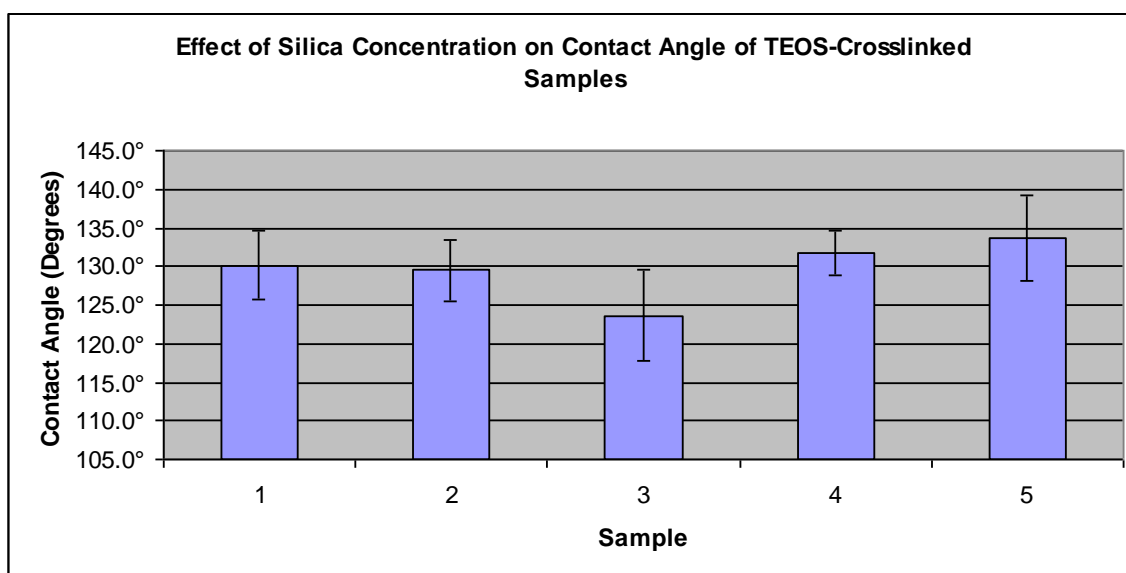


Figure 5.6 Graph Comparing Contact Angle on Samples using TEOS, n-Octyltrimethoxysilane, and Aerosil[®] 200 at Five Different Concentrations.

where:

- 1 is TEOS, n-Octyltrimethoxysilane, and 0.0% o.w.b. Aerosil[®] 200
- 2 is TEOS, n-Octyltrimethoxysilane, and 0.02% o.w.b. Aerosil[®] 200
- 3 is TEOS, n-Octyltrimethoxysilane, and 0.05% o.w.b. Aerosil[®] 200
- 4 is TEOS, n-Octyltrimethoxysilane, and 0.1% o.w.b. Aerosil[®] 200
- 5 is TEOS, n-Octyltrimethoxysilane, and 0.2% o.w.b. Aerosil[®] 200

With the exception of the sample containing 0.05% o.w.b. Aerosil[®] 200, the other four samples performed similarly; there was a standard deviation between them of 1.91°. The sample with 0.2% o.w.b. Aerosil[®] performed the best with an average contact angle of

133.8°. As can be seen in **Appendix A**, the range of contact angles for the samples tested all shared similar maximum and minimum values, though with some occurring more than other and influencing the results as such.

5.2.3. Results of Two Samples Created with n-Octadecylmethyldimethoxysilane

As a preemptive measure, two samples created with the hydrophobe n-

octadecylmethyldimethoxysilane were tested to make its ruling out a finality. The

performance of samples created with this hydrophobe compared to those created with n-

octyltrimethoxysilane is poorer. The graph in **Figure 5.7** shows a comparison of average

WCAs for two sample fabrics made with TEOS, n-octadecylmethyldimethoxysilane, and

either 0% or 0.2% Aerosil® 90 silica nanoparticles.

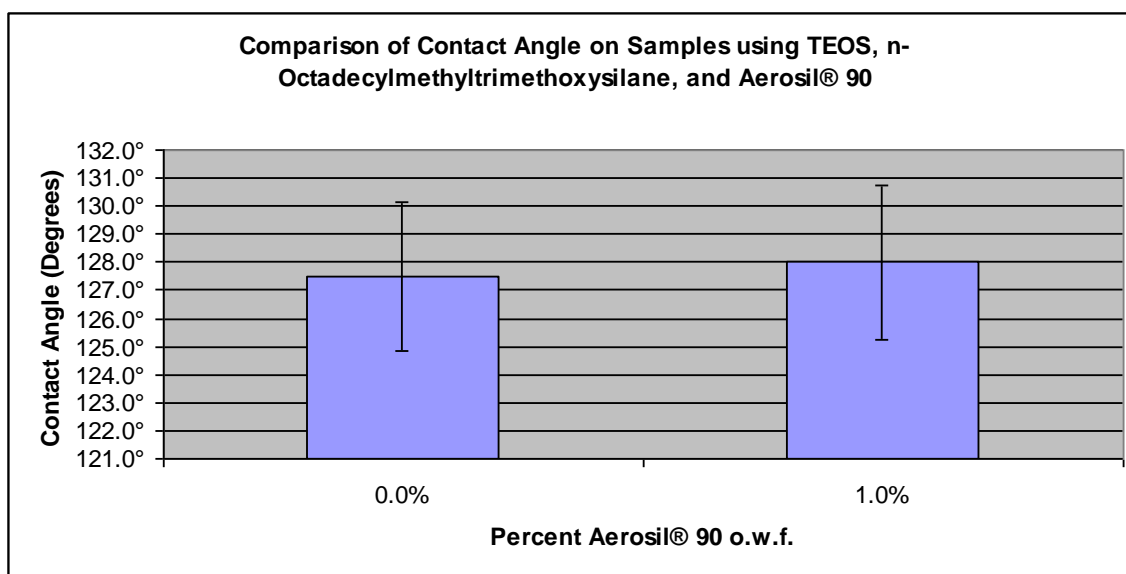


Figure 5.7 Graph Comparing Contact Angle on Two Samples Containing TEOS, n-Octadecylmethyldimethoxysilane, (left) 0% and (right) 0.2% Aerosil® 90.

From this simple two sample test (i.e. one fabric sample treated each chemical

combination, with three spots tested on each sample fabric) it can be seen that the silica

only has an effect of 0.5° on the water repellency of the sample. It is due to this small difference and the other reasons that were outlined in **Section 4.3** that the use of this hydrophobe was discontinued.

5.3. Results from the Design of Experiments

The design of experiments yielded thirty chemical combinations that were applied each to three fabrics. Each of the three fabrics was tested in three places, with each place giving two measurements. This gave a total of eighteen contact angle measurements for each chemical combination applied to a fabric. The following section will analyze the effect that each chemical type and individual chemical had on the process. **Table 5.1** below shows the key used in all the proceeding graphs as well as the average water contact angle and standard deviation for all of the samples.

Table 5.1 Design of Experiments Results (In Water Contact Angle, WCA)			
Sample:	Key:	Mean WCA:	Std. Dev.:
TEOS, n-Octyltrimethoxysilane, Aerosil® 90	TE-O-9	131.8°	3.6°
TEOS, n-Octyltrimethoxysilane, Aerosil® 150	TE-O-1	131.4°	3.6°
TEOS, n-Octyltrimethoxysilane, Aerosil® 200	TE-O-2	132.8°	4.9°
TEOS, n-Octyltrimethoxysilane, Aerosil® 380	TE-O-3	132.4°	2.3°
TEOS, n-Octyltrimethoxysilane, Aerosil® R805	TE-O-R	134.7°	2.6°
TEOS, n-Decyltriethoxysilane, Aerosil® 90	TE-D-9	139.3°	2.8°
TEOS, n-Decyltriethoxysilane, Aerosil® 150	TE-D-1	139.2°	3.7°
TEOS, n-Decyltriethoxysilane, Aerosil® 200	TE-D-2	138.7°	3.9°
TEOS, n-Decyltriethoxysilane, Aerosil® 380	TE-D-3	140.5°	2.5°
TEOS, n-Decyltriethoxysilane, Aerosil® R805	TE-D-R	142.5°	3.3°
TMOS, n-Octyltrimethoxysilane, Aerosil® 90	TM-O-9	133.6°	2.1°
TMOS, n-Octyltrimethoxysilane, Aerosil® 150	TM-O-1	134.9°	4.4°
TMOS, n-Octyltrimethoxysilane, Aerosil® 200	TM-O-2	132.8°	2.2°
TMOS, n-Octyltrimethoxysilane, Aerosil® 380	TM-O-3	129.7°	2.0°
TMOS, n-Octyltrimethoxysilane, Aerosil® R805	TM-O-R	132.4°	3.3°
TMOS, n-Decyltriethoxysilane, Aerosil® 90	TM-D-9	140.8°	1.9°
TMOS, n-Decyltriethoxysilane, Aerosil® 150	TM-D-1	142.9°	4.7°
TMOS, n-Decyltriethoxysilane, Aerosil® 200	TM-D-2	138.5°	3.6°
TMOS, n-Decyltriethoxysilane, Aerosil® 380	TM-D-3	144.2°	5.5°
TMOS, n-Decyltriethoxysilane, Aerosil® R805	TM-D-R	141.7°	3.6°
Bis(triethoxysilyl)ethane, n-Octyltrimethoxysilane, Aerosil® 90	B-O-9	139.1°	5.8°
Bis(triethoxysilyl)ethane, n-Octyltrimethoxysilane, Aerosil® 150	B-O-1	135.3°	4.5°
Bis(triethoxysilyl)ethane, n-Octyltrimethoxysilane, Aerosil® 200	B-O-2	135.3°	3.9°
Bis(triethoxysilyl)ethane, n-Octyltrimethoxysilane, Aerosil® 380	B-O-3	134.5°	4.2°
Bis(triethoxysilyl)ethane, n-Octyltrimethoxysilane, Aerosil® R805	B-O-R	133.8°	4.9°
Bis(triethoxysilyl)ethane, n-Decyltriethoxysilane, Aerosil® 90	B-D-9	137.8°	3.3°
Bis(triethoxysilyl)ethane, n-Decyltriethoxysilane, Aerosil® 150	B-D-1	137.7°	4.8°
Bis(triethoxysilyl)ethane, n-Decyltriethoxysilane, Aerosil® 200	B-D-2	132.2°	3.7°
Bis(triethoxysilyl)ethane, n-Decyltriethoxysilane, Aerosil® 380	B-D-3	130.1°	5.9°
Bis(triethoxysilyl)ethane, n-Decyltriethoxysilane, Aerosil® R805	B-D-R	136.7°	5.0°

Explanation of key in table:

The key is given in 3 sets of letters and numbers. The first letter(s) denote crosslinker type: TE for tetraethoxysilane, TM for tetramethoxysilane, and B for bis(triethoxysilyl)ethane. The second letter denotes the hydrophobe type: O for n-octyltrimethoxysilane and D for n-decyltriethoxysilane. The third letter or number denotes silica type: 9 for Aerosil® 90, 1 for Aerosil® 150, 2 for Aerosil® 200, 3 for Aerosil® 380 and R for Aerosil® R805.

5.3.1. Samples Using the Crosslinker Tetraethoxysilane

This section will present the analysis of two graphs, **Figure 5.8** and **Figure 5.9**. **Figure**

5.8 shows the comparison of samples made using tetraethoxysilane, n-octyltrimethoxysilane, and the five types of Aerosil[®] silica.

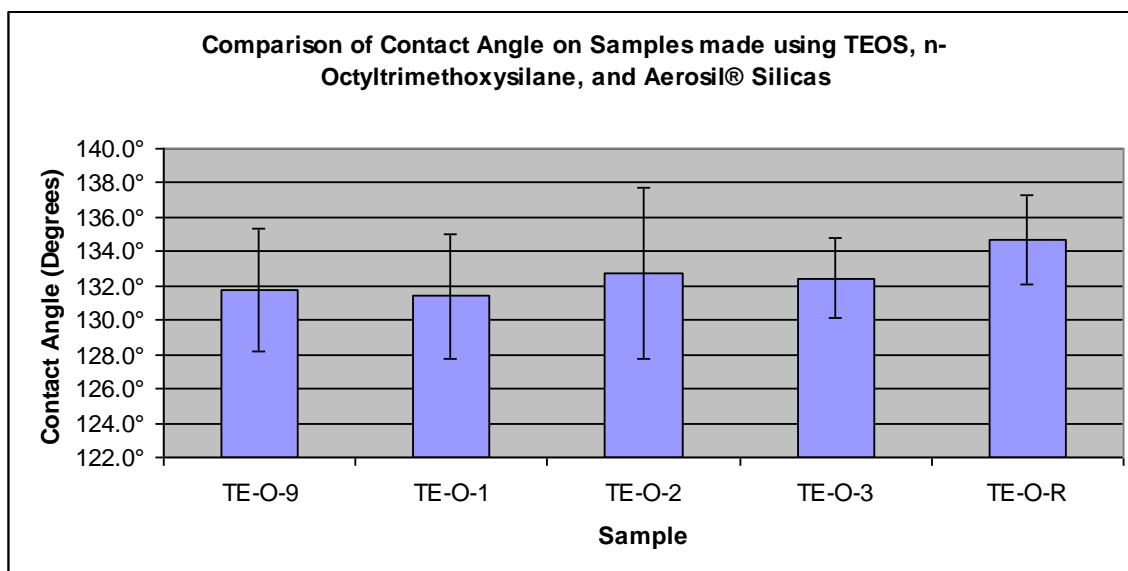


Figure 5.8 Graph Comparing Contact Angle on Samples Using TEOS, n-Octyltrimethoxysilane, and Five Types of Aerosil[®] Silica.

Figure 5.9 shows the comparison of samples made using tetraethoxysilane, n-decyltriethoxysilane, and the five types of Aerosil[®] silica.

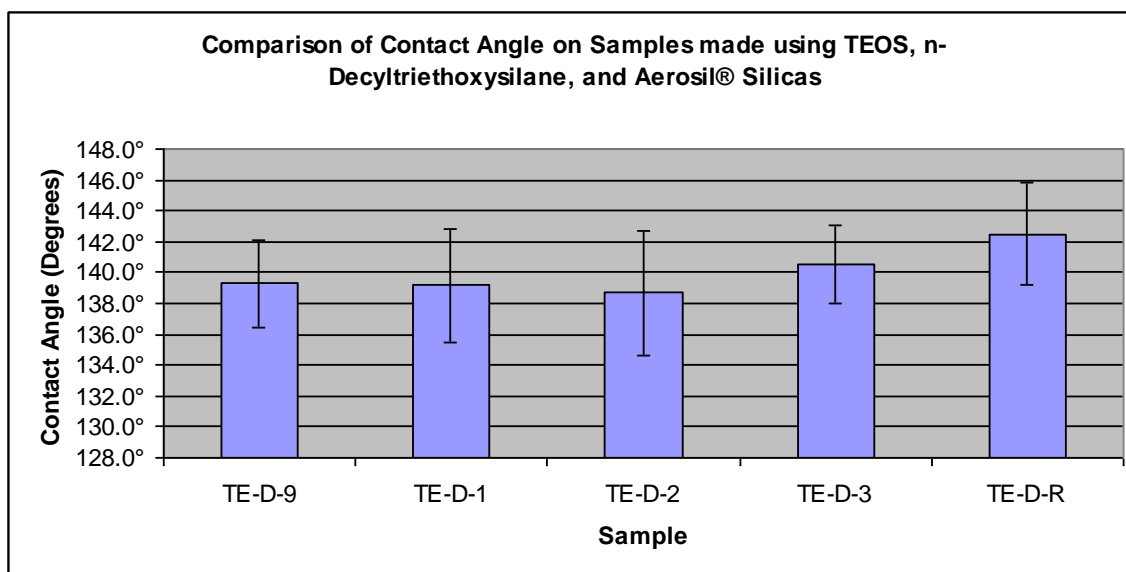


Figure 5.9 Graph Comparing Contact Angle on Samples Using TEOS, n-Decyltriethoxysilane, and Five Types of Aerosil® Silica.

The trends in these graphs will be discussed in the following sections.

5.5.1.1. Effect of Silica Type on Hydrophobicity on TEOS Crosslinked Samples

Though the effect of the silica type appears to be profound when looking at the graphs, the scale must be kept in mind during the analysis. Samples made with n-octyltrimethoxysilane only display a range of 3.3°. There appears to be no significant difference between the four types of hydrophilic silicas and only a slight increase is obtained by using hydrophobic silica. No trend is seen with changing silica types and good hydrophobicity is obtained with all samples. The minimum value of 131.4° is obtained with the combination of tetraethoxysilane, n-octyltrimethoxysilane, and Aerosil® 150. The maximum value obtained with the hydrophobic Aerosil® R805 silica, tetraethoxysilane, and n-octyltrimethoxysilane was 134.7°. Regarding variability introduced by taking an average of eighteen measurements, the average standard

deviation of the five samples made with tetraethoxysilane and n-octyltrimethoxysilane was 3.44° .

Similar results were obtained with samples made with n-decyltriethoxysilane. The range with this sample set is 3.8° . This again suggests that silica type does not play a significant part in the contact angle of these samples. Using hydrophobic silica only offers an increase of 2.0° degrees over the highest hydrophilic silica value. The overall hydrophobicity of these samples is very good, with the highest water contact angle coming from the sample made with the hydrophobic Aerosil[®] R805 silica, tetraethoxysilane, and n-decyltriethoxysilane at 142.5° . The lowest recorded value was from the sample made with Aerosil[®] 200 silica, tetraethoxysilane, and n-decyltriethoxysilane at 138.7° . The average standard deviation for these five samples was 3.28° .

5.5.1.2. Effect of Silane Hydrophobe Chain Length on Hydrophobicity of TEOS Crosslinked Samples

Chain length of the alkyltrialkoxysilane hydrophobes proved to be a significant factor in these samples. Overall, the samples made using n-decyltriethoxysilane were more hydrophobic than those made with n-octyltrimethoxysilane. This effect was expected, as the two extra carbon groups in the backbone of the n-decyltriethoxysilane chains make for a more hydrophobic molecule and increase water-droplet distance from the surface of an excessively hydrophilic neat-cotton surface. In all, there was an average increase in water contact angle of 7.4° in the n-decyltriethoxysilane samples over those using n-octyltrimethoxysilane. The average of the five n-decyltriethoxysilane samples was

140.2°, with a high of 142.5°. The average of the five n-octyltrimethoxysilane samples was 132.6° with a high value of 134.7°. Both sets of samples made with tetraethoxysilane had similar average standard deviations, with values of 3.44° (n-octyltrimethoxysilane) and 3.28° (n-decyltriethoxysilane).

5.3.2. Samples Using the Crosslinker Tetramethoxysilane

This section will present the analysis of two graphs, **Figure 5.10** and **Figure 5.11**.

Figure 5.10 shows the comparison of samples made using tetramethoxysilane, n-octyltrimethoxysilane, and the five types of Aerosil® silica.

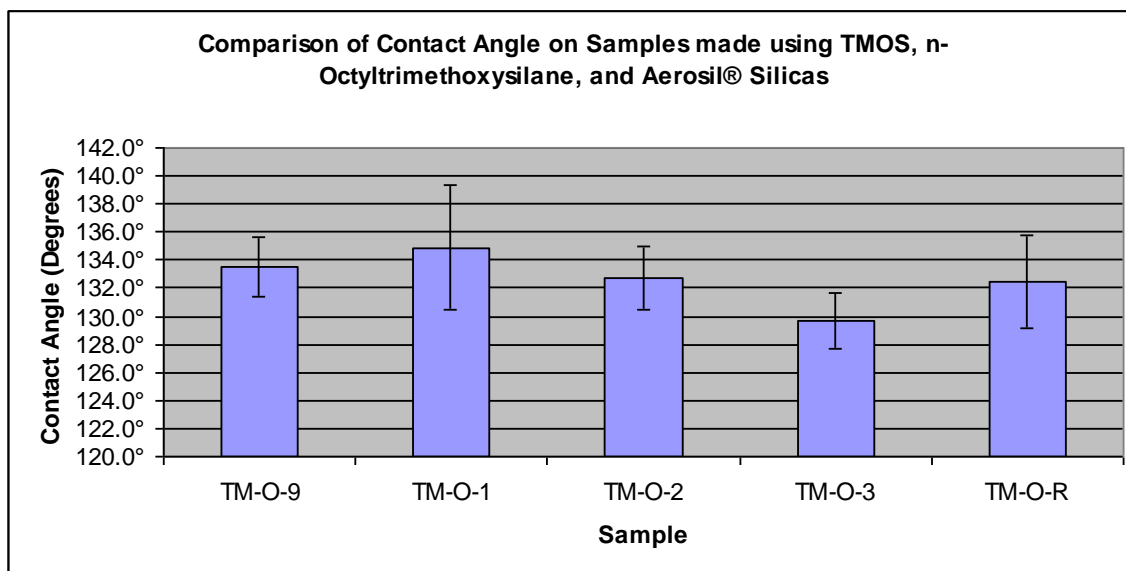


Figure 5.10 Graph Comparing Contact Angle on Samples Using TMOS, n-Octyltrimethoxysilane, and Five Types of Aerosil® Silica.

Figure 5.11 shows the comparison of samples made using tetramethoxysilane, n-decyltriethoxysilane, and the five types of Aerosil® silica.

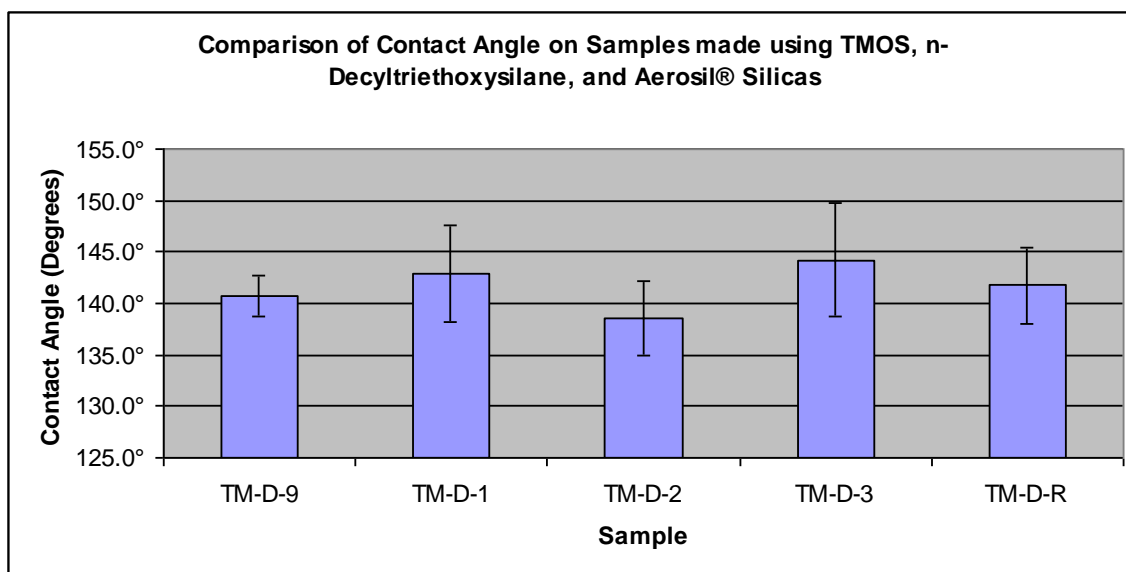


Figure 5.11 Graph Comparing Contact Angle on Samples Using TMOS, n-Decyltriethoxysilane, and Five Types of Aerosil® Silica.

The trends in these graphs will be discussed in the following sections.

5.5.2.1. Effect of Silica Type on Hydrophobicity on TMOS Crosslinked Samples

The samples made with tetramethoxysilane, n-octyltrimethoxysilane, and the five types of Aerosil® silica do not exhibit any trends regarding contact angle. This suggests that no particular type of silica or silica diameter will result in a clear advantage in processing. An important difference to note here is the difference in ranges between samples made with tetramethoxysilane and tetraethoxysilane. The range for the five samples is 5.2° , compared to their TEOS equivalent's value of 3.3° . Though there was a larger difference between samples, the within-sample variation was the lowest of all thirty samples tested with an average standard deviation of the five samples being 2.84° . The maximum value obtained with the sample made with tetramethoxysilane, n-octyltrimethoxysilane, and Aerosil® 150 was 134.9° . The minimum recorded average value was 129.7° , recorded

with the sample prepared from tetramethoxysilane, n-octyltrimethoxysilane, and Aerosil[®] 380.

The samples made with n-decyltriethoxysilane showed similar results to their n-octyltrimethoxysilane counterparts, in that there was no clear trend due to silica type. There is no clear reason to suggest why the sample made with Aerosil[®] 380 should give the highest contact angle when made with n-decyltriethoxysilane as opposed to when made with n-octyltrimethoxysilane. This sample had a value of 144.2° and was the highest of the five samples. The lowest water contact angle came from the sample with tetramethoxysilane, n-decyltriethoxysilane, and Aerosil[®] 200, at 138.5°. The samples made with n-decyltriethoxysilane had a similar range as the n-octyltrimethoxysilane samples at 5.7°. The average standard deviation from these samples was higher, though, at a value of 3.90°.

5.5.2.2. Effect of Silane Hydrophobe Chain Length on Hydrophobicity on TMOS Crosslinked Samples

Due to the similar chemical structures of the crosslinkers tetramethoxysilane and tetraethoxysilane, similar behavior ensued concerning the effect of the hydrophobic additives. Again, the n-decyltriethoxysilane samples showed significantly higher contact angles than the n-octyltrimethoxysilane samples. The average value for the n-decyltriethoxysilane samples was 141.6°, giving a difference of 8.9° between those samples and the average value of the average contact angle of the n-octyltrimethoxysilane samples at 132.7°. The recorded high average value for both sets of tetramethoxysilane samples (and of all made samples) came from the sample made with tetramethoxysilane,

n-decyltriethoxysilane, and Aerosil[®] 380 at 144.2°. The highest average value recorded for a sample made with n-octyltrimethoxysilane was 134.9°, from the sample made from tetramethoxysilane, n-decyltriethoxysilane, and Aerosil[®] 150.

5.3.3. Samples Using the Crosslinker Bis(triethoxysilyl)ethane

This section will present the analysis of two graphs, **Figure 5.12** and **Figure 5.13**.

Figure 5.12 shows the comparison of samples made using bis(triethoxysilyl)ethane, n-octyltrimethoxysilane, and the five types of Aerosil[®] silica.

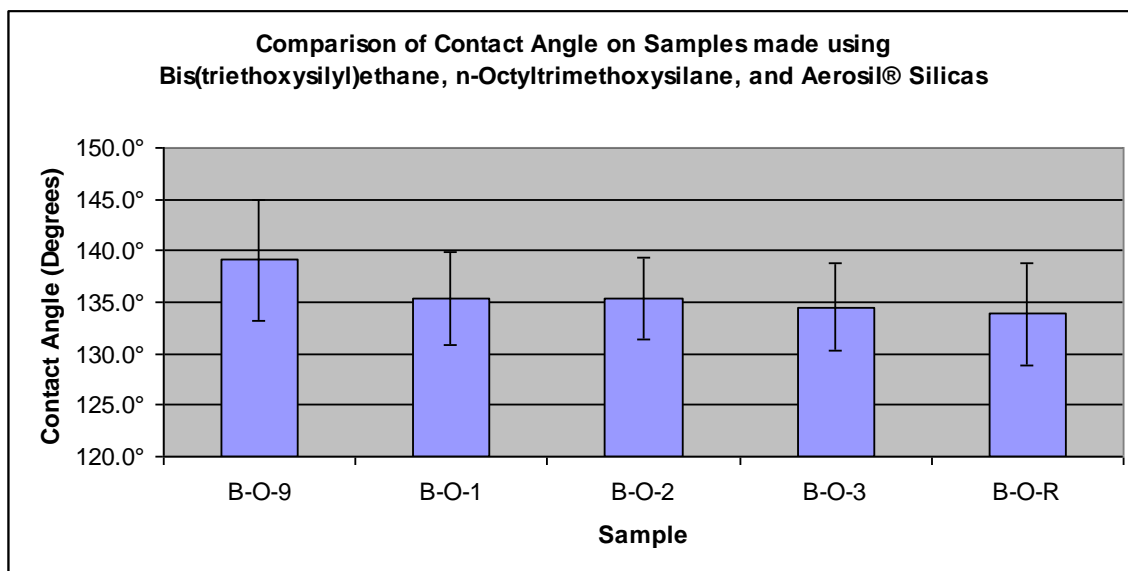


Figure 5.12 Graph Comparing Contact Angle on Samples Using Bis(triethoxysilyl)ethane, n-Octyltrimethoxysilane, and Five Types of Aerosil[®] Silica.

Figure 5.13 shows the comparison of samples made using bis(triethoxysilyl)ethane, n-decyltriethoxysilane, and the five types of Aerosil[®] silica.

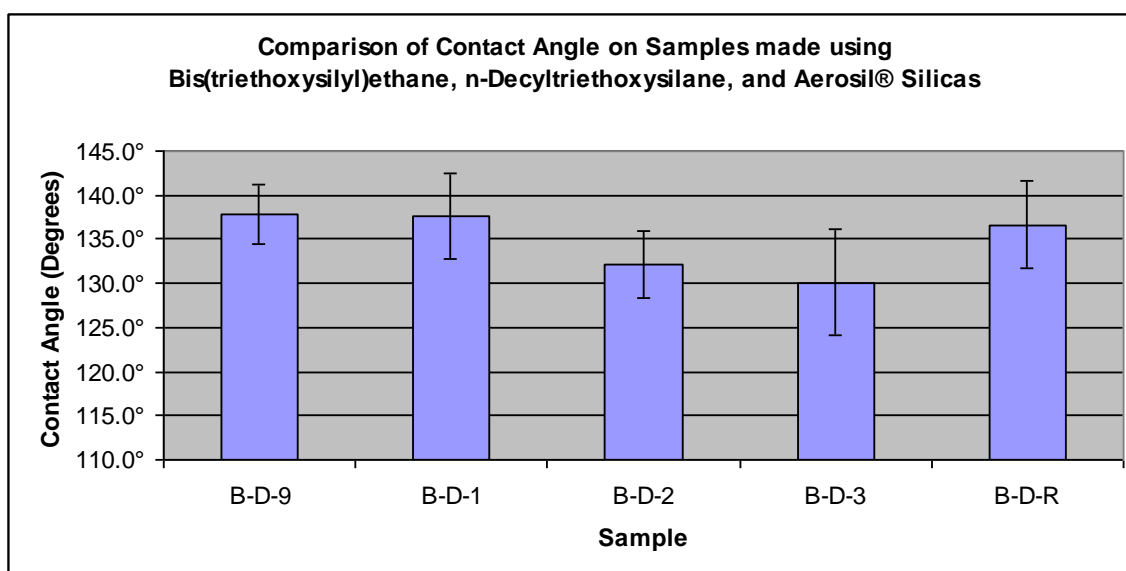


Figure 5.13 Graph Comparing Contact Angle on Samples Using Bis(triethoxysilyl)ethane, n-Decyltriethoxysilane, and Five Types of Aerosil® Silica.

The trends in these graphs will be discussed in the following sections.

5.5.3.1. Effect of Silica Type on Hydrophobicity on Bis(triethoxysilyl)ethane Crosslinked Samples

The samples prepared with n-octyltrimethoxysilane displayed, if anything, an opposite trend compared to their tetraethoxysilane counterparts. The graph shows a decreasing trend in contact angle with decreasing particle diameter and the hydrophobic silica giving the lowest contact angle of all the samples, at 133.8°. This contact angle of this sample was 5.3° lower than the best-performing sample made from bis(triethoxysilyl)ethane, n-octyltrimethoxysilane, and Aerosil® 90 which had a contact angle of 139.1°. This sample set had the greatest amount of measured variability when the average values were taken, giving an average standard deviation of 4.72°, the highest of all the sample sets.

The samples made with n-decyltriethoxysilane were similar to their tetramethoxysilane counterparts in that there was no clear trend or dominant sample in the set. Three

samples had a contact angle value of at least 6.0° higher than the lowest value. In this set, the samples with the highest contact angles were different only by 0.1° . These samples were made from bis(triethoxysilyl)ethane, n-decyltriethoxysilane, and Aerosil[®] 90 and 150 (values of 137.8° and 137.7° respectively). This sample set also had the highest range of any of the sample sets tested, with a value of 7.7° . Similar to the samples made with bis(triethoxysilyl)ethane and n-octyltrimethoxysilane, these samples had a high average-standard deviation of 4.59° .

5.5.3.2. Effect of Silane Hydrophobe Chain Length on Hydrophobicity on Bis(triethoxysilyl)ethane Crosslinked Samples

Most likely due to the different chemical structure of the crosslinker, the samples made with bis(triethoxysilyl)ethane did not follow the same trends as the samples made with either tetramethoxysilane or tetraethoxysilane. The two types of hydrophobes did not have a significant effect on the average hydrophobicity of either sample set. The contact angles for the set made with n-octyltrimethoxysilane (135.6°) and the set made with n-decyltriethoxysilane (134.9°) differed by only 0.7° . The most interesting aspect to point out is that the fabric samples made with bis(triethoxysilyl)ethane, Aerosil[®] silica, and n-octyltrimethoxysilane had a higher contact angle, on average, than those made with the longer-chain alkyltrialkoxysilane. This is counterintuitive to thought and to the behavior displayed by the samples made with the crosslinkers tetraethoxysilane and tetramethoxysilane.

5.3.4. Comparison of Hydrophilic Silica to Hydrophobic Silica Regarding Hydrophobicity

Only on two occasions did using hydrophobic silica result in a higher overall contact angle than the hydrophilic silica types. The samples made with the tetraethoxysilane crosslinker and Aerosil[®] R805 hydrophobic silica gave a contact angle increase of 1.9° in the case of n-octyltrimethoxysilane and an increase of 2.0°. Though these numbers don't suggest a significant increase due to the change in silica, a trend was seen in the graphs and the numbers. The real test of the benefits offered by the hydrophilic silica over the hydrophobic silica may be seen when testing for washing and crocking durability. The abundance of hydroxyl groups on the surface of the hydrophilic silicas should offer better covalent attachment to the fabric surface and therefore better fastness properties. This issue will be addressed in **Sections 5.6** and **5.7**.

5.3.5. Analysis of the Design as a Whole

An analysis done with JMP6.0 statistical software showed certain trends displayed by all thirty samples, in comparison to one another. In order to see how the samples related to one another, **Figure 5.14** below should be referenced (note: the key is located in **Table 5.1**).

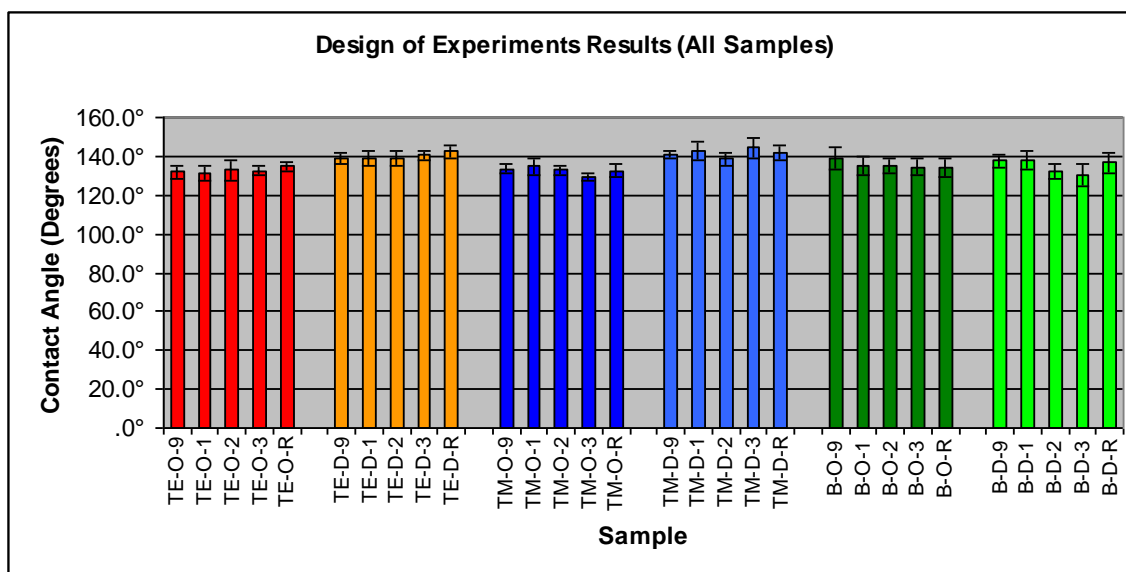


Figure 5.14 Graph Comparing Contact Angle Results for All Samples Prepared for the Design of Experiments.

This graph is assembled from **Figures 5.8 to 5.13**. It helps to show trends in the design as a whole. When the individual components are analyzed with statistical software, those trends start to take on significant meaning. When referring to the table in **Figure 5.15**, it can be seen that two parameters have a significant effect on the resulting water contact angle.

Effect Tests					
Source	Nparm	DF	Sum of Squares	F Ratio	Prob > F
Crosslinker	2	2	18.16267	2.3615	0.1563
Hydrophobe	1	1	204.36300	53.1423	<.0001*
Silica Type	4	4	24.45867	1.5900	0.2670
Crosslinker*Hydrophobe	2	2	134.31200	17.4632	0.0012*
Crosslinker*Silica Type	8	8	46.12733	1.4994	0.2900
Hydrophobe*Silica Type	4	4	14.68533	0.9547	0.4813

Figure 5.15 Statistical Data Showing Results from an Effects Test.

Where:

- **Source:**
 - lists the names of the effects in the model.
- **Nparm:**
 - is the number of parameters associated with the effect. Continuous effects have one parameter. Nominal effects have one less parameter than the number of levels. Crossed effects multiply the number of parameters for each term. Nested effects depend on how levels occur.
- **DF:**
 - is the degrees of freedom for the effect test. Ordinarily Nparm and DF are the same. They are different if there are linear combinations found among the regressors such that an effect cannot be tested to its fullest extent. Sometimes the DF will even be zero, indicating that no part of the effect is testable. Whenever DF is less than Nparm, the note Lost DFs appears to the right of the line in the report.
- **Sum of Squares:**
 - is the sum of squares for the hypothesis that the listed effect is zero.
- **F Ratio:**
 - is the F-statistic for testing that the effect is zero. It is the ratio of the mean square for the effect divided by the mean square for error. The mean square for the effect is the sum of squares for the effect divided by its degrees of freedom.
- **Prob>F:**
 - is the significance probability for the F-ratio. It is the probability that if the null hypothesis is true, a larger F-statistic would only occur due to random error. Values less than 0.0005 appear as 0.0000, which is conceptually zero.

The two parameters with an asterisk accompanying the Prob>F value signify that they are statistically significant. This means, as expected, that the hydrophobe type does indeed have an effect on the water contact angle of a given sample. This is especially true, and verified, by the effect of the Crosslinker*Hydrophobe parameter. As pointed out in **Sections 5.3.1, 5.3.2, and 5.3.3**, the use of n-decyltriethoxysilane in the place of n-octyltrimethoxysilane does offer a noticeable difference in the contact angle of the

sample. In the similar cases, the samples made with tetramethoxysilane and tetraethoxysilane as opposed to bis(triethoxysilyl)ethane have a statistically significant difference in the contact angle. To help display other trends that may be difficult to see in either **Table 5.1** or **Figure 5.14**, refer to **Figure 5.16**.

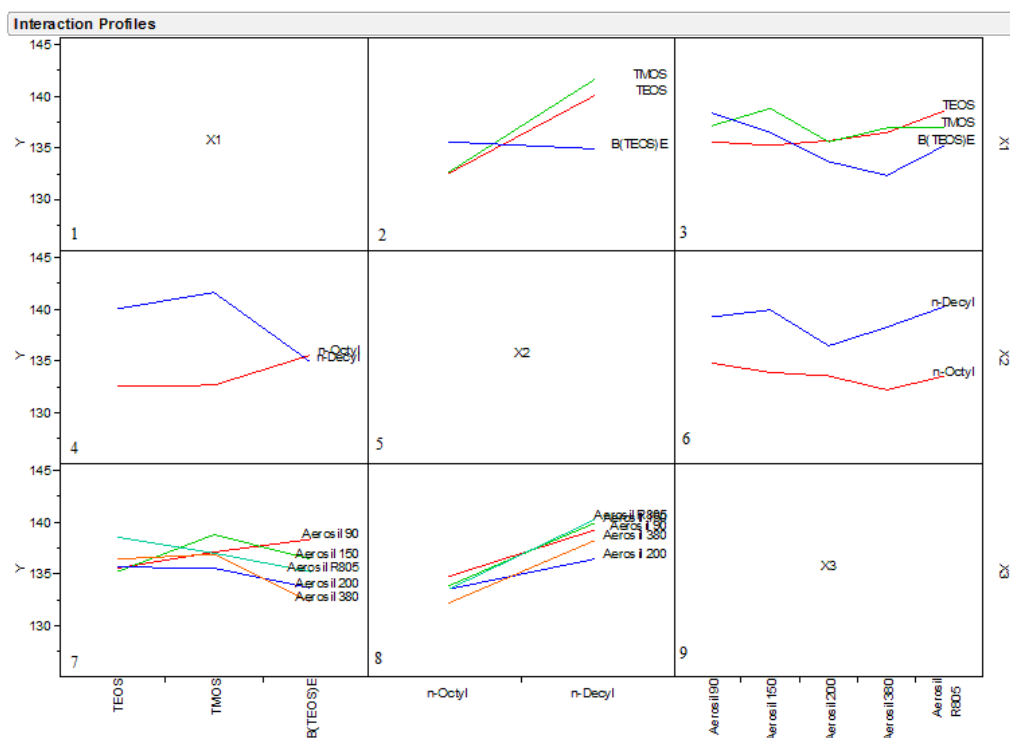


Figure 5.16 Interaction Profiles for the Design of Experiments.

Where:

- **Y** denotes resultant average contact angle
- **X1** denotes crosslinker type
- **X2** denotes hydrophobe type
- **X3** denotes silica nanoparticle type

This figure makes viewing trends and interactions a lot easier. The most prominent trends are perhaps those of between the hydrophobes and crosslinkers. These can be seen in the second and fourth plots from the top left-hand side of the figure. The sharp

positive slopes of the TMOS and TEOS lines in the Contact Angle vs. Hydrophobe plot shows the effect that n-decyltriethoxysilane has on those two crosslinkers. It can be seen, too, that the hydrophobes do not have an effect on the crosslinker bis(triethoxysilyl)ethane. This same effect is shown, though in a different way, in the fourth plot in the figure. The distance between the two lines again shows that there is a significant difference between TEOS samples made with n-octyltrimethoxysilane and n-decyltriethoxysilane. This statement holds true for samples made with TMOS as well. Plots three, six, and seven do not display any significant trends or behavior. These plots all suggest that a change in silica type (hydrophilic, hydrophobic, and particle diameter) will not make a significant change in the resultant water contact angle for the systems used in this study.

5.4. Comparison of Three DOE Samples to Their Counterparts Without Silica

Once the best samples from each set of crosslinkers was determined and their non-silica counterparts were made and tested for contact angle, a comparison was done. This was to show the benefit that the addition of the silica nanoparticles makes to the overall hydrophobic system. The graph in **Figure 5.17** shows the comparison of the samples and **Table 5.2** gives the data shown in the graph.

Sample:	Key:	Average WCA:	Std. Dev.:
TEOS, n-Decyltriethoxysilane, Aerosil® R805	TE-D-R	142.5°	3.3°
TEOS, n-Decyltriethoxysilane, NO Silica	TE-D	131.8°	3.9°
TMOS, n-Decyltriethoxysilane, Aerosil® 380	TM-D-3	144.2°	5.5°
TMOS, n-Decyltriethoxysilane, NO Silica	TM-D	133.2°	2.9°
Bis(triethoxysilyl)ethane, n-Octyltrimethoxysilane, Aerosil® 90	B-O-9	139.1°	5.8°
Bis(triethoxysilyl)ethane, n-Octyltrimethoxysilane, NO Silica	B-O	126.2°	4.2°

Note: In the key, where there is no third letter or number, it means silica was omitted from the recipe.

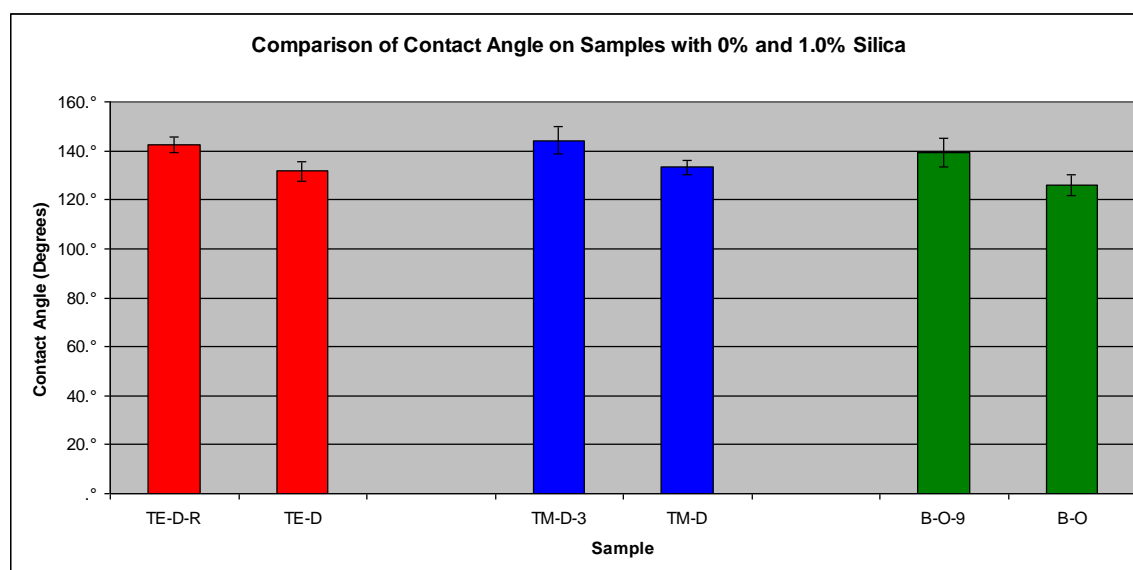


Figure 5.17 Graph Comparing Contact Angle on Samples Chosen from the DOE Made With and Without Silica Nanoparticles.

An obvious trend is seen here. Each of the samples, when prepared using silica nanoparticles, has a higher contact angle than the samples without the silica. Each of the samples boasts a difference of at least 10.0°. The samples prepared with bis(triethoxysilyl)ethane, n-octyltrimethoxysilane, and Aerosil® 90 had a contact angle (139.1°) that was 12.9° higher than the samples prepared with bis(triethoxysilyl)ethane,

n-octyltrimethoxysilane, and no silica (126.2°). The tetraethoxysilane and tetramethoxysilane samples had similar decreases in contact angle when prepared without silica. The difference between tetraethoxysilane samples was 10.7° and the difference between tetramethoxysilane samples was 11.1°. The addition of silica nanoparticles certainly advances the contact angle of the samples to which they are applied. They are certainly achieving their job of greatly increasing the surface microroughness of the samples to increase the contact angle of the samples. An analysis of how the silica nanoparticles affect the durability of the samples is given in **Sections 5.5** and **5.6**.

5.5. Results of Samples After Washing to Those Before Washing, With and Without Heat Drying

The contact angle results of the tetraethoxysilane and tetramethoxysilane samples after being subjected to the accelerated laundering tests were poor. There was no consistency within or between these sample sets. However, the samples made with the crosslinker bis(triethoxysilyl)ethane showed promising behavior. At least one sample tested for average water contact angle in the sets made from either tetraethoxysilane or tetramethoxysilane displayed absorbent behavior. Because there was so much disparity in the samples tested, showing graphical representations or data tables of the results will not give an accurate idea of the behavior. It is not expressly believed that the absorbance of water by some of the samples was due to residual detergent on the surface of the textiles. It is most likely due to the de-crystallization of the alkyl chains on the fabric surface. When not in crystalline form, these chains do not have the ability to give the fabric a high contact angle.

5.5.1. Samples Made With Bis(triethoxysilyl)ethane

Of all the samples tested, only those made with bis(triethoxysilyl)ethane retained their hydrophobic nature. This may have been due to the fact that they were made with the crosslinker bis(triethoxysilyl)ethane or the hydrophobe n-octyltrimethoxysilane. It is true that the stiffer nature of these samples helped them to withstand the vigor of the accelerated laundering test in comparison to the samples made with TEOS and TMOS, which did lose their shape and some yarns from the strong mechanical action. Graphical comparisons can be made here from the samples because of the nature of the results. **Figure 5.20** shows a comparison of the samples, both with and without silica, to those before the laundering tests.

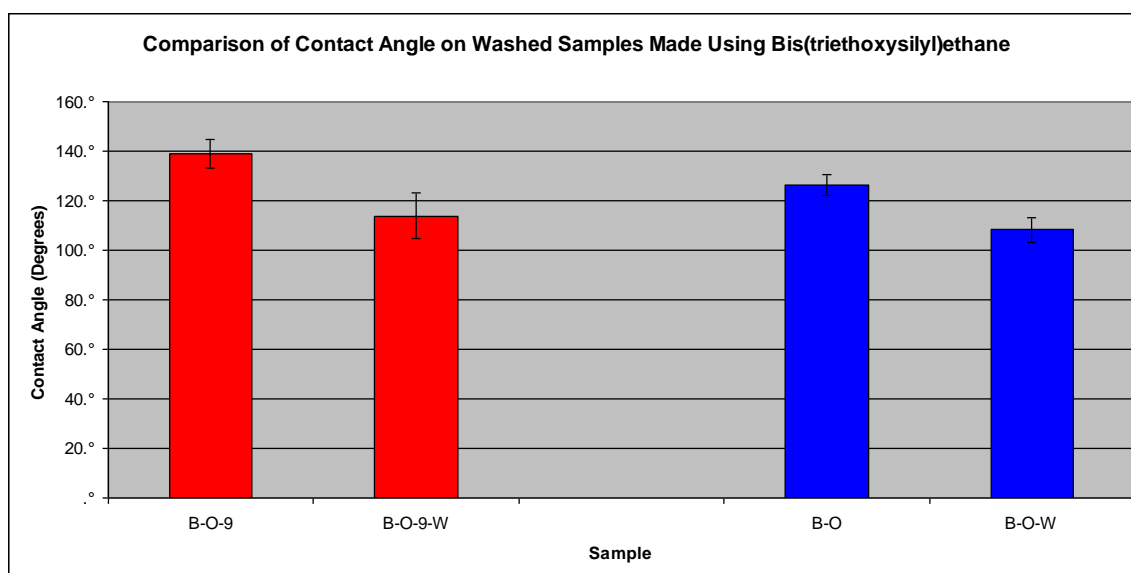


Figure 5.20 Graph Comparing Contact Angle on Bis(triethoxysilyl)ethane Samples Before and After the Accelerated Laundering Test.

where:

- B-O-9 is Bis(triethoxysilyl)ethane, n-Octyltrimethoxysilane, Aerosil® 90
- B-O-9-W is Bis(triethoxysilyl)ethane, n-Octyltrimethoxysilane, Aerosil® 90 - Washed
- B-O is Bis(triethoxysilyl)ethane, n-Octyltrimethoxysilane, No Silica
- B-O-W is Bis(triethoxysilyl)ethane, n-Octyltrimethoxysilane, No Silica - Washed

Though there are some larger differences between the unwashed and the washed samples, the results are somewhat encouraging because the washed samples did maintain some of their hydrophobic nature. There was a difference of 25.3° between the washed and unwashed samples made using Aerosil® 90 silica. The washed samples had an average value of 113.8° with a standard deviation of 9.34° , which is a little higher than would be liked. The samples without silica had a lower difference than those with silica, at 17.9° . Though the average value of the non-silica containing samples was 108.2° and lower than the silica containing samples, the standard deviation was lower (5.14° , lowest of all washed samples tested). There was a difference of 5.6° between the washed samples

(silica containing to non-silica containing), but because of the high standard deviation value of the silica samples, this difference in values may be non-significant. This suggests that the presence of silica in the samples does not have a significant effect on the contact angle of the samples after laundering.

When these samples were again subjected to the heat drying step, a significant improvement was seen in the samples prepared with silica. The heat dried silica-containing samples had a contact angle of 121.2°, an improvement of 7.4° when compared to the value of 113.8° for the air-dried samples. It is clear that the silica nanoparticles do offer a significant improvement in the heat drying step. There was only a minor difference of 1.2° between the non-silica samples. These differences are best seen in **Table 5.5** and **Figure 5.21** below.

Table 5.3 Comparison of Contact Angle on Washed and Unwashed Samples Made With Bis(triethoxysilyl)ethane			
Sample:	Key:	Average WCA:	Std. Dev.:
Bis(triethoxysilyl)ethane, n-Octyltrimethoxysilane, Aerosil® 90	B-O-9	139.1°	5.8°
Bis(triethoxysilyl)ethane, n-Octyltrimethoxysilane, Aerosil® 90 - Wash Sample	B-O-9-W	113.8°	9.3°
Bis(triethoxysilyl)ethane, n-Octyl, Aerosil® 90 - Wash & Heat Dried	B-O-9-W-HD	121.2°	5.8°
Bis(triethoxysilyl)ethane, n-Octyltrimethoxysilane, NO Silica	B-O	126.2°	4.2°
Bis(triethoxysilyl)ethane, n-Octyltrimethoxysilane, NO Silica - Wash Sample	B-O-W	108.2°	5.1°
Bis(triethoxysilyl)ethane, n-Octyl, No Silica - Wash & Heat Dried	B-O-W-HD	109.4°	5.0°

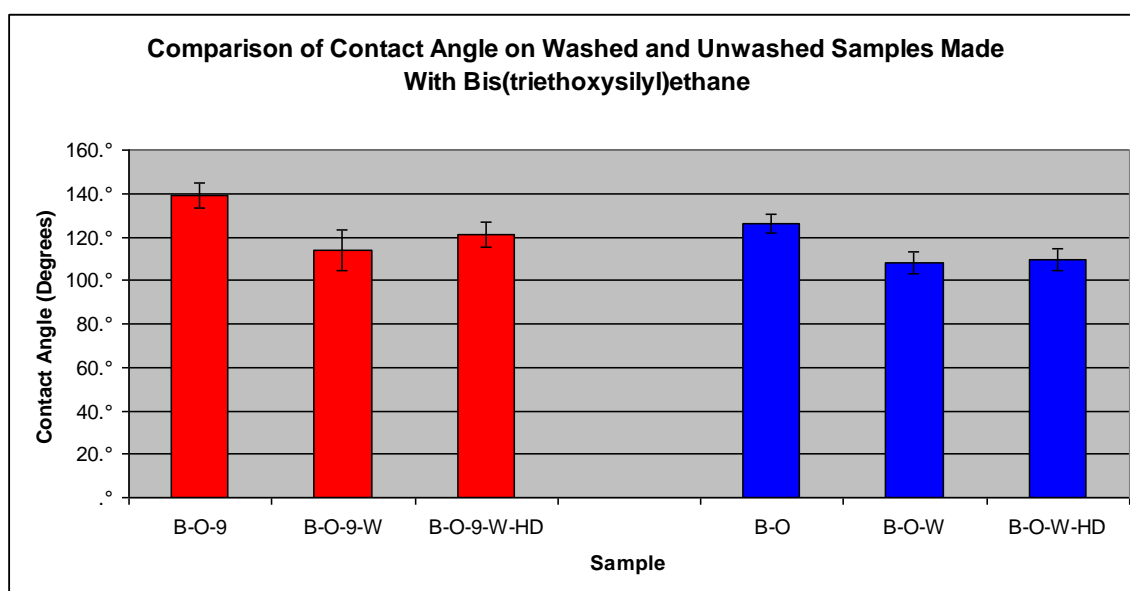


Figure 5.21 Graph Comparing Contact Angle on Washed and Unwashed Samples Made With Bis(triethoxysilyl)ethane.

Not only did the samples that were heat dried have higher contact angles, but they also had lower standard deviations especially the silica-containing sample. This means that more samples were centered around those mean values. The performance of the samples prepared with bis(triethoxysilyl)ethane, n-octyltrimethoxysilane, and Aerosil[®] 90 after laundering and heat drying were so good, that they were almost able to reach the contact angle values of the samples prepared with bis(triethoxysilyl)ethane, n-octyltrimethoxysilane, and no silica before they were washed. There was only a difference of 4.9° between the two.

5.5.2. Samples Made With Tetraethoxysilane

Perhaps the most inconsistent set of samples tested were those made with tetraethoxysilane, n-decyltriethoxysilane, and Aerosil[®] R 805. Of the three samples in the set tested, one sample was weakly absorbent. When the sample was placed on the

goniometer for contact angle testing and a water droplet was placed on the surface, the contact angle changed from approximately 90° to 40° until the droplet was absorbed into the fabric. Equally as odd, the remaining two samples in the set tested had average contact angles of 114.7° and 82.5° , respectively. This set, having one sample being absorbent, one being weakly hydrophilic, and one weakly hydrophobic shows no consistency and offers no confidence in the ability of the sample to resist laundering. The samples made without silica (tetraethoxysilane and n-decyltriethoxysilane) showed somewhat more consistent behavior. In spite of the more consistent nature, the samples tested could not be considered wholly hydrophobic. On all but two occasions, the samples had contact angles under 90° and one spot in the first sample absorbed the droplet after 90 sec. Disregarding the absorbent spot, the other sixteen measurements taken had an average of 82.6° with a standard deviation of 13.01° . The standard deviation of these measurements shows the amount of variability in the samples. Regardless of the variability, these samples do show the tendency to be more hydrophilic than hydrophobic.

When the same samples were subjected to a heat drying step after they were washed and rinsed, improvement was shown. The samples resisted the absorbance of water and showed contact angles greater than 90° . **Table 5.3** and **Figure 5.18** show a comparison of the DOE samples (both with and without silica) made with tetraethoxysilane to those that were subjected to laundering and a heat drying step.

Table 5.4 Comparison of Contact Angle on Washed & Heat Dried TEOS Samples to DOE Samples			
Sample:	Key:	Average WCA:	Std. Dev.:
TEOS, n-Decyltriethoxysilane, Aerosil [®] R805	TE-D-R	142.5°	3.3°
TEOS, n-Decyl, Aerosil [®] R805 - Washed & Heat Dried	TE-D-R-W-HD	100.4°	10.1°
TEOS, n-Decyltriethoxysilane, NO Silica	TE-D	131.8°	3.9°
TEOS, n-Decyl, No Silica - Washed & Heat Dried	TE-D-W-HD	96.3°	7.5°

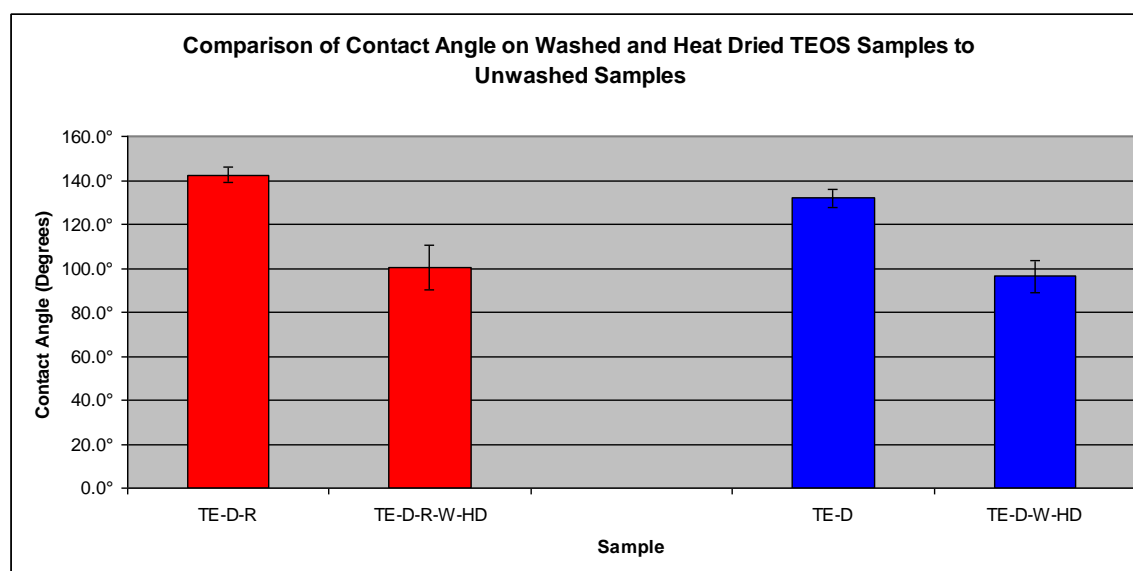


Figure 5.18 Graph Comparing Contact Angle of Washed and Heat Dried TEOS Samples to Unwashed Samples.

Though there was nowhere near 100% contact angle recovery, the heat drying step is a large improvement over the behavior of the air-dried samples. The samples made with silica show only a slight, if at all significant, advantage over those made without silica. However, the difference between the washed and unwashed samples was greater in the silica-containing samples, at 42.1° (versus the non-silica samples at 35.5°).

Unfortunately, the silica-containing sample that was washed and heat-dried had a very

high standard deviation. As can be seen in **Appendix A**, the measured values that constitute the average given were extremely varied. The values varied from just under 90° to just over 110° . However, the larger values outweighed the smaller values giving an overall average of over 100° , suggesting that the overall sample was slightly hydrophobic.

5.5.3. Samples Made With Tetramethoxysilane

The samples made with tetramethoxysilane, n-decyltriethoxysilane, and Aerosil[®] 380 were the most absorbent of all the samples tested. Five of the nine spots tested in the three samples absorbed water after approximately 90 sec. The remaining four spots had an average contact angle of 80.4° and a standard deviation of 6.50° . Again, the behavior displayed here shows that even when the samples did not eventually absorb water, they were weakly hydrophilic due to the average contact angle being less than 90° .

The other set of samples made with tetramethoxysilane, n-decyltriethoxysilane, and no silica behaved slightly better than those with silica. One of the samples in the set of three was absorbent in all spots. However, unlike the samples made with silica, the samples started to absorb water after 60 sec instead of 90 sec. The remaining two samples that were not absorbent had an average contact angle of 79.7° and a standard deviation of 6.43° . These values are essentially equivalent to the values of the samples made with silica. This suggests that the silica nanoparticles do not play a significant role in the washfastness of the hydrophobic treatments made with either tetraethoxysilane or tetramethoxysilane.

These samples, when subjected to the heat drying step, did not show as much improvement as the samples made with tetraethoxysilane. The samples prepared with silica did not at all absorb water, but had an average contact angle of 80.2°. This was a 64.0° departure from the original DOE sample. The non-silica sample had a very slightly hydrophobic contact angle at 92.3°. **Table 5.4** and **Figure 5.19** show a comparison of the DOE samples (both with and without silica) made with tetramethoxysilane to those that were subjected to laundering and a heat drying step.

Table 5.5 Comparison of Contact Angle on Washed & Heat Dried TMOS Samples to DOE Samples			
Sample:	Key:	Average WCA:	Std. Dev.:
TMOS, n-Decyltriethoxysilane, Aerosil® 380	TM-D-3	144.2°	5.5°
TMOS, n-Decyl, Aerosil® 380 - Wash & Heat Dried	TM-D-3-W-HD	80.2°	4.4°
TMOS, n-Decyltriethoxysilane, NO Silica	TM-D	133.2°	2.9°
TMOS, n-Decyl, No Silica - Wash & Heat Dried	TM-D-W-HD	92.3°	13.6°

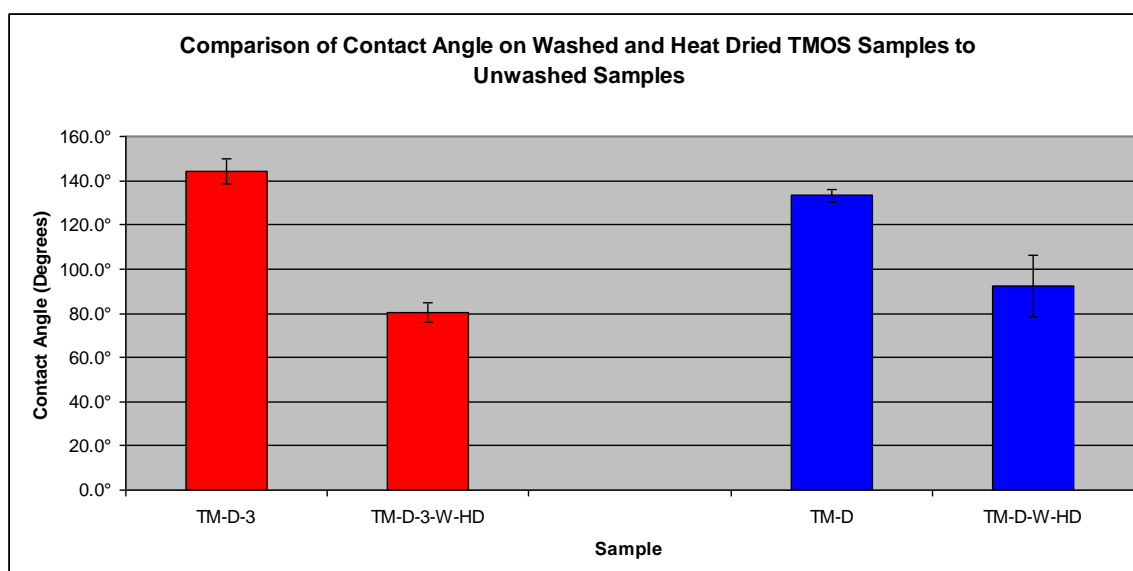


Figure 5.19 Graph Comparing Contact Angle of Washed and Heat Dried TMOS Samples to Unwashed Samples.

As can be seen in the table, the washed and heat dried sample prepared without silica has an extremely high standard deviation. The measured values for this sample (in **Appendix A**) ranged from 77° to 127°. The chance of one of these samples having a contact angle above 90° is just as good as it having a contact angle below 90°. Again, the samples prepared with tetramethoxysilane showed very varied and inconsistent behavior.

5.6. Results of Samples Produced With Ultrasonicated Solutions and Subjected to Laundering

The results described in the preceding sections show that the use of silica nanoparticles in conjunction with certain chemicals can certainly enhance the washfastness of the treatment. However, it is limited in some respects and has room for improvement. The theory behind using a solution to coat the fabric that has been subjected to ultrasonic energy is to further break up the silica nanoparticle agglomerates for better fixation to the

fabric. It was evident that a method needed to be examined after the washfastness performance of the samples prepared with both tetramethoxysilane and tetraethoxysilane. The following sections will address the usefulness of the sonication procedure.

5.6.1. Comparison of Sonicated Samples to DOE Samples

All of the samples, when prepared with ultrasonicated solutions, had a lower average contact angle than their DOE counterparts. The differences did not exceed 10° in the three instances, but they should be noted. The largest difference came with the sample prepared with bis(triethoxysilyl)ethane, n-octyltrimethoxysilane, and Aerosil[®] 90. The difference was on the order of 9.4° . **Table 5.6** and **Figure 5.22** show a comparison of the samples prepared with sonicated solutions to the normal DOE samples.

Table 5.6 Comparison of Contact Angle on Sonicated Samples to Unsonicated Samples			
Sample:	Key:	Average WCA:	Std. Dev.:
TEOS, n-Decyltriethoxysilane, Aerosil [®] R805	X	142.5°	3.3°
TEOS, n-Decyl, Aerosil [®] R805 - Sonicated	X-s	138.0°	4.6°
TEOS, n-Decyltriethoxysilane, NO Silica	X-a	131.8°	3.9°
TMOS, n-Decyltriethoxysilane, Aerosil [®] 380	XIX	144.2°	5.5°
TMOS, n-Decyl, Aerosil [®] 380 - Sonicated	XIX-s	136.4°	4.8°
TMOS, n-Decyltriethoxysilane, NO Silica	XIX-a	133.2°	2.9°
Bis(triethoxysilyl)ethane, n-Octyltrimethoxysilane, Aerosil [®] 90	XXI	139.1°	5.8°
Bis(triethoxysilyl)ethane, n-Octyl, Aerosil [®] 90 - Sonicated	XXI-s	129.7°	3.5°
Bis(triethoxysilyl)ethane, n-Octyltrimethoxysilane, NO Silica	XXI-a	126.2°	4.2°

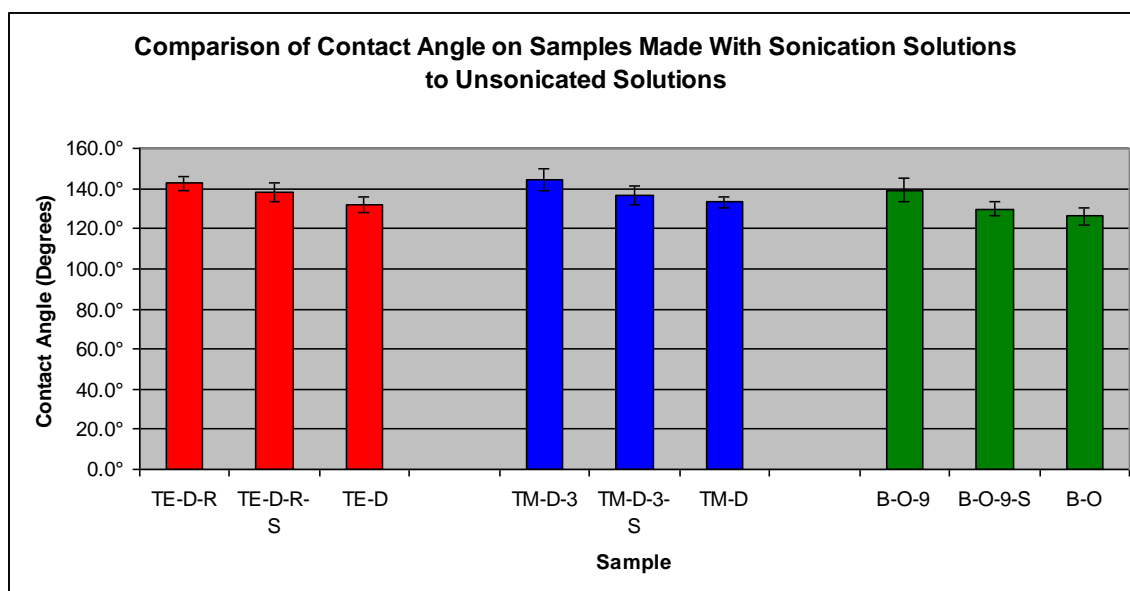


Figure 5.22 Graph Comparing Contact Angle on DOE Samples to Samples Made With Sonicated Solutions and Samples Made Without Silica.

The tetraethoxysilane samples had the smallest difference, at 4.5° . The samples prepared with tetramethoxysilane had a difference of 7.8° . These differences will be important for later analysis of how the washed samples compare to both the samples with and without sonicated solutions. It is possible that because the agglomerates were broken up that some of the repellent effect that the microroughness created was lost. A more even coating due to the more individualized particles could be the cause of a loss in the microroughness. Whether or not the sacrifice in initial contact angle was acceptable remains to be seen in the washfastness data, because if the samples are able to retain or achieve a higher contact angle after washing than the DOE samples, the treatment will have been a success. As the graphical trends show, though the sonicated samples all have lower collective contact angles than the non-sonicated, silica containing samples, these

sonicated samples still have higher contact angles than the samples prepared without silica.

5.6.2. Comparison of Washfastness Results of Sonicated Samples to Non-Sonicated Samples

The sonication process had varying results on the washfastness of the samples that were treated. In general, the sonicated solutions made with both tetraethoxysilane and tetramethoxysilane produced samples that absorbed water after washing (when air-dried). The sonicated-solution sample of bis(triethoxysilyl)ethane had an average contact angle of 107.6° after washing and air-drying, which is comparable to the non-sonicated sample made with bis(triethoxysilyl)ethane, n-octyltrimethoxysilane, and no silica (108.2° , after washing and air-drying).

When subjected to a heat drying step, all of the samples made with sonicated solutions showed much improved behavior when tested for contact angle (in comparison to the same samples that were air-dried). The samples prepared with tetraethoxysilane and tetramethoxysilane resisted the absorption of water, but gave low, hydrophilic contact angles of 79.8° and 77.6° , respectively. The sample made with bis(triethoxysilyl)ethane, on the other hand, gave the highest contact angle of all the samples tested after laundering (including non-sonicated solution samples and those subjected to drying). It had an average contact angle of 123.1° , which is only a 6.6° difference from the original sample before laundering.

Since a lot of comparisons can be made from this sample set, it is best to refer to **Table 5.7** and **Figure 5.23**.

Sample:	Key:	Average WCA:	Std. Dev.:
TEOS, n-Decyltriethoxysilane, Aerosil® R805	TE-D-R	142.5°	3.3°
TEOS, n-Decyltriethoxysilane, Aerosil® R805 - Wash Sample	TE-D-R-W	abs	abs
TEOS, n-Decyl, Aerosil® R805 - Washed & Heat Dried	TE-D-R-W-HD	100.4°	10.1°
TEOS, n-Decyltriethoxysilane, NO Silica	TE-D	131.8°	3.9°
TEOS, n-Decyltriethoxysilane, NO Silica - Wash Sample	TE-D-W	abs	abs
TEOS, n-Decyl, No Silica - Washed & Heat Dried	TE-D-W-HD	96.3°	7.5°
TEOS, n-Decyl, Aerosil® R805 - Sonicated	TE-D-R-S	138.0°	4.6°
TEOS, n-Decyl, Aerosil® R805 - Sonicated & Washed	TE-D-R-S-W	abs	abs
TEOS, n-Decyl, Aerosil® R805 - Sonicated, Washed, & Heat Dried	TE-D-R-S-W-HD	79.8°	5.0°
TMOS, n-Decyltriethoxysilane, Aerosil® 380	TM-D-3	144.2°	5.5°
TMOS, n-Decyltriethoxysilane, Aerosil® 380 - Wash Sample	TM-D-3-W	abs	abs
TMOS, n-Decyl, Aerosil® 380 - Wash & Heat Dried	TM-D-3-W-HD	80.2°	4.4°
TMOS, n-Decyltriethoxysilane, NO Silica	TM-D	133.2°	2.9°
TMOS, n-Decyltriethoxysilane, NO Silica - Wash Sample	TM-D-W	abs	abs
TMOS, n-Decyl, No Silica - Wash & Heat Dried	TM-D-W-HD	92.3°	13.6°
TMOS, n-Decyl, Aerosil® 380 - Sonicated	TM-D-3-S	136.4°	4.8°
TMOS, n-Decyl, Aerosil® 380 - Sonicated & Washed	TM-D-3-S-W	abs	abs
TMOS, n-Decyl, Aerosil® 380 - Sonicated, Washed, & Heat Dried	TM-D-3-S-W-HD	77.6°	5.3°
Bis(triethoxysilyl)ethane, n-Octyltrimethoxysilane, Aerosil® 90	B-O-9	139.1°	5.8°
Bis(triethoxysilyl)ethane, n-Octyltrimethoxysilane, Aerosil® 90 - Wash Sample	B-O-9-W	113.8°	9.3°
Bis(triethoxysilyl)ethane, n-Octyl, Aerosil® 90 - Wash & Heat Dried	B-O-9-W-HD	121.2°	5.8°
Bis(triethoxysilyl)ethane, n-Octyltrimethoxysilane, NO Silica	B-O	126.2°	4.2°
Bis(triethoxysilyl)ethane, n-Octyltrimethoxysilane, NO Silica - Wash Sample	B-O-W	108.2°	5.1°
Bis(triethoxysilyl)ethane, n-Octyl, No Silica - Wash & Heat Dried	B-O-W-HD	109.4°	5.0°
Bis(triethoxysilyl)ethane, n-Octyl, Aerosil® 90 - Sonicated	B-O-9-S	129.7°	3.5°
Bis(triethoxysilyl)ethane, n-Octyl, Aerosil® 90 - Sonicated & Washed	B-O-9-S-W	107.6°	3.7°
Bis(triethoxysilyl)ethane, n-Octyl, Aerosil® 90 - Sonicated, Washed, & Heat Dried	B-O-9-S-W-HD	123.1°	4.8°

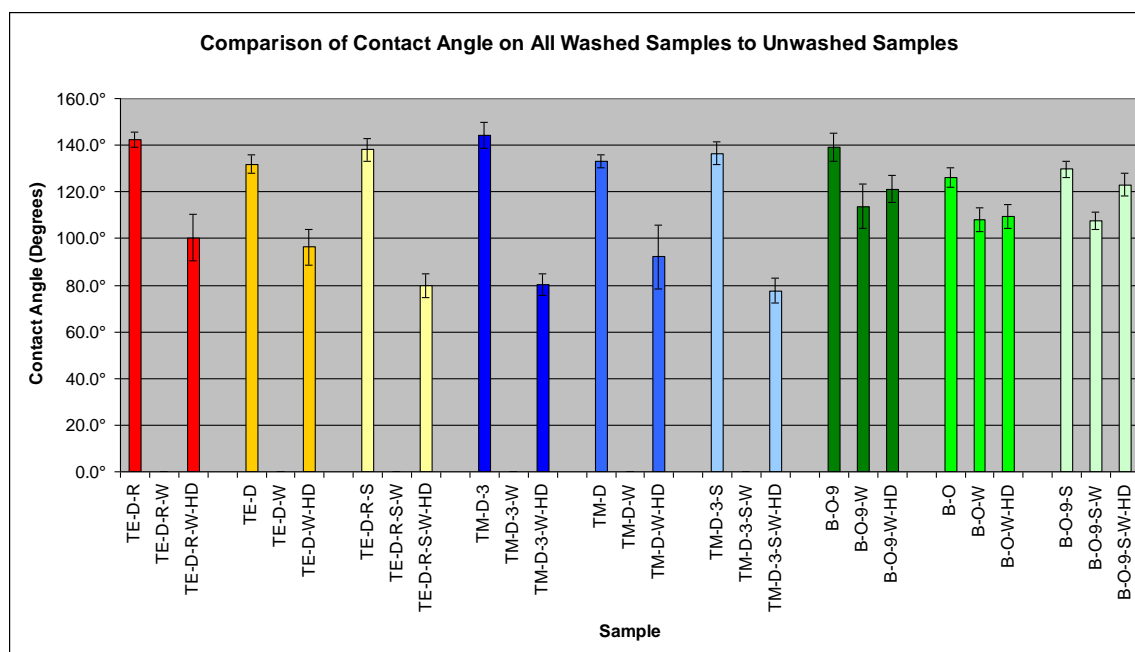


Figure 5.23 Graph Comparing Contact Angle on All Unwashed and Washed Samples.

Where no bar is seen, it is represented by the abbreviation “abs” in the table, taken to mean fully or partially absorbent and no value is given. The results from all of the samples made with the crosslinker bis(triethoxysilyl)ethane, especially when made from sonicated solutions, are the most interesting and of note. This is because the sonication process hurt the contact angle of the heat dried samples prepared with tetraethoxysilane and tetramethoxysilane. Both of these sub-80° values were less than the heat dried samples than their DOE counterparts, both with and without silica. This suggests that the sonication was actually a step backward in the processing of these samples. However, great promise is shown in the bis(triethoxysilyl)ethane samples when prepared from sonicated solutions. The 123.1° average contact angle obtained from this sample is only 3.1° from the unlaundered sample prepared from bis(triethoxysilyl)ethane, n-

octyltrimethoxysilane, and no silica. This high recovery due to the heat drying step is very promising that with some work on process optimization the samples could approach 100% recovery.

5.7. Results of Samples After Crocking to Those Before Crocking

The samples subjected to the AATCC modified crocking test displayed a lot of variability and inconsistency between and within similar sample sets. The differences between samples ranged from a negligible 1.2° to a substantial 26.1°. The data for the differences between the crocked and uncrocked samples is shown in **Table 5.8** and represented graphically in **Figure 5.24**.

Table 5.8 Comparison of Contact Angle on Crocked Samples to Uncrocked Samples			
Sample:	Key:	Average WCA:	Std. Dev.:
TEOS, n-Decyltriethoxysilane, Aerosil® R805	TE-D-R	142.5°	3.3°
TEOS, n-Decyltriethoxysilane, Aerosil® R805 - Crock Sample	TE-D-R-C	130.7°	3.2°
TEOS, n-Decyltriethoxysilane, NO Silica	TE-D	131.8°	3.9°
TEOS, n-Decyltriethoxysilane, NO Silica - Crock Sample	TE-D-C	123.4°	3.4°
TMOS, n-Decyltriethoxysilane, Aerosil® 380	TM-D-3	144.2°	5.5°
TMOS, n-Decyltriethoxysilane, Aerosil® 380 - Crock Sample	TM-D-3-C	118.1°	8.1°
TMOS, n-Decyltriethoxysilane, NO Silica	TM-D	133.2°	2.9°
TMOS, n-Decyltriethoxysilane, NO Silica - Crock Sample	TM-D-C	123.4°	7.3°
Bis(triethoxysilyl)ethane, n-Octyltrimethoxysilane, Aerosil® 90	B-O-9	139.1°	5.8°
Bis(triethoxysilyl)ethane, n-Octyltrimethoxysilane, Aerosil® 90 - Crock Sample	B-O-9-C	118.6°	6.8°
Bis(triethoxysilyl)ethane, n-Octyltrimethoxysilane, NO Silica	B-O	126.2°	4.2°
Bis(triethoxysilyl)ethane, n-Octyltrimethoxysilane, NO Silica - Crock Sample	B-O-C	124.9°	3.9°

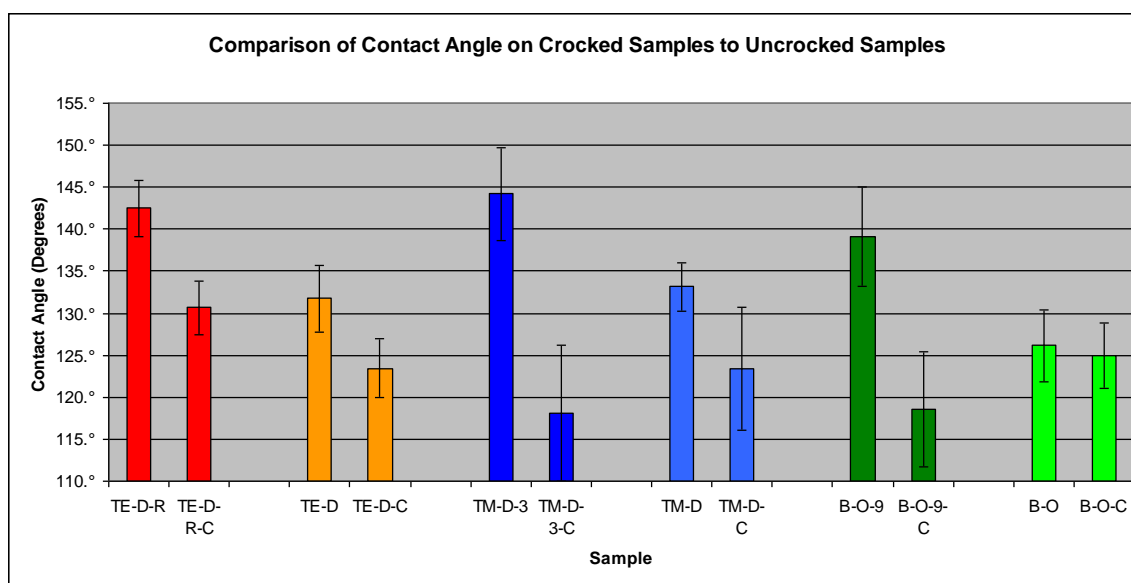


Figure 5.24 Graph Comparing Contact Angle on Samples Chosen from the DOE Subjected to Crocking (Before and After).

As can be seen, these results are very mixed. The highest difference came from the samples prepared with tetramethoxysilane, n-decyltriethoxysilane, and Aerosil[®] 380 at 26.1°. The next highest value difference came from the samples prepared with bis(triethoxysilyl)ethane, n-octyltrimethoxysilane, and Aerosil[®] 90 at 20.5°. In fact, all of the samples prepared with silica nanoparticles exhibited lower resistance to crocking than the samples prepared without silica. The silica nanoparticles, though nanometer sized, are still macroscopic materials. The abrasion of the fabric from the crocking motion is more likely to wear off the particles from the surface (which have silane hydrophobes covalently bonded to them) than samples containing only silane hydrophobes covalently bonded to the surface of the fabric.

Most of the samples tested after being subjected to crocking showed a lot of variability during the contact angle testing. This is shown in the standard deviation values in **Table**

5.7. The variability could easily be due to the state of the samples after they were subjected to crocking. Random selection of spots to test on the samples after crocking and uneven surfaces could easily cause this. Crocking may not occur in a perfectly even fashion on the surface of the fabric, much like everyday abrasion situations in the use of common textiles.

5.8. Comparison of Results from This Research to Literature

When conducting research, the performance and results are the samples are most oftentimes meaningless unless compared to the results of other or similar samples. In this case, we are able to compare our results to those researchers mentioned in the literature review as well as to other samples prepared with different water repellent finish types (fluorochemical and silicone).

5.8.1. Comparison of Results to Literature Review Samples

Without restating the whole of **Section 2.7.4**, it can be seen by comparison that the contact angle values of the samples prepared in this research (before laundering or crocking) were comparable to or better than those prepared by researchers using similar chemicals. It must be noted, however, that not all researchers were using the same base substrate as was used in this research. On samples of polyamide (nylon) and polyester/cotton, Mahltig and Böttcher [24] showed that contact angles between 112° and 135° could be achieved with the hydrophobic additive octyltrimethoxysilane to sols prepared from tetraethoxysilane and tetraethoxysilane/ 3-glycidyloxypropyltriethoxysilane. Referring back to **Table 2.3**, it can be seen that on a polyester/cotton fabric that with a C16 hydrophobe (Hexadecyltrimethoxysilane) at 4.0

wt. % that a contact angle of 142° was achieved. This value compares with the samples prepared in this research with TEOS and TMOS crosslinkers, silica nanoparticles and a C10 hydrophobe (highest value being greater than 144°). With these samples, Mahltig and Böttcher [24] reported that after leaching with SDS solution at 40°C and drying at room temperature only coatings containing C8, C16 and TF hydrophobes contain still water repellent properties and contact angles in range of 127° to 131° were determined on the coated polyester/cotton. Though they did not follow the exact procedure as in this research, our samples prepared with the sonicated bis(triethoxysilyl)ethane, n-octyltrimethoxysilane, and Aerosil[®] 90 had similar contact angle values.

Daoud et al. [13] also prepared samples with similar results. Their fabrics prepared with TEOS, 3-glycidoxypropyltrimethoxysilane (GPTMS), and hexadecyltrimethoxysilane (HDTMS) on a woven cotton had a contact angle value of 135° after coating and 105° after 30 wash cycles. Again, these values are very comparable to those from this research, though our best performing samples did outperform those made from Daoud et al.'s [13] process. Textor et al. [52] also used 3-glycidoxypropyltrimethoxysilane to crosslink with the catalyst 1-methylimidazol and tridecafluoro-1,1,2,2-tetrahydrooctyl triethoxysilane as a fluorosilane hydrophobe on technical polyester fabric. They reported results of contact angle of up to 95° with as little as 1-2% added to the sol, far below our lowest reported value (note the use of a fluorosilane in Textor et al.'s [52] work). Yu et al. [59] reported contact angle values between 134° and 145° using sols made from TEOS and a perfluorooctylated quaternary ammonium silane coupling agent.

Perhaps the work most similar to many aspects of this research was that of Pipatchanchai and Srikulkit [38]. Their results of their direct usage of silica nanoparticles and sonication can be seen in **Table 2.8**. In this table, paying particular attention to their first two results columns, it can be seen that the coatings prepared in this research were far superior before laundering and comparable after laundering and heat-drying. At the highest concentration of both silica nanoparticles and silane hydrophobe, their values never exceed 122° .

5.8.2. Comparison of Results to Samples Made from Alternate Methods

In his 2007 thesis for the Institute, David Wade Tyner [55] evaluated the contact angle and water repellent performance of a traditional fluoropolymer finish applied by the pad-dry-cure method. His finish was applied to a twill-woven cotton substrate of $6.7 \text{ oz} / \text{yd}^2$ basis weight. With this finish, a contact angle of 157° was achieved before laundering. After 5 laundering cycles, a contact angle of 145° remained. These values translated to AATCC spray-test ratings of 100 and 95 (before laundering and after 5 laundering cycles respectively).

To compare to a traditional silicone finish, Gao and McCarthy [17] were able to create an ultrahydrophobic surface on a microfiber polyester fabric treated with a dimethylsilicone exhibiting advancing and receding contact angles of 170° and 165° , respectively.

Chapter 6: Conclusions and Recommendations for Future Work

6.1. Summary of Results

The scope of this work was primarily to determine what combinations and concentrations of silica nanoparticles and silane chemistry applied to a prepared (desized, scoured, bleached, and undyed) 100% cotton fabric would give the highest contact angle and water repellency. In addition, determining the effect of modified abrasion and laundering on the durability of the best-performing finishes was investigated.

- Water-repellent finishes can be produced on 100% cotton fabrics using a combination of silane hydrophobes (such as alkyltrialkoxysilanes) and silane crosslinkers (such as tetraethoxysilane).
- The contact angle of said water-repellent finishes can be increased at least 10° with the introduction of silica nanoparticles.
- The increase in chain length of the silane hydrophobe does increase the water contact angle of samples prepared with the crosslinkers tetraethoxysilane and tetramethoxysilane 7.4° and 6.9° , respectively. The increase in chain length of the silane hydrophobe does not increase the water contact angle of samples prepared with the crosslinker bis(triethoxysilyl)ethane.
- The finishes applied to the fabrics show better fastness to crocking than they do to laundering. The lowest contact angle of all the crocked samples was 118.1° , whereas the lowest contact angle for a laundered sample was 0° .

- The samples made with tetraethoxysilane and tetramethoxysilane that were subjected to heat-drying after laundering did not absorb water like those that were simply air-dried.
- The samples prepared with sonicated solutions had lower contact angles than solutions without sonicated solutions but higher contact angles than those prepared without silica:
 - Tetraethoxysilane, n-Decyltriethoxysilane, Aerosil® R805: 4.5° lower than unsonicated sample, 6.2° higher than non-silica sample.
 - Tetramethoxysilane, n-Decyltriethoxysilane, Aerosil® 380: 7.8° lower than unsonicated sample, 3.2° higher than non-silica sample.
 - Bis(triethoxysilyl)ethane, n-Octyltrimethoxysilane, Aerosil® 90: 9.4° lower than unsonicated sample, 3.5° higher than non-silica sample.
- The laundered and heat-dried samples prepared with sonicated and unsonicated bis(triethoxysilyl)ethane solutions the best washfastness:
 - Bis(triethoxysilyl)ethane, n-Octyltrimethoxysilane, Aerosil® 90 (Laundered and Heat-Dried): 121.2° (Unlaundered: 139.1°, 87.1% Recovery)
 - Bis(triethoxysilyl)ethane, n-Octyltrimethoxysilane, Aerosil® 90 (Sonicated Solution, Laundered and Heat-Dried): 123.1° (Sonicated, Unlandered: 129.7°, 94.9% Recovery)
- The most durable samples prepared in this research resulted in a good technology on which optimizations need to be done.

6.2. Recommendations for Future Work

There are several steps that can be taken to make this research even more valuable. Not all steps are related, but all would be valuable to broaden the range of this work. It is recommended that:

- This research should be continued and adapted to more common textile processing equipment and chemicals. Working in a water based medium (as opposed to ethanol) would be very important; however, steps would need to be taken so that process still produced good results. It would be equally as important, when working with water, to also adapt the process for padding machinery so that it would be easier to adapt for a scale-up and to help reduce the % solids on the fabric. When working with water, it would be important that the chemicals are *not* stirred for 24 hours as they are when made with ethanol, as this could cause polymerization of the silanes. Dispersement of the silica should be done for 24 hours and then the silane chemicals should be added to the mixture immediately before coating. This way, the hydrolysis of the silanes would take place on the fabric surface and more reaction would take place with the fabric itself as opposed to in the solution.
- This work should be continued on dyed, 100% cotton fabric. It would be important to apply the treatment to fabrics dyed with as many dye types as possible. It is possible that fabrics treated with reactive dyes may have less affinity for the treatment since hydroxyl sites are being occupied by colorants. This work would also be important for the evaluation of color change due to the

- water repellent treatment. Knowing the effect of color change (ΔE_{cmc}) would be an important aspect for the application of the treatment onto fabrics where aesthetics are important. Thirdly, since color leaching was a problem in the treatment of wool, polyester, and nylon fabrics, it would be important that solutions in which the fabrics are treated do not do the same to cotton fabrics.
- In the same vein, one type of testing that could not be done that may be of interest would be an AATCC test for a change in whiteness. In some cases during this research, some samples turned a pale yellow or brown color after the curing step in the laboratory oven. The laboratory ovens used in this study did not promote even heating or absolutely constant temperature. It may have been that some of the browning occurred for samples nearest the heating source. It would be a good test to evaluate for whiteness change if the samples were heated in a tenter or a line-curing system where the fabric is heated evenly and equidistant from the heating source.
 - For the samples that were prepared and tested for contact angle, it is of important interest to continue preparing fabric samples in the same way and test them using standard AATCC test methods for water repellency (spray test, impact penetration test, etc.). High contact angle does not always translate to high water repellency. This is necessary work because it will show the correlation between the samples with high contact angle and those are highly water repellent and further show the usefulness of this type of coating technology.

- A more detailed study of non-cellulosic fabrics should be done. Fabrics supplied by International Textile Group were used as-received and therefore may have had chemicals on them that did not allow for the treatment to fully function. Due to time constraints detailed work was not done to investigate the effect of the finishing.
- Experiments should be done on this work with the lower purity TEOS and TMOS chemicals (refer to **Section 4.3**). If the treatment research in this project were to be adapted by a company, it would be of special interest to know if the lower purity chemicals behaved on par with the high purity chemicals. The difference in cost is significant.
- Perhaps most importantly, this technology needs to be optimized now that the base work has been done to investigate it. A good combination of chemicals at various combinations processed at varying parameters should be investigated to give the best fabric hand and durability to laundering and crocking.

Chapter 7: References

- [1] *AATCC Test Method 8-2005 Colorfastness to Crocking: AATCC Crockmeter Method*; AATCC Technical Manual; 2007; Vol. 82, pp 17.
- [2] *AATCC Test Method 61-2006 Colorfastness to Laundering, Home and Commercial: Accelerated*; AATCC Technical Manual; 2007; Vol. 82, pp 86.
- [3] *AATCC Test Method 127-2003 Water Resistance: Hydrostatic Pressure Test*; AATCC Technical Manual; 2007; Vol. 82, pp 207.
- [4] Anamelechi, Charles C., George A. Truskey, and W. Monty Reichert. "Mylar™ and Teflon-AF™ as cell culture substrates for studying endothelial cell adhesion." *Biomaterials* 26 (2005), 6887–6896.
- [5] Anonymous. "Funding Opportunities." National Nanotechnology Initiative. 2007. National Nanotechnology Coordination Office. Feb. 28, 2007. <http://www.nano.gov/html/funding/home_funding.html>.
- [6] Arkles, Barry. Silanes Coupling Agents: Connecting Across Boundaries. 2nd Version. Morrisville, PA: Gelest, Inc., 2006.
- [7] Arkles, Barry and Gerald Larson. Metal-Organics for Materials, Polymers and Synthesis: A Survey of Properties and Chemistry. Morrisville, PA: Gelest, Inc., 2005.
- [8] Arkles, Barry and Gerald Larson. Silicon Compounds: Silanes and Silicons: A Survey of Properties and Chemistry. Morrisville, PA: Gelest, Inc., 2004.
- [9] Barthlott, W. and C. Neinhuis. "Purity of the sacred lotus, or escape from contamination in biological surfaces." *Planta* 202 (1997), 1-8.
- [10] Brown, John J., and Ralph A. Rusca. "The Effect of Fabric Structure on Fabric Properties." *Textile Research Journal* 25 (1955), 472-476.
- [11] Burton, Zachary and Bharat Bhushan. "Surface Characterization and Adhesion and Friction Properties of Hydrophobic Leaf Surfaces and Nanopatterned Polymers for Superhydrophobic Surfaces." *Applied Scanning Probe Methods III*. Ed.s B. Bhusan and H. Fuchs. Berlin: Springer, 2006. 55-81.
- [12] Černe, Lidija, and Barbara Simončič. "Influence of repellent finishing on the surface free energy of cellulosic textile substrates." *Text. Res. J.* 74 (2004), 426-432.

- [13] Daoud, Walid A., John H. Xin, and Xiaoming Tao. "Superhydrophobic silica nanocomposite coating by a low-temperature process." J. Am. Ceram. Soc. 87 (2004), 1782-1784.
- [14] Donath, Steffen, Holger Militz and Carsten Mai. "Creating water-repellent effects on wood by treatment with silanes." Holzforschung 60 (2006), 40-46.
- [15] Ebbing, Darrell D. and Steven D. Gammon. General Chemistry. 7th Edition. Boston: Houghton Mifflin, 2002.
- [16] El Ola, Samiha Mohamed Abo, Richard Kotek, W. Curtis White, John Allan Reeve, Peter Hauser, and Joon Ho Kim. "Unusual Polymerization of 3-(trimethoxysilyl)-propyldimethyloctadecyl Ammonium Chloride on PET Substrates." Polymer 45 (2004), 3215-3225.
- [17] Gao, Lichao and Thomas J. McCarthy. "'Artificial lotus leaf' prepared using 1 1945 patent and a commercial textile." Langmuir 22 (2006), 5998-6000.
- [18] Haas, Karl-Heinz, Sabine Amberg-Schwab, and Klaus Rose. "Functionalized coating materials based on inorganic-organic polymers." Thin Solid Films 351 (1999), 198-203.
- [19] Kaelble, D.H. "Dispersion-polar surface tension properties of organic solids." J. Adhesion 2 (1970), 66-81.
- [20] Lewandowski, Grzegorz, Egbert Meissner, and Eugeniusz Milchert. "Review: Special applications of fluorinated organic compounds." J. Haz. Mat. A136 (2006), 385-391.
- [21] Lichstein, Bernard M. "Stain and Water Repellency of Textiles." Surface Characteristics of Fibers and Textiles. Ed. M. J. Schick. New York, NY: Marcel Dekker, Inc., 1975. 495-524.
- [22] Ma, Minglin, and Randal M. Hill. "Superhydrophobic Surfaces." Current Opinion in Colloid & Interface Science 11 (2006), 193-202.
- [23] Mahltig, Boris, F. Audenaert, and Horst Böttcher. "Hydrophobic Silica Sol Coatings on Textiles—the Influence of Solvent and Sol Concentration." J. Sol-Gel Sci. Technol. 34 (2005), 103-109.
- [24] Mahltig, Boris, and Horst Böttcher. "Modified silica sol coatings for water-repellent textiles." J. Sol-Gel Sci. Technol. 27(2003), 43-52.

- [25] Mahltig, Boris, and Horst Böttcher. "Refining of textiles by nanosol coating." Melliand Textilber 83 (2002), 251-253.
- [26] Mahltig, Boris, Horst Böttcher, D. Knittel and E. Schollmeyer. "Incorporation of triarylmethane dyes into sol-gel matrices deposited on textiles." J. Sol-Gel Sci. Technol. 31 (2004), 293-297.
- [27] Mahltig, Boris, Helfried Haufe, and Horst Böttcher. "Functionalization of textiles by inorganic sol-gel coatings." J. Mater. Chem. 15 (2005), 4385-4398.
- [28] Mai, Carsten, and Holger Militz. "Modification of wood with silicon compounds. Inorganic silicon compounds and sol-gel system: a review." Wood Sci. Technol. 37 (2004), 339-348.
- [29] Mai, Carsten, and Holger Militz. "Modification of wood with silicon compounds. Treatment systems based on organic silicon compounds - a review." Wood Sci. Technol. 37 (2004), 453-461.
- [30] Michael, G., and Ferch, H. Basic Characteristics of Aerosil. Degussa Technical Bulletin Pigment no. 11. 1998.
- [31] Mondea, Takashi, Hiroyuki Fukubea, Fujito Nemotoa, Toshinobu Yokob and Takeo Konakahara. "Preparation and surface properties of silica-gel coating films containing branched-polyfluoroalkylsilane." Journal of Non-Crystalline Solids 246 (1999), 54-64.
- [32] Moses, Christopher D. "Fluid Flow in Nonwovens: Empirical Characterization of Multiphase Transport Properties." Research Proposal, May 10, 2004.
- [33] Nakagawa, Tohru, and Tatsuya Hiwatashi. "Water-repellent thin film with high alkali resistance using the sol-gel method for ink jet printer head." Jpn. J. Appl. Phys. 41 (2002), 3896-3901.
- [34] Nave, C.R. "Surface Tension." Hyperphysics. 2005. Georgia State University. 24 Feb. 2007 <<http://hyperphysics.phy-astr.gsu.edu/hbase/surten.html>>.
- [35] Owens, Jeffery R. *Microwave Promoted Coupling of Siloxanes to Hydroxyl Containing Substrates for Facile Synthesis of Chemical and Biological Warfare Agent Reactive Polymers*. Graduate Seminar. Textile & Apparel, Technology & Management Department, North Carolina State University, USA. 06 February 2008.
- [36] Owens, D.K., and R.C. Wendt. "Estimation of the surface free energy of polymers." J. Appl. Polym. Sci. 13 (1969), 1741-1747.

[37] Pilotek, S., and H.K. Schmidt. "Wettability of Microstructured Hydrophobic Sol-Gel Coatings." J. Sol-Gel Sci. Technol. 26 (2003), 789-792.

[38] Pipatchanchai, Thanwarat, and Kawee Srikulkit. "Hydrophobicity Modification of Woven Cotton Fabric by Hydrophobic Fumed Silica Coating." J. Sol-Gel Sci. Technol. 44 (2007), 119-123.

[39] Protective Chemical PM-490; MSDS No. 17-9595-4; Minnesota Mining and Manufacturing Company : St. Paul, MN, August 29, 2006.

[40] Protective Chemical PM-490; Product Bulletin No. 98-0212-0931-1; Minnesota Mining and Manufacturing Company : St. Paul, MN, September, 2002.

[41] Protective Chemical PM-930; MSDS No. 18-3561-0; Minnesota Mining and Manufacturing Company : St. Paul, MN, September 15, 2006.

[42] Protective Chemical PM-930; Product Bulletin No. 98-0212-0971-7; Minnesota Mining and Manufacturing Company : St. Paul, MN, March, 2003.

[43] Reusch, William. "Carbohydrates." Natural Products. 1999. Michigan State University. 26 Feb. 2007
<<http://www.cem.msu.edu/~reusch/VirtualText/carbhyd.htm#carb8>>.

[44] Sakurai, Yoshiaki, Shigeki Okuda, Norio Nagayama, and Masaaki Yokoyama. "Novel microlens array fabrication utilizing UV-photodecomposition of polysilane." J. Mat. Chem. 11 (2001), 1077-1080.

[45] Schmidt, Helmut. "Considerations about the sol-gel process: From the classical sol-gel route to advanced chemical nanotechnologies." J. Sol-Gel. Sci. Techn. 40 (2006), 115-130.

[46] Schmuckler, Joe, and Mark Michalovic. "Faces in Polymers." Faces in Molecular Sciences. 2001. The Chemical Heritage Foundation. 26 Feb. 2007
<<http://www.chemheritage.org/EducationalServices/faces/teacher/poly/pop/pet.htm>>.

[47] Slade, Phillip E. Handbook of Fiber Finish Technology. New York, NY: Marcel Dekker, Inc, 1998.

[48] Soeno, Takuji, Kohei Inokuchi, and Seimei Shiratori. "Ultra-water-repellent surface: fabrication of complicated structure of SiO₂ nanoparticles by electrostatic self-assembled films." Appl. Surf. Sci. 237 (2004), 543-547.

[49] Teflon AP Fabric Protector; MSDS No. DU008183; E.I. du Pont de Nemours and Company : Wilmington, DE, October 16, 2000.

- [50] Teflon AP-II; MSDS No. 10378PP; E.I. du Pont de Nemours and Company : Wilmington, DE, June 26, 2006.
- [51] Textor, Torsten, Thomas Bahners and Eckhard Schollmeyer. "Modern Approaches for Intelligent Surface Modification." Journal of Industrial Textiles 32 (2003), 279-289.
- [52] Textor, T., T. Bahners, and E. Schollmeyer. "Organically modified ceramics for coating textiles materials." Prog. Colloid Polym. Sci. 117 (2001), 76-79.
- [53] Thim, Gilmar P., Maria A.S. Oliveira, Evandro D.A. Oliveira, and Francisco C.L. Melo. "Sol-gel silica film preparation from aqueous solutions for corrosion protection." Journal of Non-Crystalline Solids 273 (2000), 124-128.
- [54] Tomasino, Charles. Chemistry & Technology of Fabric Preparation & Finishing. Raleigh, NC: North Carolina State University, 1992.
- [55] Tyner, David Wade. "Evaluation of Repellent Finishes Applied by Atmospheric Plasma." MS Thesis. North Carolina State University, 2007.
- [56] Warner, Steven B. Fiber Science. Upper Saddle River, NJ: Prentice-Hall, 1995.
- [57] Whang, Hyun Suk. "Wetting Characteristics and Surface Energy Properties of Cellulosic and Noncellulosic Fibers." Diss. North Carolina State University, 1997.
- [58] Yoneda, Takashige, and Takeshi Morimoto. "Mechanical durability of water repellent glass." Thin Solid Films 351 (1999), 279-283.
- [59] Yu, Minghua, Guotuan Gu, Wei-Dong Meng, and Feng-Ling Qing. "Superhydrophobic cotton fabric coating based on a complex layer of silica nanoparticles and perfluorooctylated quaternary ammonium silane coupling agent." Applied Surface Science 253 (2007), 3669–3673.
- [60] Zhang, Xiangwu, and Peter S. Fedkiw. "Ionic transport and interfacial stability of sulfonate-modified fumed silicas as nanocomposite electrolytes." J. Electrochem. Soc. 152 (2005), A2413-A2420.

Appendices

Appendix A: Raw Data Used to Make Graphs and Tables
Data from **Figure 5.5**

TEOS + 0.02% o.w.b. SiO ₂						
	Location 1		Location 2		Location 3	
	Angle 1	Angle 2	Angle 1	Angle 2	Angle 1	Angle 2
Sample 1	132	131	127	123	125	135
Sample 2	135	131	130	133	125	135
Sample 3	131	125	123	132	130	128
				129.5	±	4.0
TEOS + 0.2% o.w.b. SiO ₂						
	Location 1		Location 2		Location 3	
	Angle 1	Angle 2	Angle 1	Angle 2	Angle 1	Angle 2
Sample 1	128	147	136	135	128	137
Sample 2	129	131	135	132	137	132
Sample 3	124	131	142	139	130	135
				133.8	±	5.5
TMOS + 0.02% o.w.b. SiO ₂						
	Location 1		Location 2		Location 3	
	Angle 1	Angle 2	Angle 1	Angle 2	Angle 1	Angle 2
Sample 1	118	119	115	116	120	126
Sample 2	120	120	115	115	121	119
Sample 3	119	130	118	118	115	116
				118.9	±	3.9
TMOS + 0.2% o.w.b. SiO ₂						
	Location 1		Location 2		Location 3	
	Angle 1	Angle 2	Angle 1	Angle 2	Angle 1	Angle 2
Sample 1	123	124	130	145	133	116
Sample 2	140	136	128	128	140	138
Sample 3	133	125	126	126	127	129
				130.4	±	7.2
Bis(triethoxysilyl)ethane + 0.02% o.w.b. SiO ₂						
	Location 1		Location 2		Location 3	
	Angle 1	Angle 2	Angle 1	Angle 2	Angle 1	Angle 2
Sample 1	125	121	120	120	132	132
Sample 2	132	132	125	130	130	129
Sample 3	134	134	127	123	127	129
				127.9	±	4.6
Bis(triethoxysilyl)ethane + 0.2% o.w.b. SiO ₂						
	Location 1		Location 2		Location 3	
	Angle 1	Angle 2	Angle 1	Angle 2	Angle 1	Angle 2
Sample 1	132	131	136	144	131	134
Sample 2	139	135	133	138	131	136
Sample 3	142	137	130	132	135	136
				135.1	±	3.8

Data from **Figure 5.6**

TEOS + 0% o.w.b. SiO ₂						
	Location 1		Location 2		Location 3	
	Angle 1	Angle 2	Angle 1	Angle 2	Angle 1	Angle 2
Sample 1	130	130	130	133	136	131
Sample 2	134	136	129	127	133	130
Sample 3	120	122	128	125	133	135
				130.1	±	4.4
TEOS + 0.01% o.w.b. SiO ₂						
	Location 1		Location 2		Location 3	
	Angle 1	Angle 2	Angle 1	Angle 2	Angle 1	Angle 2
Sample 1	132	131	127	123	125	135
Sample 2	135	131	130	133	125	135
Sample 3	131	125	123	132	130	128
				129.5	±	4.0
TEOS + 0.025% o.w.b. SiO ₂						
	Location 1		Location 2		Location 3	
	Angle 1	Angle 2	Angle 1	Angle 2	Angle 1	Angle 2
Sample 1	121	126	115	120	118	114
Sample 2	131	123	124	118	123	120
Sample 3	132	134	123	124	129	131
				123.7	±	5.8
TEOS + 0.05% o.w.b. SiO ₂						
	Location 1		Location 2		Location 3	
	Angle 1	Angle 2	Angle 1	Angle 2	Angle 1	Angle 2
Sample 1	125	125	134	132	133	134
Sample 2	134	131	133	133	134	130
Sample 3	134	132	132	135	130	131
				131.8	±	2.8
TEOS + 0.02% o.w.b. SiO ₂						
	Location 1		Location 2		Location 3	
	Angle 1	Angle 2	Angle 1	Angle 2	Angle 1	Angle 2
Sample 1	128	147	136	135	128	137
Sample 2	129	131	135	132	137	132
Sample 3	124	131	142	139	130	135
				133.8	±	5.5

Data from **Figure 5.7**

TEOS, Octadecylmethyldimethoxysilane, NO Silica						
	Location 1		Location 2		Location 3	
	Angle 1	Angle 2	Angle 1	Angle 2	Angle 1	Angle 2
Sample 1	130	131	126	128	124	126
				127.5	±	2.6
TEOS, Octadecylmethyldimethoxysilane, Aerosil 90						
	Location 1		Location 2		Location 3	
	Angle 1	Angle 2	Angle 1	Angle 2	Angle 1	Angle 2
Sample 1	125	129	131	125	131	127
				128.0	±	2.7

Data from **Figure 5.8**

TEOS, n-Octyltrimethoxysilane, Aerosil® 90						
	Location 1		Location 2		Location 3	
	Angle 1	Angle 2	Angle 1	Angle 2	Angle 1	Angle 2
Sample 1	132	131	134	132	126	127
Sample 2	130	131	133	134	136	138
Sample 3	130	138	133	133	128	126
				131.8	±	3.6
TEOS, n-Octyltrimethoxysilane, Aerosil® 150						
	Location 1		Location 2		Location 3	
	Angle 1	Angle 2	Angle 1	Angle 2	Angle 1	Angle 2
Sample 1	130	129	130	125	135	136
Sample 2	140	135	127	130	133	128
Sample 3	130	130	133	129	133	132
				131.4	±	3.6
TEOS, n-Octyltrimethoxysilane, Aerosil® 200						
	Location 1		Location 2		Location 3	
	Angle 1	Angle 2	Angle 1	Angle 2	Angle 1	Angle 2
Sample 1	134	131	131	132	134	141
Sample 2	130	131	122	124	128	134
Sample 3	134	137	134	134	138	141
				132.8	±	4.9
TEOS, n-Octyltrimethoxysilane, Aerosil® 380						
	Location 1		Location 2		Location 3	
	Angle 1	Angle 2	Angle 1	Angle 2	Angle 1	Angle 2
Sample 1	134	132	130	127	133	129
Sample 2	130	132	135	133	132	135
Sample 3	133	135	133	131	134	136
				132.4	±	2.3
TEOS, n-Octyltrimethoxysilane, Aerosil® R805						
	Location 1		Location 2		Location 3	
	Angle 1	Angle 2	Angle 1	Angle 2	Angle 1	Angle 2
Sample 1	132	132	131	132	135	137
Sample 2	130	139	137	135	136	139
Sample 3	135	133	135	137	135	135
				134.7	±	2.6

Data from **Figure 5.9**

TEOS, n-Decyltriethoxysilane, Aerosil® 90						
	Location 1		Location 2		Location 3	
	Angle 1	Angle 2	Angle 1	Angle 2	Angle 1	Angle 2
Sample 1	138	141	140	136	137	139
Sample 2	144	140	142	144	141	141
Sample 3	139	140	139	136	137	133
				139.3	±	2.8
TEOS, n-Decyltriethoxysilane, Aerosil® 150						
	Location 1		Location 2		Location 3	
	Angle 1	Angle 2	Angle 1	Angle 2	Angle 1	Angle 2
Sample 1	138	143	147	145	137	140
Sample 2	139	139	133	140	140	133
Sample 3	138	136	142	140	140	135
				139.2	±	3.6
TEOS, n-Decyltriethoxysilane, Aerosil® 200						
	Location 1		Location 2		Location 3	
	Angle 1	Angle 2	Angle 1	Angle 2	Angle 1	Angle 2
Sample 1	139	138	141	134	139	145
Sample 2	144	142	141	132	135	135
Sample 3	142	139	143	140	134	133
				138.7	±	3.9
TEOS, n-Decyltriethoxysilane, Aerosil® 380						
	Location 1		Location 2		Location 3	
	Angle 1	Angle 2	Angle 1	Angle 2	Angle 1	Angle 2
Sample 1	143	141	138	139	142	143
Sample 2	141	143	142	142	135	136
Sample 3	141	140	139	145	139	140
				140.5	±	2.5
TEOS, n-Decyltriethoxysilane, Aerosil® R805						
	Location 1		Location 2		Location 3	
	Angle 1	Angle 2	Angle 1	Angle 2	Angle 1	Angle 2
Sample 1	142	142	144	144	140	143
Sample 2	143	138	145	141	147	138
Sample 3	139	138	149	145	147	140
				142.5	±	3.3

Data from **Figure 5.10**

TMOS, n-Octyltrimethoxysilane, Aerosil® 90						
	Location 1		Location 2		Location 3	
	Angle 1	Angle 2	Angle 1	Angle 2	Angle 1	Angle 2
Sample 1	136	135	135	132	138	134
Sample 2	133	136	133	132	131	132
Sample 3	131	134	135	132	135	130
				133.6	±	2.1
TMOS, n-Octyltrimethoxysilane, Aerosil® 150						
	Location 1		Location 2		Location 3	
	Angle 1	Angle 2	Angle 1	Angle 2	Angle 1	Angle 2
Sample 1	142	145	135	132	136	135
Sample 2	128	130	137	137	135	132
Sample 3	135	132	130	130	137	140
				134.9	±	4.4
TMOS, n-Octyltrimethoxysilane, Aerosil® 200						
	Location 1		Location 2		Location 3	
	Angle 1	Angle 2	Angle 1	Angle 2	Angle 1	Angle 2
Sample 1	132	135	129	133	133	133
Sample 2	132	136	132	135	134	137
Sample 3	131	135	132	129	132	130
				132.8	±	2.2
TMOS, n-Octyltrimethoxysilane, Aerosil® 380						
	Location 1		Location 2		Location 3	
	Angle 1	Angle 2	Angle 1	Angle 2	Angle 1	Angle 2
Sample 1	130	128	131	129	129	131
Sample 2	131	129	132	124	129	132
Sample 3	132	128	132	128	129	130
				129.7	±	2.0
TMOS, n-Octyltrimethoxysilane, Aerosil® R805						
	Location 1		Location 2		Location 3	
	Angle 1	Angle 2	Angle 1	Angle 2	Angle 1	Angle 2
Sample 1	135	134	135	133	130	133
Sample 2	134	130	133	130	130	124
Sample 3	133	130	131	140	134	135
				132.4	±	3.3

Data from **Figure 5.11**

TMOS, n-Decyltriethoxysilane, Aerosil® 90						
	Location 1		Location 2		Location 3	
	Angle 1	Angle 2	Angle 1	Angle 2	Angle 1	Angle 2
Sample 1	140	142	143	143	143	141
Sample 2	140	141	140	143	136	139
Sample 3	141	139	143	142	139	139
				140.8	±	1.9
TMOS, n-Decyltriethoxysilane, Aerosil® 150						
	Location 1		Location 2		Location 3	
	Angle 1	Angle 2	Angle 1	Angle 2	Angle 1	Angle 2
Sample 1	139	150	139	144	149	147
Sample 2	146	147	145	140	149	143
Sample 3	135	137	143	135	144	141
				142.9	±	4.7
TMOS, n-Decyltriethoxysilane, Aerosil® 200						
	Location 1		Location 2		Location 3	
	Angle 1	Angle 2	Angle 1	Angle 2	Angle 1	Angle 2
Sample 1	134	137	139	131	141	137
Sample 2	140	138	137	145	137	135
Sample 3	138	135	141	143	144	141
				138.5	±	3.6
TMOS, n-Decyltriethoxysilane, Aerosil® 380						
	Location 1		Location 2		Location 3	
	Angle 1	Angle 2	Angle 1	Angle 2	Angle 1	Angle 2
Sample 1	142	143	155	157	149	148
Sample 2	146	146	146	136	141	141
Sample 3	144	137	144	140	141	140
				144.2	±	5.5
TMOS, n-Decyltriethoxysilane, Aerosil® R805						
	Location 1		Location 2		Location 3	
	Angle 1	Angle 2	Angle 1	Angle 2	Angle 1	Angle 2
Sample 1	137	143	141	148	138	146
Sample 2	140	135	140	138	143	146
Sample 3	143	146	138	141	145	143
				141.7	±	3.6

Data from **Figure 5.12**

Bis(triethoxysilyl)ethane, n-Octyltrimethoxysilane, Aerosil® 90						
	Location 1		Location 2		Location 3	
	Angle 1	Angle 2	Angle 1	Angle 2	Angle 1	Angle 2
Sample 1	145	137	150	142	144	143
Sample 2	141	136	137	132	128	135
Sample 3	132	135	147	141	144	135
				139.1	±	5.8
Bis(triethoxysilyl)ethane, n-Octyltrimethoxysilane, Aerosil® 150						
	Location 1		Location 2		Location 3	
	Angle 1	Angle 2	Angle 1	Angle 2	Angle 1	Angle 2
Sample 1	142	139	139	144	135	139
Sample 2	133	136	133	127	139	135
Sample 3	135	134	133	132	127	133
				135.3	±	4.5
Bis(triethoxysilyl)ethane, n-Octyltrimethoxysilane, Aerosil® 200						
	Location 1		Location 2		Location 3	
	Angle 1	Angle 2	Angle 1	Angle 2	Angle 1	Angle 2
Sample 1	130	130	130	135	134	132
Sample 2	131	132	141	142	138	135
Sample 3	138	137	134	138	138	141
				135.3	±	3.9
Bis(triethoxysilyl)ethane, n-Octyltrimethoxysilane, Aerosil® 380						
	Location 1		Location 2		Location 3	
	Angle 1	Angle 2	Angle 1	Angle 2	Angle 1	Angle 2
Sample 1	142	142	134	137	135	132
Sample 2	131	130	132	126	136	136
Sample 3	133	132	133	132	141	137
				134.5	±	4.2
Bis(triethoxysilyl)ethane, n-Octyltrimethoxysilane, Aerosil® R805						
	Location 1		Location 2		Location 3	
	Angle 1	Angle 2	Angle 1	Angle 2	Angle 1	Angle 2
Sample 1	145	143	141	134	131	131
Sample 2	135	130	130	137	130	130
Sample 3	133	133	131	126	135	134
				133.8	±	4.9

Data from **Figure 5.13**

Bis(triethoxysilyl)ethane, n-Decyltriethoxysilane, Aerosil® 90						
	Location 1		Location 2		Location 3	
	Angle 1	Angle 2	Angle 1	Angle 2	Angle 1	Angle 2
Sample 1	135	137	138	141	135	137
Sample 2	136	140	141	138	132	135
Sample 3	142	135	137	135	143	144
				137.8	±	3.3
Bis(triethoxysilyl)ethane, n-Decyltriethoxysilane, Aerosil® 150						
	Location 1		Location 2		Location 3	
	Angle 1	Angle 2	Angle 1	Angle 2	Angle 1	Angle 2
Sample 1	136	145	140	131	142	138
Sample 2	145	136	145	140	143	134
Sample 3	133	130	133	138	135	135
				137.7	±	4.8
Bis(triethoxysilyl)ethane, n-Decyltriethoxysilane, Aerosil® 200						
	Location 1		Location 2		Location 3	
	Angle 1	Angle 2	Angle 1	Angle 2	Angle 1	Angle 2
Sample 1	140	125	135	135	133	130
Sample 2	131	130	131	130	132	130
Sample 3	133	132	130	125	134	125
				131.2	±	3.7
Bis(triethoxysilyl)ethane, n-Decyltriethoxysilane, Aerosil® 380						
	Location 1		Location 2		Location 3	
	Angle 1	Angle 2	Angle 1	Angle 2	Angle 1	Angle 2
Sample 1	136	141	128	121	126	125
Sample 2	138	138	125	120	134	133
Sample 3	125	129	129	129	131	134
				130.1	±	5.9
Bis(triethoxysilyl)ethane, n-Decyltriethoxysilane, Aerosil® R805						
	Location 1		Location 2		Location 3	
	Angle 1	Angle 2	Angle 1	Angle 2	Angle 1	Angle 2
Sample 1	137	135	134	132	143	140
Sample 2	144	142	134	127	137	135
Sample 3	134	145	130	132	140	139
				136.7	±	5.0

Data for Washing, Crocking, and Non-Silica Comparison Samples

TEOS, n-Decyltriethoxysilane, Aerosil® R805 - Crock Sample						
	Location 1		Location 2		Location 3	
	Angle 1	Angle 2	Angle 1	Angle 2	Angle 1	Angle 2
Sample 1	131	130	135	131	132	126
Sample 2	128	128	136	133	137	129
Sample 3	130	128	131	126	133	128
				130.7	±	3.2
TEOS, n-Decyltriethoxysilane, Aerosil® R805 - Wash Sample						
	Location 1		Location 2		Location 3	
	Angle 1	Angle 2	Angle 1	Angle 2	Angle 1	Angle 2
Sample 1	abs	abs	abs	abs	abs	Abs
Sample 2	118	123	98	115	106	128
Sample 3	83	82	70	90	88	82
				98.6	±	18.9
TEOS, n-Decyltriethoxysilane, NO Silica						
	Location 1		Location 2		Location 3	
	Angle 1	Angle 2	Angle 1	Angle 2	Angle 1	Angle 2
Sample 1	128	134	134	139	134	126
Sample 2	132	130	132	125	135	132
Sample 3	128	132	128	129	136	138
				131.8	±	3.9
TEOS, n-Decyltriethoxysilane, NO Silica - Crock Sample						
	Location 1		Location 2		Location 3	
	Angle 1	Angle 2	Angle 1	Angle 2	Angle 1	Angle 2
Sample 1	128	124	121	121	121	123
Sample 2	123	125	126	120	122	120
Sample 3	131	118	126	123	129	121
				123.4	±	3.4
TEOS, n-Decyltriethoxysilane, NO Silica - Wash Sample						
	Location 1		Location 2		Location 3	
	Angle 1	Angle 2	Angle 1	Angle 2	Angle 1	Angle 2
Sample 1	75	81	abs	abs	73	74
Sample 2	104	98	79	80	90	97
Sample 3	99	75	85	90	64	58
				82.6	±	13.0

TMOS, n-Decyltriethoxysilane, Aerosil® 380 - Crock Sample						
	Location 1		Location 2		Location 3	
	Angle 1	Angle 2	Angle 1	Angle 2	Angle 1	Angle 2
Sample 1	128	126	120	124	100	104
Sample 2	120	116	125	109	131	115
Sample 3	121	113	123	116	120	115
				118.1	±	8.1
TMOS, n-Decyltriethoxysilane, Aerosil® 380 - Wash Sample						
	Location 1		Location 2		Location 3	
	Angle 1	Angle 2	Angle 1	Angle 2	Angle 1	Angle 2
Sample 1	abs	abs	83	70	85	85
Sample 2	85	70	82	83	abs	abs
Sample 3	abs	abs	abs	abs	abs	abs
				80.3	±	6.5
TMOS, n-Decyltriethoxysilane, NO Silica						
	Location 1		Location 2		Location 3	
	Angle 1	Angle 2	Angle 1	Angle 2	Angle 1	Angle 2
Sample 1	131	135	136	133	136	132
Sample 2	127	132	131	132	132	130
Sample 3	135	130	136	138	134	137
				133.2	±	2.8
TMOS, n-Decyltriethoxysilane, NO Silica - Crock Sample						
	Location 1		Location 2		Location 3	
	Angle 1	Angle 2	Angle 1	Angle 2	Angle 1	Angle 2
Sample 1	132	128	125	132	116	119
Sample 2	122	121	131	131	130	125
Sample 3	126	125	123	118	112	105
				123.4	±	7.3
TMOS, n-Decyltriethoxysilane, NO Silica - Wash Sample						
	Location 1		Location 2		Location 3	
	Angle 1	Angle 2	Angle 1	Angle 2	Angle 1	Angle 2
Sample 1	abs	abs	abs	abs	abs	abs
Sample 2	73	75	73	75	78	77
Sample 3	76	83	94	87	80	85
				79.7	±	6.4

Bis(triethoxysilyl)ethane, n-Octyltrimethoxysilane, Aerosil® 90 - Crock Sample						
	Location 1		Location 2		Location 3	
	Angle 1	Angle 2	Angle 1	Angle 2	Angle 1	Angle 2
Sample 1	125	113	126	118	126	125
Sample 2	107	105	118	113	125	120
Sample 3	123	111	114	118	120	127
				118.6	±	6.8
Bis(triethoxysilyl)ethane, n-Octyltrimethoxysilane, Aerosil® 90 - Wash Sample						
	Location 1		Location 2		Location 3	
	Angle 1	Angle 2	Angle 1	Angle 2	Angle 1	Angle 2
Sample 1	104	101	107	107	119	119
Sample 2	104	101	114	120	129	129
Sample 3	124	123	119	115	105	109
				113.8	±	9.3
Bis(triethoxysilyl)ethane, n-Octyltrimethoxysilane, NO Silica						
	Location 1		Location 2		Location 3	
	Angle 1	Angle 2	Angle 1	Angle 2	Angle 1	Angle 2
Sample 1	126	126	114	120	126	125
Sample 2	120	126	124	125	127	128
Sample 3	124	128	126	125	126	133
				124.9	±	3.9
Bis(triethoxysilyl)ethane, n-Octyltrimethoxysilane, NO Silica - Crock Sample						
	Location 1		Location 2		Location 3	
	Angle 1	Angle 2	Angle 1	Angle 2	Angle 1	Angle 2
Sample 1	129	121	132	127	130	125
Sample 2	135	127	132	123	126	127
Sample 3	125	122	122	127	120	121
				126.2	±	4.2
Bis(triethoxysilyl)ethane, n-Octyltrimethoxysilane, NO Silica - Wash Sample						
	Location 1		Location 2		Location 3	
	Angle 1	Angle 2	Angle 1	Angle 2	Angle 1	Angle 2
Sample 1	117	100	112	118	112	106
Sample 2	113	110	101	107	106	100
Sample 3	106	105	111	108	108	108
				108.2	±	5.1

TEOS, n-Decyl, Aerosil® R805 - Wash & Heat Dried						
	Location 1		Location 2		Location 3	
	Angle 1	Angle 2	Angle 1	Angle 2	Angle 1	Angle 2
Sample 1	85	87	100	97	88	90
Sample 2	94	97	95	97	111	116
Sample 3	108	111	112	112	112	95
				100.4	±	10.1
TEOS, n-Decyl, No Silica - Wash & Heat Dried						
	Location 1		Location 2		Location 3	
	Angle 1	Angle 2	Angle 1	Angle 2	Angle 1	Angle 2
Sample 1	96	90	91	95	93	87
Sample 2	96	90	95	88	115	95
Sample 3	96	97	100	98	97	114
				96.3	±	7.5
TEOS, n-Decyl, Aerosil® R805 - Sonicated & Washed						
	Location 1		Location 2		Location 3	
	Angle 1	Angle 2	Angle 1	Angle 2	Angle 1	Angle 2
Sample 1	73	77	82	81	78	73
Sample 2	abs	abs	abs	abs	abs	abs
Sample 3	abs	abs	abs	abs	abs	abs
				77.3	±	3.8
TEOS, n-Decyl, Aerosil® R805 - Sonicated, Washed, & Heat Dried						
	Location 1		Location 2		Location 3	
	Angle 1	Angle 2	Angle 1	Angle 2	Angle 1	Angle 2
Sample 1	78	74	76	76	90	72
Sample 2	83	85	80	78	84	85
Sample 3	75	81	85	75	75	85
				79.8	±	5.0
TEOS, n-Decyl, Aerosil® R805 – Sonicated						
	Location 1		Location 2		Location 3	
	Angle 1	Angle 2	Angle 1	Angle 2	Angle 1	Angle 2
Sample 1	135	130	135	136	142	145
Sample 2	147	141	140	138	134	134
Sample 3	136	130	138	142	141	140
				138.0	±	4.6

TMOS, n-Decyl, Aerosil® 380 - Wash & Heat Dried						
	Location 1		Location 2		Location 3	
	Angle 1	Angle 2	Angle 1	Angle 2	Angle 1	Angle 2
Sample 1	77	78	75	77	79	80
Sample 2	80	90	85	83	88	78
Sample 3	78	75	78	76	81	86
				80.2	±	4.4
TMOS, n-Decyl, No Silica - Wash & Heat Dried						
	Location 1		Location 2		Location 3	
	Angle 1	Angle 2	Angle 1	Angle 2	Angle 1	Angle 2
Sample 1	80	88	81	80	81	77
Sample 2	90	100	84	111	127	115
Sample 3	85	88	100	95	92	87
				92.3	±	13.7
TMOS, n-Decyl, Aerosil® 380 - Sonicated & Washed						
	Location 1		Location 2		Location 3	
	Angle 1	Angle 2	Angle 1	Angle 2	Angle 1	Angle 2
Sample 1	abs	abs	abs	abs	abs	abs
Sample 2	abs	abs	abs	abs	abs	abs
Sample 3	abs	abs	abs	abs	abs	abs
				#DIV/0!	±	#DIV/0!
TMOS, n-Decyl, Aerosil® 380 - Sonicated, Washed, & Heat Dried						
	Location 1		Location 2		Location 3	
	Angle 1	Angle 2	Angle 1	Angle 2	Angle 1	Angle 2
Sample 1	82	72	84	89	72	78
Sample 2	76	75	76	77	70	76
Sample 3	83	76	79	70	86	76
				77.6	±	5.3
TMOS, n-Decyl, Aerosil® 380 – Sonicated						
	Location 1		Location 2		Location 3	
	Angle 1	Angle 2	Angle 1	Angle 2	Angle 1	Angle 2
Sample 1	142	142	139	138	127	132
Sample 2	125	137	144	137	135	140
Sample 3	135	135	135	137	140	135
				136.4	±	4.8

Bis(triethoxysilyl)ethane, n-Octyl, Aerosil® 90 - Wash & Heat Dried						
	Location 1		Location 2		Location 3	
	Angle 1	Angle 2	Angle 1	Angle 2	Angle 1	Angle 2
Sample 1	121	122	122	127	125	120
Sample 2	129	130	121	121	122	115
Sample 3	113	108	130	121	119	116
				121.2	±	5.8
Bis(triethoxysilyl)ethane, n-Octyl, No Silica - Wash & Heat Dried						
	Location 1		Location 2		Location 3	
	Angle 1	Angle 2	Angle 1	Angle 2	Angle 1	Angle 2
Sample 1	113	107	104	111	113	99
Sample 2	108	110	110	114	121	106
Sample 3	104	116	110	108	109	106
				109.4	±	5.0
Bis(triethoxysilyl)ethane, n-Octyl, Aerosil® 90 - Sonicated & Washed						
	Location 1		Location 2		Location 3	
	Angle 1	Angle 2	Angle 1	Angle 2	Angle 1	Angle 2
Sample 1	111	112	111	110	113	108
Sample 2	111	110	108	104	109	105
Sample 3	101	106	104	106	100	107
				107.6	±	3.7
Bis(triethoxysilyl)ethane, n-Octyl, Aerosil® 90 - Sonicated, Washed, & Heat Dried						
	Location 1		Location 2		Location 3	
	Angle 1	Angle 2	Angle 1	Angle 2	Angle 1	Angle 2
Sample 1	127	122	125	124	128	125
Sample 2	118	122	115	110	121	127
Sample 3	127	127	125	128	123	121
				123.1	±	4.8
Bis(triethoxysilyl)ethane, n-Octyl, Aerosil® 90 – Sonicated						
	Location 1		Location 2		Location 3	
	Angle 1	Angle 2	Angle 1	Angle 2	Angle 1	Angle 2
Sample 1	132	130	133	135	134	136
Sample 2	131	130	130	129	129	129
Sample 3	127	129	123	124	125	128
				129.7	±	3.5

Appendix B: Calculations

Making of 0.01 N HCl Solution:

Start with 37% HCl_{aq}

$$37\% \text{ HCl} = 37 \text{ g HCl} \times (1 \text{ mol HCl} / 36.5 \text{ g HCl}) = 1.01 \text{ mol HCl}$$

$$\text{If } 100 \text{ g Soln.} \times (1 \text{ mL Soln.} / 1.18 \text{ g/mL Soln.}) \times (1 \text{ L Soln.} / 1000 \text{ mL Soln.}) = .0840 \text{ L Soln.}$$

$$\text{Molarity of Solution} = 1.01 \text{ mol HCl} / .0840 \text{ L HCl} = 12.0 \text{ M HCl} [=12.0 \text{ N HCl}]$$

$$(500 \text{ mL } 0.01 \text{ N HCl})(0.01 \text{ N HCl}) = (X \text{ mL } 12.0 \text{ N HCl})(12.0 \text{ N HCl})$$

$$(500 \text{ mL})(0.01 \text{ N}) / (12.0 \text{ N}) = .417 \text{ mL of } 12.0 \text{ N HCl in } 500 \text{ mL of Water}$$

Determining the Amount of Silica Nanoparticles to Introduce to Solutions:

Silica was normally added at 0.2% and 0.02% on weight of bath.

Three pieces of 22.86 cm x 22.86 cm fabric are to be used with each solution.

Three pieces weigh approximately 22.49 grams. These calculations were used throughout, under the assumption that all pieces of fabric would weigh approximately the same amount.

$$\text{In } 0.02\% \text{ o.w.b. solutions, } 22.49 \text{ g} \times 0.001 = 0.0225 \text{ g Silica}$$

$$\text{In } 0.2\% \text{ o.w.b. solutions, } 22.49 \text{ g} \times 0.01 = 0.225 \text{ g Silica}$$

In terms of square yardage:

Fabric was about 4 oz. / yd²

$$4 \text{ oz.} \times 0.01 = 0.04 \text{ oz. of silica per yd}^2$$

$$0.04 \text{ oz. of silica} = 1.13 \text{ g of silica}$$

Silica used:

$$1.13 \text{ g} / \text{yd}^2 \text{ of fabric}$$